Université d'Ottawa • University of Ottawa

Université d'Ottawa · University of Ottawa

FACULTÉ DES ÉTUDES SUPÉRIEURES ET POSTDOCTORALES

FACULTY OF GRADUATE AND POSTDOCTORAL STUDIES

Julie Kathleen LALONDE

AUTEUR DE LA THÈSE - AUTHOR OF THESIS

M. Sc. (Cellular and Molecular Medicine)

GRADE - DEGREE

Department of Cellular and Molecular Medicine

FACULTÉ, ÉCOLE, DÉPARTEMENT - FACULTY, SCHOOL, DEPARTMENT

TITRE DE LA THÈSE - TITLE OF THE THESIS

TC10, a Mammalian Rho CTPase Responsible for Actin Cytoskeleton Reorganization and Cardiac Hypertrophy in the Murine Heart

L. Megeney

DIRECTEUR DE LA THÈSE - THESIS SUPERVISOR

CO-DIRECTEUR DE LA THÈSE - THESIS CO-SUPERVISOR

EXAMINATEURS DE LA THÈSE - THESIS EXAMINERS

R. Kothary

L. Sabourin

J.-M. De Koninck, Ph.D.

LE DOYEN DE LA FACULTÉ DES ÉTUDES SUPÉRIEURES ET POSTDOCTORALES

SIGNATURE

DEAN OF THE FACULTY OF GRADUATE AND POSTDOCTORAL STUDIES

TC10, a mammalian Rho GTPase responsible for actin cytoskeleton reorganization and cardiac hypertrophy in the murine heart

by

Julie Kathleen Lalonde

This thesis is submitted as a partial fulfillment of the M.Sc. program in

Cellular and Molecular Medicine

Department of Cellular and Molecular Medicine

Faculty of Medicine

University of Ottawa

November 3, 2003

Your file Votre référence
ISBN: 0-612-90102-5
Our file Notre référence
ISBN: 0-612-90102-5

Abstract

Rho guanosine triphosphatases (GTPases) act as molecular switches, cycling between two conformational states: an active, GTP-bound state and an inactive, GDP-bound state to control many complex cellular events in eukaryotic cells. Many Rho GTPases, including RhoA, Cdc42 and Rac1, have been extensively characterized and are involved in actin reorganization, activation of MAPK cascades, cell cycle progression, cellular proliferation, invasion, differentiation and apoptosis. TC10 was identified and classified as a Rho GTPase over ten years ago, however the precise role of this protein, which is highly expressed in cardiac and skeletal muscle, has only recently been explored *in vitro* and remains unexplored *in vivo*. Based on the unique expression pattern of TC10, we set out to investigate the role of TC10 by generating transgenic mice over-expressing activated TC10Q75L under the control of the cardiac-specific α-myosin heavy chain promoter. Transgenic mice expressing high levels of TC10Q75L showed pronounced atrial enlargement, evidence of left ventricular hypertrophy and diminished cardiomyocyte membrane integrity. *In vitro*, transgenic primary cardiomyocytes showed marked reorganization of the actin cytoskeleton, leading to the formation of actin-containing filopodial extensions, loss of stress fibers and actin aggregation. Together, these data suggest that TC10 functions to regulate cellular signalling to the actin cytoskeleton and processes associated with cell growth, leading to cardiac hypertrophy in TC10Q75L transgenic mice.

Table of Contents

List of Figures

List of Tables

List of Abbreviations

ACK1	Activated Cdc42-binding kinase
ANF	Atrial natriuretic factor
APS	Adapter containing pleckstrin and Scr homology domain
ATP	Adenosine triphosphate
Borg	Binder of Rho GTPase
BSA	Bovine serum albumin
C2C12 cells	Mouse skeletal muscle myoblasts
CAAX	Cysteine-aliphatic-aliphatic-any amino acid
CAP	Cbl-associated protein
cDNA	Complementary deoxyribonucleic acid
COS-1 cells	African green monkey kidney cells
CRIB domain	Cdc42/Rac interactive binding domain
CXXC	Cysteine-any-any-cysteine amino acid
DAPI	4,6-Diamidino-2-phenylindole
DH domain	Dbl homology domain
DMEM	Dulbecco's modified Eagle medium media
DNA	Deoxyribonucleic acid
EBD	Evans blue dye
EDTA	Ethylenediaminetetraacetic acid
ERK	Extracellular signal-regulated kinase
F-actin	Filamentous actin
FBS	Fetal bovine serum

GAP	GTPase-activating protein
GAPDH	Glyceraldehyde-3-phosphate dehydrogenase
GDP	Guanosine diphosphate
GEF	Guanine nucleotide exchange factor
GTP	Guanosine triphosphate
H9C2 cells	Rat cardiomyocytes
HA	Hemagglutinin
Hgh	Human growth hormone
HIS	Histidine
IgG	Immunoglobulin G
IP	Immunoprecipitation
IPTG	Isopropyl β-D-thiogalactoside
JMEM	Joklik's modified Eagle's medium
JNK	c-Jun NH_2-terminal kinase
kDa	kilodalton
MEF2	Myocyte enhancer factor 2
MHC	Myosin heavy chain
MAPK	Mitogen-activated protein kinase
MBP	Myelin basic protein
$MgCl_2$	Magnesium chloride
MLK	Mixed-lineage kinase
MRCK	Myotonic dystrophy kinase-related Cdc42-binding kinase
MSE55	Murine stromal and epithelial protein of 55kDa

N1E-115 cells	Neuroblastoma cells
Na_3VO_4	Sodium orthovanadate
NaCl	Sodium chloride
NaF	Sodium fluoride
NFAT	Nuclear factor of activated T-cell
NF-κB	Nuclear factor κB
N-WASP	Neural-Wiskott-Aldrich syndrome protein
PAGE	Polyacrylamide gel electrophoresis
PAK	p21-activated kinase
PC12 cells	Neuronal rat pheochromocytoma cells
PCR	Polymerase chain reaction
PH domain	Pleckstrin homology domain
PBS	Phosphate-buffered saline
PI3K	Phosphatidylinositol-3-OH kinase
PIST	PDZ domain protein interacting specifically with TC10
PDGF	Platelet-derived growth factor
PFA	Paraformaldehyde
PMSF	Phenylmethylsulfonyl fluoride
Rho GDI	Rho guanine nucleotide dissociation inhibitor
Rho GTPase	Rho guanosine triphosphatase
RhoT	Rho GTPase TC10 homologue
RNA	Ribonucleic acid
RT-PCR	Reverse transcriptase-polymerase chain reaction

SDS	Sodium dodecyl sulfate
SRF	Serum response factor
TBS	Tris-buffered saline
TCL	TC10-Like protein
TC10Q75L	Constitutively active, GTPase-defective TC10
TC10wt	Wild type TC10
Tg	Transgenic
WASP	Wiskott-Aldrich syndrome protein
Wt	Wild type

Acknowledgements

First and foremost, I would like to take this opportunity to thank my supervisor, Dr. Lynn Megeney, for providing me with an enriching laboratory environment and the freedom to explore science in an unrestricted manner. It was, and still is, very much appreciated especially considering the circumstances. Your guidance, encouragement and open nature towards science were valued.

I would also like to thank all of the other Megeney lab members, past and present, who made my journey through this molecular biology lab, a memorable and successful one: Kim Balazsi, Jacqueline Sandoz, Andrée Hierlihy, Dr. Steven Kolodziejczyk (all former members), Dr. Pasan Fernando, Beata Pekalska, Andrea Rowan, Jennifer Knudson, and Simon St-Pierre (all current members). I would especially like to acknowledge: Kim for showing me the ropes when I first came to the lab without a molecular background, Jackie for expert advice on generating and maintaining a transgenic colony, Pasan for always having words of wisdom and helpful science advice, Andrée for primary culturing and immunocytochemical advice, Andrea, Jennifer and Simon for being fellow M.Sc. students and understanding the "ups and downs," and Beata for making sure the lab was always running smoothly. I would also like to mention the new additions to the lab: Dr. Lawrence Puente, Steve Brunette, Jean-François Carrière and Rebecca Walsh. Although I didn't spend a lot of time in the lab with the "new additions," I'm sure they are just adding to the overall "Megeney" experience.

I would also like to express my appreciation towards the Kothary lab for helpful advice, reagents, and good times in the shared lab environment. I would especially like to thank Yves DeRepentigny for all his expertise in helping me generate my transgenic colony, as well as assistance with other experiments along the way, and Kevin for expert advice in the field of immunocytochemistry and microscopy.

I would also like to recognize and thank my committee members, Dr. Michael Rudnicki and Dr. Anthony Krantis, for valuable discussions and helpful guidance over the past two years. Additionally, I would like to thank Donna Hooper for always being there to lend graduate students a helpful hand whenever it was needed.

And last, but certainly not least, I would like to thank the people that are most important and central in my life, my family and friends: my fiancée, Timothy Buick, my parents, and my brother, the rest of my family, and my good friends, especially Melanie Hazelton, for always being supportive and encouraging in whatever venture I embark upon and for always being there when it was needed the most. Thank you for making me realize that I can achieve whatever I strive to accomplish and for making the not-so-good times in any researcher's life that much brighter. I would like to dedicate this thesis to Tim, my best friend. Tim, thank you for enduring the graduate student days with me, and I am looking forward to a very happy and successful future together.

CHAPTER 1

1.0 Introduction

1.1 Identification and classification of TC10

TC10, a novel human *ras*-like gene, was identified over a decade ago in a cDNA library screen designed to isolate and characterize human *ras*-related genes (Drivas et al., 1990). The *ras* superfamily of proteins, presently numbering over 60 in mammals, can be divided into five distinct sub-families, based on amino acid sequence similarities. These five groupings include: the Ras, Rab, Arf, Ran, and Rho families (Etienne-Manneville and Hall, 2002). The *rho* genes, a more distantly related sub-family share only approximately 35% amino acid identity with the *ras* proteins (Drivas et al., 1990). Consequently, TC10 was classified as a Rho guanosine triphosphatase (GTPase) based on its amino acid sequence identity with other Rho GTPases (greater than 50%), its size (approximately 200 amino acids), and the distance between its guanine nucleotide binding domains (Drivas et al., 1990; Murphy et al., 1999).

1.2 Rho guanosine triphosphatases

Rho GTPases act as molecular switches, cycling between two conformational states: an active, GTP-bound state and an inactive, GDP-bound state (Etienne-Manneville and Hall, 2002; Kjøller and Hall, 1999; Van Aelst and D'Souza-Schorey, 1997). To date, about twenty mammalian Rho GTPases have been identified, although this family of proteins is continuously expanding as new isoforms and novel proteins are discovered on a regular basis. In view of this, the currently identified Rho GTPases and their present sub–grouping within the Rho family are as follows: Rho (A, B, C); Rac (1, 2, 3), RhoG; Cdc42, TC10, TCL (RhoT); Chp (1, 2); Rnd (1, 2, 3(RhoE)); RhoBTB (1, 2); RhoD; Rif; and TTF (RhoH) (Abe et al., 2003; Neudauer et al., 1998; Etienne-Manneville and Hall,

2002; Kjøller and Hall, 1999). RhoA, Rac1, and Cdc42 are among the three most intensely studied and therefore well characterized Rho GTPases (Etienne-Manneville and Hall, 2002; Abe et al., 2003; Joberty et al., 1999). Rho GTPases are involved in many intricate, apparently diverse cellular processes including: cell transformation, gene transcription, cell cycle progression, membrane trafficking, differentiation, and apoptosis. However, these proteins are best understood for their roles as pivotal regulators of the actin cytoskeleton, influential in determining cell morphology, motility, migration, adhesion and cytokinesis (Abe et al., 2003; Neudauer et al., 1998; Murphy et al., 1999; Kjøller and Hall, 1999).

In addition to playing key roles in numerous cellular processes, the regulation and extensive list of effector proteins adds to the complexity of the study of Rho GTPases. Currently, three classes of Rho GTPase regulatory proteins exist, numbering more than 130, and over sixty target proteins have been identified, each interacting with one or several Rho GTPases (regulatory and effector proteins will be discussed in more detail in sections 1.3.3 and 1.3.5, respectively) (Etienne-Manneville and Hall, 2002; Van Aelst and D'Souza-Schorey, 1997). The immense number of regulatory and effector proteins, and the striking similarity of Rho family proteins adds to the notion that signal convergence and/or functional redundancy may exist between several Rho GTPases. However, the differing cellular and tissue localization of each Rho GTPase may account for complex signalling networks that are cooperative and coordinated in nature, and not necessarily redundant (Kjøller and Hall, 1999). The notion of separate linear signalling pathways for each Rho GTPase may no longer be a realistic one, rather Rho GTPases

may be reliant on a complex interdependent signalling network regulated by spatial and temporal cues (Etienne-Manneville and Hall, 2002).

1.3 TC10, a small Rho GTPase

TC10 was discovered and classified as a Rho GTPase over a decade ago. Despite this discovery, TC10 had remained almost completely uncharacterized until recent years (Drivas et al., 1990; Neudauer et al., 1998). More recently, the role of this Rho GTPase has been explored *in vitro* and the list of effector proteins and regulators has begun to be identified and compiled.

1.3.1 Structural and functional domains

On the basis of amino acid sequence comparisons, the classification of Rho GTPases dictates a fifty to fifty-five percent conservation in primary structure across species barriers (Van Aelst and D'Souza-Schorey, 1997). Additionally, the isoforms within a given Rho subfamily usually share greater than 90% sequence homology (Murphy et al., 1999). TC10 is most closely related to Cdc42, with 67% identity, Rac1, with 63% identity, and RhoA, with 51% identity (Murphy et al., 1999; Murphy et al., 2001). Although TC10 shares significant homology with other Rho GTPases, both in amino acid sequence similarity and in structural motifs, it is unique in that it possesses a short extension at its amino terminal (Kanzaki et al., 2002). In comparison to human TC10, the mouse homolog diverges by two amino acids, whereas rat TC10 only diverges by one amino acid (Chiang et al., 2002).

The human TC10 gene contains five exons spanning thirty-eight kilobases (Chiang et al., 2002). It encodes a protein of 205 to 213 amino acids, depending on a choice of methionine initiation codons at amino acid positions one and nine, resulting in a protein ranging in molecular mass from 23.4 to 24.3 kDa (Drivas et al., 1990; Murphy et al., 1999). TC10 contains four conserved GTP-binding motifs (G1-G4), an effector domain, switch I and II domains, a Rho insert domain, and a carboxyl terminal CAAX (cysteine-aliphatic-aliphatic-any) box amino acid motif (Abe et al., 2003). The G1 to G4 domains are core motifs required for GTP/GDP-binding and GTPase activity (Abe et al., 2003). The effector domain, which closely overlaps with the Switch I domain, is involved in effector interactions, while the Switch I and II domains participate in regulatory and effector protein binding (Murphy et al., 1999). These domains are nearly identical between the closely related TC10, Cdc42 and Rac1 (Figure 1) (Neudauer et al., 1998). The Rho insert is a thirteen amino acid region, specific to Rho GTPases, which has been shown to be involved in effector protein binding and interactions with regulatory proteins, specifically Rho GDP-dissociation inhibitors (Rho GDIs) (Wu et al., 1997; Abe et al., 2003). The CAAX box motif directs specific post-translational modifications, namely isoprenylation of the cysteine residue, followed by proteolytic removal of the three terminal amino acids and carboxymethylation, which is necessary for appropriate trafficking, membrane localization, and signalling specificity (Murphy et al., 1999; Murphy et al., 2001; Watson et al., 2003; Abe et al., 2003). Additionally, TC10 has a CXXC (cysteine-any-any-cysteine) amino acid sequence directly upstream of the CAAX box sequence, which directs palmitoylation of the cysteine residues and farnesylation, serving as membrane-targeting sites (Watson et al., 2001; Chiang et al., 2002; Abe et al.,

2003). These protein modifications suggest that TC10 is membrane-associated, and may be an important consideration in determining TC10's function in a physiological context (Murphy et al., 1999).

Initial characterization of TC10 function has revealed both overlapping and distinct roles for this GTPase in comparison to other Rho proteins. For example, gain-of-function (constitutively active, GTPase-defective) TC10 (TC10Q75L) induced peripheral membrane extensions, longer and more in number than those induced by Cdc42 (Neudauer et al., 1998). In addition, loss of stress fibers and formation of peripheral extensions were observed in the transfected NIH3T3 fibroblasts. In contrast, gain-of-function Cdc42 induced the formation of peripheral extensions and membrane ruffling in the same cell type (Neudauer et al., 1998). Activated Rac1 caused increased peripheral membrane ruffling and lamellipodial formation, while activated RhoA increased actin stress fibers in fibroblast cells (Neudauer et al., 1998). In COS cells, transfection of wild type TC10 (TC10wt) resulted in a significant percentage of cells displaying multiple short filopodia, while following transfection with TC10Q75L a high percentage of cells exhibited multiple long filopodia (Murphy et al., 1999). A carboxyl terminal deletion, GTPase-defective double mutant (TC10Q75L/Cdel) obliterates the phenotype seen with the TC10Q75L mutant. Finally, a constitutively active/effector double mutant of TC10 only reduces the phenotype seen with TC10Q75L by about one half (Murphy et al., 1999). Despite the significant homology and largely overlapping set of effectors for TC10, Rac1 and Cdc42, TC10 appears to produce a distinct phenotype *in vitro*. Clearly, the basis for the variable physiological effects needs to be firmly established.

Figure 1. Structural similarity between TC10 and Rho GTPase proteins.

A comparison of the amino acid sequence similarities of mouse TC10 and other related Rho GTPase proteins is shown. Alignment was performed by the method of Lipman and Pearson. Amino acids sharing greater than 50% identity with each other are shown in red. Functional domains are shown in green (*G1-G4*, core motifs for GTP/GDP-binding and hydrolysis; *E*, effector domain). The *switch I* and *switch II*, *Rho insert* and *CAAX* motifs are also shown. This figure was adapted from: Abe et al., 2003.

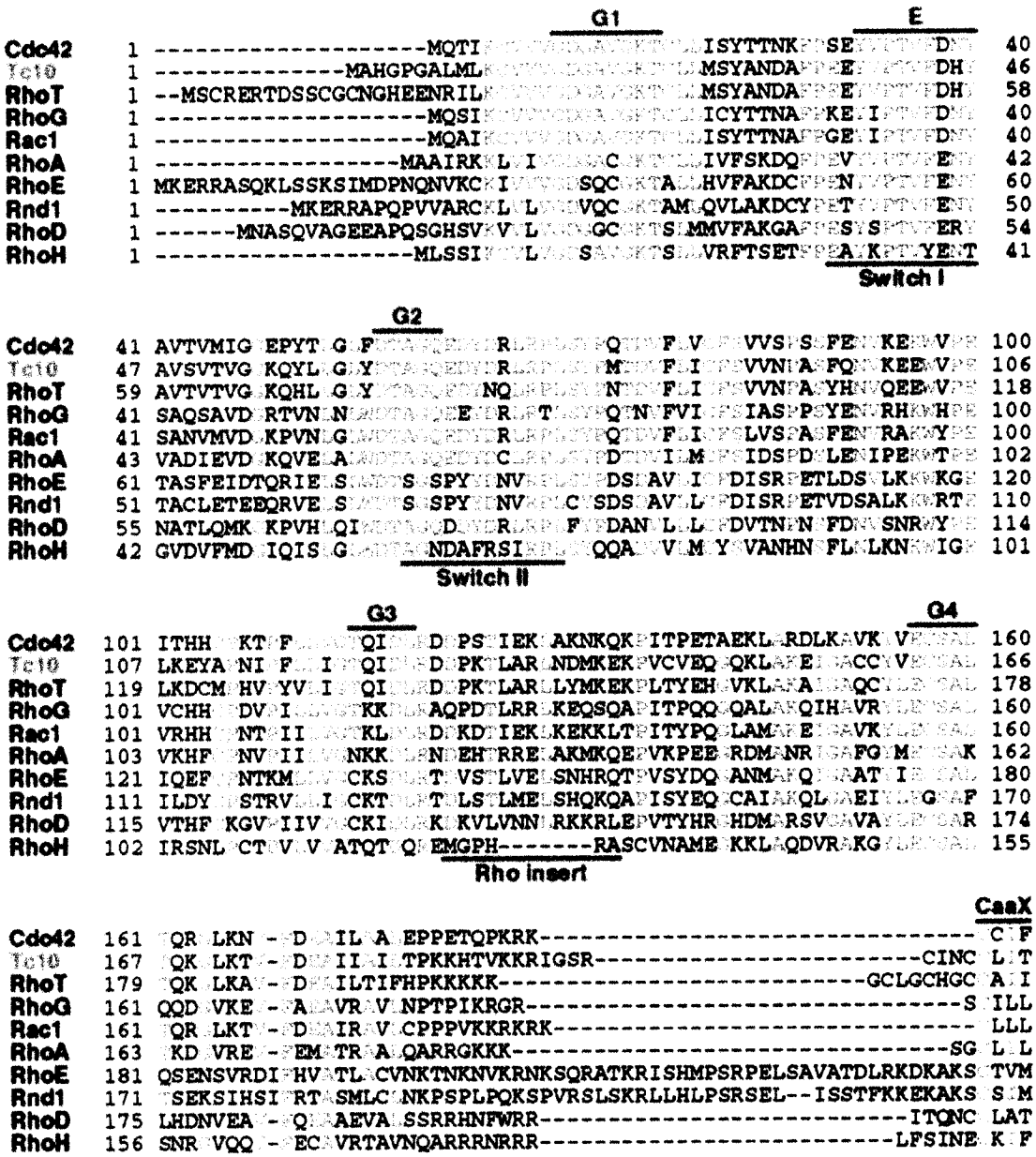

Adapted from Abe et al., 2003.

1.3.2 Cellular and tissue localization

It is important to consider that, while maintaining key structural similarities, Rho GTPases appear to have unique physiological roles, which is now thought to be largely dependent upon cell-context and precise cellular localization (Heo and Meyer, 2003). While TC10 is most closely related to Cdc42 and the recently discovered RhoT (also known as TCL), it is interesting to note that all three Rho GTPases have different tissue expression profiles (Neudauer et al., 1998; Abe et al., 2003).

Preliminary northern blot analyses revealed high TC10 expression in cardiac and skeletal muscle, whereas its closest relative, Cdc42 had a lower, more ubiquitous expression level (Neudauer et al., 1998). More recently, TC10 was found to be highly expressed in cardiac, skeletal and smooth muscle. It was remarkably upregulated forty-eight hours after the induction of differentiation in C2C12 skeletal muscle cells, and expression remained high in terminally differentiated myotubes (Abe et al., 2003). Low TC10 expression was also detected in the embryonic brain, which gradually increased with developmental stage and TC10 expression was induced during neuronal differentiation of PC12 and N1E-115 cells (Tanabe et al., 2000; Abe et al., 2003). Again, Cdc42 expression displayed more of a ubiquitous profile in all tissues examined and during differentiation of C2C12 skeletal muscle cells. Cdc42 was downregulated during neuronal rat pheochromocytoma PC12 cell and N1E-115 neuroblastoma cell differentiation. In contrast, RhoT expression was predominantly seen in the smooth muscle of the uterus and in the heart, with very low expression detected in skeletal muscle and brain, and displayed a constant, low level of expression during C2C12 muscle

cell differentiation and was undetected in the PC12 and N1E-115 neuronal cells examined (Abe et al., 2003).

TC10 subcellular localization studies have provided evidence that wild type and various mutant forms of TC10 are distributed in both the cell membrane and intracellular membranes to varying extents (Murphy et al., 2001). Wild type TC10 resides primarily in the cell membrane, whereas constitutively active, GTPase defective TC10 is found in the plasma membrane and the perinuclear region, GTP-binding defective TC10 is found primarily in a cytoplasmic perinuclear distribution pattern, and the carboxyl terminal deletion mutant of TC10 resides predominantly in the nucleus (Murphy et al., 1999; Murphy et al., 2001). These studies revealed that TC10 localization within the cell is a dynamic process, dependent upon GTP hydrolysis, GTP binding and the C-terminal CXXCCAAX motif. It was also noted that wild type TC10 co-localized with cortical filamentous actin, which is required for TC10 plasma membrane localization, as evidenced by disruption of this cytoskeletal component by the marine sponge toxin Latrunculin B (Murphy et al., 2001). Furthermore, TC10 has been shown to localize specifically to lipid raft microdomains, which are specialized structures within the plasma membrane with a distinct lipid and protein composition (Watson et al., 2001; Kanzaki and Pessin, 2002; Watson et al., 2003). The major structural component of these specialized sub-domains is caveolin, which forms characteristic invaginations of the cellular periphery called caveolae (Galbiati et al., 2001; Watson et al., 2001). Caveolae have recently emerged as important sites of dynamic events at the plasma membrane, including vesicular trafficking and signal transduction (Zhao et al., 2002). As

endogenous TC10 co-localizes with caveolin, it is probable that this Rho GTPase plays an important tissue-specific role in signal transduction and vesicular trafficking in heart and skeletal muscle cells (Watson et al., 2001).

1.3.3 Regulation of enzymatic activity in the Rho GTPase family

Similar to *ras*-related proteins, Rho GTPases assume either an active GTP-bound or an inactive GDP-bound state, acting as switches to control many cellular events in eukaryotic cells (Vignal et al., 2000). Presently, three different classes of Rho GTPase regulatory proteins have been identified. These include: (1) guanine nucleotide exchange factors (GEFs), (2) GTPase-activating proteins (GAPs) and (3) Rho guanine nucleotide dissociation inhibitors (Rho GDIs). These regulatory proteins control the activity of Rho GTPases by allowing them to cycle between GDP- and GTP-bound states (Bar-Sagi and Hall, 2000; Ridley, 2000).

Rho GTPases are positively regulated by GEFs, as they facilitate the exchange of GDP for GTP, activating the Rho GTPase, which then permits an interaction with specific effector proteins (Bishop and Hall, 2000; Kjøller and Hall, 1999). To date, over sixty GEFs have been identified. All Rho GEFs contain a Dbl homology domain (DH) and a neighbouring pleckstrin homology (PH) domain. The DH domain catalyzes the exchange reaction, while the PH domain serves to target the molecules to specific cellular targets (Ren et al., 1998; Zhou et al., 1998; Michaelson et al., 2001). GAPs and Rho GDIs represent the two known classes of Rho GTPase inhibitors and number over seventy in mammals. GAPs increase the intrinsic rate of GTPase hydrolysis to accelerate the return

of the proteins to the inactive conformation (Moon and Zheng, 2003; Fidyk and Cerione, 2002), whereas Rho GDIs sequester GDP-bound Rho GTPases and have the ability to solubilize membrane-associated Rho GTPases (Hoffman et al., 2000; Michaelson et al., 2001).

The regulation of TC10 is speculated to be an important difference between TC10 and Cdc42 (Neudauer et al., 1998). Although the GTP off-rates for both GTPases are similar, the intrinsic GTPase activity of TC10 was determined to be fivefold lower than that of Cdc42 (Neudauer et al., 1998). It has been reported that Dbl, a GEF specific to Cdc42 and Rac1, and Lbc, a RhoA specific GEF, do not affect the dissociation rate of GDP from TC10 (Hart et al., 1994; Zheng et al., 1995). To date, C3G is the only reported GEF specific for TC10 (Chiang et al., 2001). TC10 also has a lower affinity for, but a greater responsiveness to, the p50 RhoGAP than Cdc42 (Neudauer et al., 1998). Similarly, experimental evidence has demonstrated that TC10, in contrast to Cdc42 and Rac1, does not interact with RhoGDIα (Murphy et al., 2001). Taken together, these results suggest that the regulation of TC10 is divergent from that of other Rho proteins.

1.3.4 Activation of TC10

Probable activators of TC10 and extracellular stimuli responsible for TC10 activation remain largely unknown (Murphy et al., 2001). Although GEF proteins represent likely regulatory factors, confirmation of GEFs within this context remains unrealized (Vignal et al., 2000). Recently, it has been observed that insulin serves as an indirect upstream activator of TC10, via the C3G GEF (Chiang et al., 2001; Watson et al., 2001). This has

led to the characterization of a novel insulin signalling pathway involving TC10 that is independent of the well-characterized phosphatidylinositol-3-OH kinase (PI3K) pathway (see Section 1.4) (Khan and Pessin, 2002; Chang et al., 2002).

1.3.5 Downstream effectors

The multiplicity of functions that are controlled by Rho GTPases requires that these proteins interact with a diverse array of target effector proteins. However, prior to attaining a comprehensive understanding of the functions of Rho GTPases, the identification of all of their effector proteins may be required (Joberty et al., 1999).

Experimental observations have demonstrated that TC10, Cdc42 and Rac1 interact with an overlapping set of effectors (Neudauer et al., 1998; Neudauer et al., 2001). However distinct morphologies induced by gain-of-function TC10 and Cdc42 mutants suggest that the complete set of effectors may be somewhat divergent (Neudauer et al., 1998). Using activated TC10 fused to the GAL4 DNA-binding domain as bait in a saturating yeast two-hybrid screen of a total mouse embryo library, nine common effectors for TC10 and Cdc42 were characterized: IQGAP1, α-, β- and γPAK (p21-activated kinase), MRCKα/β (myotonic dystrophy kinase-related Cdc42-binding kinase α/β), MLK2 (mixed-lineage kinase 2), N-WASP (neural-Wiskott-Aldrich syndrome protein) and MSE55 (murine stromal and epithelial protein of 55kDa), later renamed Borg5 (binder of Rho GTPase 5) (Neudauer et al., 1998; Joberty et al., 1999; Osada et al., 2000; Abe et al., 2003). Eight of these nine effectors contain a CRIB (Cdc42/Rac interactive binding) domain, which contains a sixteen-residue sequence with eight core amino acids and is necessary and

sufficient for GTP-bound Rho GTPases to associate with their effectors (Joberty et al., 1999; Burbelo et al, 1995; Neudauer et al., 1998). However, unlike Cdc42, TC10 did not interact with MLK3 (mixed-lineage kinase 3) or WASP (Wiskott-Aldrich syndrome protein), despite high sequence similarity in the CRIB domains of these proteins or related proteins such as, MLK2 and N-WASP (Neudauer et al., 1998). TC10 interacted weakly with ACK1 (activated Cdc42-binding kinase 1) and did not interact with Borg3 (Joberty et al., 1999; Neudauer et al., 1998). Presently, TC10 has been shown to interact with at least two distinct effectors, PIST (PDZ domain protein interacting specifically with TC10) (Neudauer et al., 2001) and Exo70, a component of the exocyst complex, implicated in the tethering or docking of secretory vesicles (Inoue et al., 2003). When co-expressed *in vitro*, GTP-bound, active TC10 and Cdc42 were both able to stimulate α-p21-activated kinase (PAK) activity and JNK kinase activity (Neudauer et al., 1998).

1.4 TC10's role in insulin-stimulated GLUT-4 translocation

Insulin-stimulated glucose uptake in adipose and striated muscle cells is accomplished by GLUT-4 translocation from intracellular storage sites to the cell surface membrane (Khan and Pessin, 2002; Chiang et al., 2001; Chang et al., 2002; Kanzaki and Pessin, 2002). Signalling events regulating this highly complex and dynamic trafficking process are initiated by the receptor-catalyzed tyrosine phosphorylation of intracellular substrates (Chang et al., 2002; Kanzaki and Pessin, 2002). The classic signalling pathway regulating insulin-stimulated glucose uptake is dependent upon phosphatidylinositol 3-kinase (PI3K), whereas the more recently discovered signalling pathway required for this

essential biological process is independent of PI3K, involving TC10 and other novel signalling intermediates (Chiang et al., 2002; Chang et al., 2002).

1.4.1 A TC10-dependent insulin signalling pathway

Compelling data acquired over the last several years has indicated that the PI3K-dependent pathway is necessary, but not sufficient for insulin-stimulated glucose transport. Firstly, growth factors other than insulin, such as Platelet-Derived Growth Factor (PDGF), can stimulate PI3K activity but cannot cause GLUT-4 translocation or glucose uptake. In addition, experimental evidence in 3T3L1 adipocytes using an acetoxy-methyl (AM) derivative of $PI(3,4,5)P_3$/AM, a membrane permeable, biologically active, product of the PI3K pathway, did not affect basal glucose uptake. Furthermore, inhibition of the PI3K pathway with wortmannin, followed by the addition of insulin and $PI(3,4,5)P_3$/AM almost completely restored glucose uptake, suggesting the presence of an additional, insulin-stimulated pathway, independent of PI3K and uninhibited by the known PI3K inhibitor (Khan and Pessin, 2002).

Recent reports illustrate a second requisite pathway necessary for insulin-stimulated glucose transport involving the activation of TC10. This pathway is dependent on insulin receptor signalling that originates from the caveolae of lipid raft microdomains and other signalling intermediates (Khan and Pessin, 2002; Chiang et al., 2002; Chang et al., 2002). Cbl is recruited to the insulin receptor by APS (adapter containing pleckstrin and Scr homology domains) along with CAP (a Cbl-associated protein). The carboxyl-terminal SH3 domain of CAP associates with the proline-rich domain of Cbl, allowing its amino-

terminal SH domain to interact with the lipid raft protein flotillin, stabilizing the complex in the lipid raft microdomain (Chang et al., 2002; Chiang et al., 2001; Chiang et al., 2002). Phosphorylated Cbl in the lipid raft microdomains then recruits the CrkII/C3G complex. C3G acts as a GEF for TC10, activating this small Rho GTPase, by exchanging GDP for GTP. Activated TC10 then stimulates GLUT-4 translocation, accomplished by modifying cortical actin and stimulating actin polymerization on GLUT-4 compartments (Khan and Pessin, 2002; Saltiel and Pessin, 2002; Gual et al., 2002). A yeast two-hybrid screen revealed CIP4/2 (Cdc42-interacting protein 4/2) as a potentially important downstream effector of TC10 in this signalling pathway, as it is recruited to the plasma membrane in response to insulin and plays a critical part in the regulation of insulin-stimulated glucose transport (Chang et al., 2002). Similarly, TC10 was shown to interact with the exocyst complex, Exo70, which may play an important role in targeting the GLUT-4 vesicle to the cellular membrane, perhaps directing proper fusion of the vesicle (Inoue et al., 2003). Recently, the compartmentalization of TC10 within lipid raft microdomains was shown to be essential for insulin-dependent activation of TC10 and GLUT-4 translocation (Watson et al., 2001). Specifically, expression of chimeric TC10 proteins containing the COOH-terminal domains of H-Ras (which targets the protein to the lipid raft microdomains), disrupted GLUT-4 translocation; whereas, a TC10/K-Ras chimera, directed to the non-lipid raft microdomains was unaffected by insulin and did not affect GLUT-4 translocation events (Watson et al., 2001). Furthermore, these data offered evidence supporting the importance of precise cellular localization of TC10 in signalling cascades and provided a molecular basis for the specificity of insulin signalling with respect to glucose transport (Watson et al., 2001).

1.5 TC10's involvement in the regulation of cytoskeletal dynamics

The actin cytoskeleton is an essential component in determining cell shape and morphology. Actin-containing lamellipodial and filopodial extensions from the cellular membrane are thought to depend on the activation of small Rho GTPases (Vidal et al., 2002). Thus, Rho GTPases are presently seen as central regulators of the actin cytoskeleton and associated cytoarchitectures responsible for cell morphology, motility, migration, adhesion and cytokinesis in a variety of cell types (Abe et al., 2003). Recent experimental evidence has also implicated TC10 in the regulation of cytoskeletal dynamics. In fibroblasts, constitutively active TC10Q75L induced the formation of actin-containing filopodial extensions concomitant with a reduction in actin stress fibers. However, wild type TC10 had a minimal effect on fibroblast cell morphology, suggesting that the downstream effectors necessary for actin remodeling may not be present in this cell type (Murphy et al., 1999; Kanzaki et al., 2002). In adipocytes, it was recently reported that TC10 differentially regulates two separate types of filamentous actin, dependent on its proper subcellular localization and the distinct functional domains of TC10 (Kanzaki et al., 2002). Specifically, expression of TC10Q75L fully disrupted cortical actin, whereas massive polymerization of the perinuclear actin was observed. Additionally, expression of an amino-terminal deletion mutant of TC10Q75L had no significant effect on cortical actin but this mutant still had the capability of inducing perinuclear actin polymerization (Kanzaki et al., 2002). Although many effector proteins connecting Rho GTPases to actin cytoskeleton reorganization have been identified, the precise signalling networks in a physiological context are still being explored. The diaphanous family of proteins has been physically linked to Rho GTPase control of the

actin filament system. The IQGAPs have been suggested to be scaffolding proteins mediating Rho GTPase-actin interactions, and the PAK family has also been implicated in coordinating the dynamics of actin and microtubule cytoskeletons following GTPase activation (Krebs et al., 2001; Olson, 2003; Bokoch, 2003; Johnson, 1999). TC10 has been shown to interact with IQGAP1 and the PAKs (α/β/γ), and has also been shown to interact with profilin, an actin-binding protein proposed to aid in the conversion of globular to filamentous actin and N-WASP, which was recently shown to induce Arp2/3-complex-mediated actin polymerization following activated TC10 binding (Neudauer et al., 1998; Murphy et al., 1999; Abe et al., 2003). From the discussion above, it is clear that a comprehensive understanding of Rho GTPase-mediated actin cytoskeleton reorganization will require the determination of Rho GTPase signalling pathways and effectors.

From what is known regarding the physiological relevance of Rho GTPases, possible functions appear to be as diverse as the tissues in which they reside. However, functional redundancy and extensive cross-talk may be a common feature in this protein family. Murphy et al. (2001) reported that signalling mediated by TC10 and Cdc42 appeared to be functionally distinct based on differences in cellular localizations, the ability to rescue certain mutations and in their response to RhoGDIα. In a recent study by Heo and Meyer (2003), a combined algorithm and genome-based experimental strategy was used to classify the functions of Rho family proteins and to understand the structural specificity for each of the functional classes and the basis for markedly different roles in a given cellular context. The roles of the majority of human Rho GTPases were classified in a

cellular morphology context and it was determined that almost half of the expressed small GTPase constructs induced marked morphological changes that could be assigned to nine distinct classes: filopodia, lamellipodia, stress fibers, cell rounding, cell shrinking, local spreading, multiple morphologies, polar or eyelash phenotypes. By creating switch-of-function mutants, Heo and Meyer (2003) identified the residues that define four of the nine induced morphologies and unexpectedly determined that the identified residues were mostly outside the known effector regions and were also distantly spaced. This experimental approach may be useful in the identification of function-specific binding partners, in the investigation of signalling cross-talk and in the testing of the physiological relevance of particular cell functions (Heo and Meyer, 2003). It is likely that the complexity of Rho GTPase signalling pathways will be resolved as tissue and cellular-dependent functions are identified.

1.6 TC10 and post-natal growth of the murine heart

In the quest to decipher the precise role for individual Rho GTPases, spatial and temporal expression gains tremendous importance. For example, given that TC10 expression is elevated in the adult myocardium and that this protein is involved in cytoskeletal remodeling, the possibility of a cardiac-specific role for this Rho GTPase becomes apparent.

1.6.1 Post-natal growth of the heart

Post-natal growth of the heart is mediated principally by cardiomyocyte hypertrophy. Hypertrophic growth is characterized by cell enlargement in the absence of cell division,

actin cytoskeleton remodeling leading to the formation of distinct sarcomeric structures, upregulation of fetal and contractile protein genes such as atrial natriuretic factor (ANF) and β-myosin heavy chain (β-MHC) and induction of immediate early genes, such as c-fos and c-myc (Pracyk et al., 1998; Sah et al., 1999). Cardiomyocyte hypertrophy also contributes to the pathology of the majority of post-natal heart disease (reviewed in Megeney et al., 1999). While this mechanism is initially compensatory in nature, sustained cardiac hypertrophy is associated with fibrotic disease, arrhythmia, decompensation, dilated cardiomyopathy and heart failure (Molkentin et al., 1998; Bueno et al., 2000). Key conduits have been identified in the regulation of cardiomyocyte hypertrophy, including calcineurin-dependent and mitogen-activated protein kinase (MAPK) signalling pathways (Molkentin et al., 1998; Molkentin, 2000). However, the fundamental molecular mechanisms regulating normal and pathologic cardiomyocyte hypertrophy remain elusive (Megeney et al., 1999). Several important factors involved in hypertrophic growth have been identified including calcineurin activation of NFAT (nuclear factor of activated T-cells) transcription factors and p38 activation of the MEF2 (myocyte enhancer factor 2) family of transcription factors (Molkentin et al., 1998; Kolodziejczyk et al., 1999). In addition, Rho GTPases have been implicated in hypertrophic growth responses and myofibrillar organization in cardiomyocytes (Molkentin and Dorn II, 2001; Hoshijima et al., 1998; Ichida and Finkel, 2001; Aikawa et al., 1999). Clearly, the elucidation of the underlying molecular mechanisms controlling hypertrophic growth of the heart is essential to the understanding of cardiovascular biology and will be critical in developing new prevention and treatment strategies for

cardiac hypertrophy and heart failure (Molkentin et al., 1998, Molkentin and Dorn II, 2001).

1.6.2 Rho GTPases in cardiac development and hypertrophy

In cell types other than cardiomyocytes, the Ras subfamily regulates cell growth while the Rho family regulates cell morphology. Consequently, the involvement of small GTP-binding proteins in hypertrophic growth of heart cells became a focus of many investigations (Clerk and Sugden, 2000). Numerous *in vitro* and *in vivo* experiments have recently implicated a Ras-dependent signalling pathway in the regulation of cardiac hypertrophy (Molkentin and Dorn II, 2001). In rat neonatal ventricular cardiomyocytes, transfection or infection with activated Ras, RhoA, or Rac1 resulted in characteristics consistent with cardiac hypertrophy (Pracyk et al., 1998; Clerk and Sugden, 2000). Cardiac-specific over-expression of activated Ras in transgenic mice led to the development of features consistent with ventricular hypertrophy, including increased heart weight to body mass ratios, cardiomyocyte cross-sectional area and ANF expression (Thorburn et al., 1993; Hunter et al., 1995; Molkentin and Dorn II, 2001). Whereas over-expression of RhoA caused atrial enlargement, ventricular dilatation and conduction dysfunction, resulting in lethal heart failure (Sah et al., 1999). Collectively, these over-expression studies indicate that Ras and Rac participate in hypertrophic cardiac growth, while RhoA may only play a limited role in this mechanism (Molkentin and Dorn II, 2001).

More recently, the role of Rho GTPases in murine cardiac development was explored using a reverse genetic approach, i.e. over-expressing Rho GDIα in a cardiac-specific manner. Rho GDIα specifically inhibits RhoA, Rac1 and Cdc42 Rho family proteins. Over-expression of Rho GDIα resulted in a disruption of cardiac morphogenesis, with incomplete looping, lack of chamber demarcation, hypocellularity and lack of trabeculation (Wei et al., 2002). This study unequivocally revealed the importance of these three Rho family GTPases in cardiac morphogenesis.

1.6.3 Mitogen-activated protein kinase cascades and cardiac hypertrophy

Rho GTPases are widely accepted as key regulators of the actin cytoskeleton leading to cellular remodeling and growth in many cell types, conceivably exerting their effects through several different families of signalling intermediates, including the MAPKs. Mitogen-activated protein kinases, important enzymes involved in the conversion of extracellular stimuli to intracellular signals, are implicated in the control of gene expression crucial for diverse cellular events, such as cell growth, survival and adaptation (Davis, 2000; Chang and Karin, 2001; Coso et al., 1995; Minden et al., 1995). In mammalian cells, at least four known MAPK cascades exist, including c-Jun NH_2-terminal kinases (JNK1/2/3), the p38 kinase family (p38α/β/δ/γ), extracellular signal-regulated kinases (ERK1/2) and ERK5 (Chang et al., 2001; Coso et al., 1995). Experimental evidence has shown that ERKs mediate growth factor-initiated cellular responses, while JNK and p38 primarily mediate cellular responses caused by environmental stress or proinflammatory cytokines, although some degree of cross-talk exists in these signalling cascades (Aoki et al., 2000). Based on the observations that

TC10 stimulates JNK kinase activity, is involved in aspects of cell growth through remodeling of the actin cytoskeleton and is highly expressed in the adult myocardium (Neudauer et al., 1998; Murphy et al., 1999), the following discussion will be limited to examining the role of JNK kinases during cardiac adaptation.

Evidence supporting the role of JNK1 and 2 as critical regulators of cardiomyocyte adaptation has emerged in recent years (Molkentin and Dorn II, 2001). Activated MEKK1 or MKK4, both upstream activators of JNK, induced promoter expression of select hypertrophy-associated genes following transfection experiments. Likewise, transfection of a dominant-negative MEKK1-encoding expression vector attenuated ANF promoter activity (Molkentin and Dorn II, 2001; Ramirez et al., 1997; Thorburn et al., 1997; Bogoyevitch et al., 1996). Similarly, a dominant-negative MKK4 adenovirus significantly alleviated agonist-induced cardiac hypertrophy in ventricular cardiomyocytes. Moreover, dominant-negative MKK4 adenoviral delivery in aortic-banded rat hearts led to a decrease in hypertrophic growth following pressure overload (Choukroun et al., 1999). Conversely, MEKK1 transfection was reported to attenuate phenylephrine-induced sarcomeric reorganization, indicative of an antihypertrophic role in the JNK signalling pathway (Thorburn et al., 1997; Bueno et al., 2000; Molkentin and Dorn II, 2001). Furthermore, MEKK1 and JNK activation have been shown to inhibit ANF expression in neonatal cardiomyocytes in primary culture (Nemoto et al., 1998). However, whether JNK activity is primarily a prohypertrophic or a prodilatation factor has not been resolved.

1.6.4 TC10 and cardiac adaptation: A pathway mediated through JNK activation?

Although the precise physiological roles of Rho GTPases have not been fully elucidated, based on the high-cardiac expression of TC10 and the fact that this Rho GTPase is involved in aspects of cytoskeletal remodeling and JNK activation, it seems reasonable to speculate that TC10 may be an important mediator of cardiac hypertrophy and/or dilation. To date, experimental evidence exploring the effects of TC10 on actin cytoskeletal rearrangement, cellular growth and JNK activation in cardiomyocytes is lacking. However, based on TC10's ability to potently affect actin remodeling and JNK activation in other, less relevant cell types and on the experimental links made between JNK and cardiac adaptation, it seems reasonable to speculate that TC10 may play an important role in cardiac adaptation, possibly mediated through JNK activation.

1.7 Experimental rationale

Among the many reports pertaining to Rho GTPases and their biological relevance, few have addressed the notion of tissue/cell context specificity. Indeed, although the role of TC10 has been explored *in vitro*, the physiological relevance and significance of this Rho GTPase remains unknown. To explore the cardiac-specific functions of TC10, I generated transgenic mice over-expressing activated TC10 (TC10Q75L) in the post-natal myocardium. A glutamine to leucine amino acid substitution at position 75, forces the mutated protein to remain bound to GTP, thus in the active state, and to be GTPase-defective, thus unable to be inactivated by GAPs. This transgenic tool allowed us to examine the actions of TC10 in an *in vivo* context, in an attempt to decipher the cellular role of TC10 in cardiac tissue.

1.8 Hypotheses and objectives

Based on the high expression level of TC10 in the heart, my prevailing hypothesis is that TC10 has a cardiac-specific function. Within this context, I further hypothesize that:

1) Over-expression of activated TC10 *in vivo* and *in vitro* will lead to actin cytoskeleton reorganization in heart and skeletal muscle cells, causing perturbations of their plasma membrane, thus compromising overall muscle cell integrity.

2) Excessive activation of TC10 *in vivo* will activate a cardiac hypertrophy and/or dilatation program, possibly mediated through c-Jun NH_2-terminal kinase 1 (JNK1). This would prove to be detrimental to cardiac muscle cells over an extended period of time.

To investigate the role of TC10 in cardiac muscle, the phenotypic consequences of over-expressing TC10Q75L in the post-natal heart will be characterized in a gain-of-function transgenic mouse line. In addition, the *in vitro* consequences of TC10Q75L over-expression will be studied following transient transfections in C2C12 mouse myoblast and H9C2 rat cardiomyocyte cell lines. The primary objectives of this project are:

1) To establish a TC10 gain-of-function transgenic mouse line and to characterize any phenotypic consequences caused by the over-expression of constitutively active TC10 (TC10Q75L) *in vivo*.

2) To generate a reliable polyclonal TC10 antibody.

3) Ultimately, to establish any tissue-specific role(s) of TC10 in cardiac and skeletal muscle.

CHAPTER 2

2.0 Materials and Methods

2.1 Generation of the TC10 constructs

Full-length human wild type TC10 (TC10wt) and constitutively active TC10 (TC10Q75L) constructs were kindly provided by Dr. Ian Macara (University of Virginia, Charlottesville, VA, USA) in pKH3 expression vectors containing an amino-terminal triple-hemagglutinin (HA) tag. The full-length, constitutively active TC10Q75L cDNA (642 bp; see Appendix A for sequence details) was digested out of the pKH3 expression vector using *BamHI* and *EcoRI* and gel-purified using the Ultraclean DNA purification kit, according to the company's directions (Mo Bio Laboratories, Inc., Carlsbad, CA, USA). To generate a mammalian expression vector, TC10Q75L cDNA was directionally subcloned in-frame into the *SalI* multi-cloning site of the pBluescript II SK+ expression vector. The insert was ligated between the 5.5 kb murine alpha-myosin heavy chain (α-MHC) promoter, to promote post-natal, cardiac-specific expression of the transgene, and the 600 bp human growth hormone (Hgh) polyadenlyation (polyA) sequences.

To produce and purify a recombinant HIS-tagged TC10 fusion protein, the TC10wt cDNA was digested from the pKH3 vector using the *BamHI* and *EcoRI* restriction enzymes and was subcloned into the pRSET A expression vector (Invitrogen Life Technologies, Carlsbad, CA, USA).

The sequence of each DNA construct was confirmed by appropriate diagnostic restriction enzyme digests and sequence analyses (Cortec DNA Service Laboratories, Inc., Kingston, ON, Canada).

2.2 Generation of TC10Q75L transgenic mice

The α-MHC-TC10Q75L-Hgh sequence was digested from the pBluescript II SK+ expression vector using *BamHI*. The DNA fragment was subjected to TAE-agarose gel electrophoresis and the 6.68 kb construct was excised and gel purified using the Ultraclean DNA purification kit, according to the manufacturer's instructions (Mo Bio Laboratories, Inc., Carlsbad, CA, USA). The purified transgene fragment was diluted in oocyte injection buffer (2 ng/μl) and was microinjected into the pronuclei of mouse oocytes, which were implanted into the oviducts of five pseudopregnant foster mothers (B6C3F1, Charles River, Canada) (DiDonato et al., 2001; Hogan et al., 1994; Hogan and Tilly, 1977). The resulting pups were screened for the presence of the transgene by polymerase chain reaction (PCR) and the genotyping results were confirmed by Southern blot analysis (described in Sections 2.3 and 2.4; refer to Appendix B for TC10Q75L colony information).

2.3 Genomic DNA extraction and polymerase chain reaction

Tail DNA was extracted using a phenol:chloroform extraction method. Briefly, tail samples were digested in genomic DNA buffer (100 mM NaCl, 10 mM Tris-HCl, pH 8.0, 25 mM EDTA, pH 8.0, 0.5% SDS), containing 0.3 mg/mL proteinase K overnight at 55°C. Genomic DNA was precipitated with isopropanol and resuspended in 1XTE buffer (10 mM Tris-HCl, pH 8.0, 1 mM EDTA, pH 8.0). Pups were screened for the presence of the TC10Q75L transgene by PCR, using two custom primers designed to amplify a region of the transgene adjacent to the Hgh tail (~500 bp PCR product):

TC10 forward 5'-TAATAGGAACTCAGATTGATCT-3' and

Hgh reverse 5'-ACTCCAGCTTGGTTCCCGAATAGA-3'. PCR reactions were performed as follows: 94°C for 1 minute, 50°C for 1 min, 72°C for 3 minutes per cycle for 30 cycles, with a 2 minute 94°C pre-dwell and a 10 minute 72°C post-dwell.

Glyceraldehyde-3-phosphate dehydrogenase (GAPDH) was used as a loading control. The GAPDH primers were GAPDH forward 5' –TGACTCCACTCACGCCAAATTCAA –3' and GAPDH reverse 5'-TGCCTGCTTCACCACCTTCTTGAT-3'. PCR was performed as follows: 94°C for 1 minute, 52°C for 1 min, 72°C for 3 minutes per cycle for 20 cycles, with a 2 minute 94°C pre-dwell and a 10 minute 72°C post-dwell. PCR products were separated on a 1.2% agarose gel, sized with a 1-kb DNA ladder and visualized by ethidium bromide staining.

2.4 Genomic DNA digestion and Southern blot analysis

Ten micrograms of genomic DNA from each sample was digested overnight at 37°C using the *EcoRI* restriction enzyme. DNA fragments were then separated on a 0.7% TAE-agarose gel and transferred to a Hybond-N+ nylon membrane, according to the manufacturer's instructions (Amersham Pharmacia Biotech Inc., Piscataway, NJ, USA). Specific cDNA probes were generated against the Hgh region, the polyadenylation sequence found in the transgenic mice, and against Trap 3.1, an exon in close proximity to the dystonin gene locus (from Dr. Rashmi Kothary, OHRI, Ottawa, ON, Canada). The Hgh probe was used to confirm the PCR genotyping results and to identify the transgene copy number in TC10Q75L transgenic mice. The Trap 3.1 probe was used as a DNA loading control in these experiments. Probes were radiolabeled using the Rediprime II

random prime labeling system, according to the manufacturer's instructions (Amersham Pharmacia Biotech Inc., Piscataway, NJ, USA). Label incorporation was verified using a Beckman LS6500 Multi-Purpose Scintillation Counter. Labeled probes were then hybridized to the membranes overnight at 65°C in Church buffer (0.5 M sodium phosphate, pH 7.2, 7% sodium dodecyl sulfate (SDS), 1 mM EDTA). Membranes were washed accordingly and exposed to X-ray film at –80°C for varying exposure times, between 3 hours and 10 days.

2.5 RNA extraction, RT-PCR and Northern blot analysis

Total RNA was collected from various mouse tissues including heart, hind limb skeletal muscle, brain, lung, spleen, liver, kidney using the Trizol reagent, following the manufacturer's instructions (Invitrogen Life Technologies, Carlsbad, CA, USA). Total RNA was subjected to reverse transcriptase-polymerase chain reaction (RT-PCR) and northern blot analysis to confirm the presence of the transgene and to compare and quantify the expression pattern between TC10Q75L transgenic mouse lines.

Five micrograms of RNA from each tissue was reverse transcribed into its complementary DNA (cDNA) using Superscript II Reverse Transcriptase, according to the company's instructions (Invitrogen Life Technologies, Carlsbad, CA, USA). RT-PCR was used to confirm cardiac-specific expression of the transgene (as described above). Parallel RT-PCR was performed using the GAPDH template to verify the presence of cDNA in each reaction tube (as outlined above).

Fifteen micrograms of total RNA was separated on a 1.0% agarose-formaldehyde gel and transferred to a Hybond-N+ nylon membrane, following the company's instructions (Amersham Pharmacia Biotech Inc., Piscataway, NJ, USA). The RNA was cross-linked to the membrane with UV exposure and membranes were then prehybridized for 2 hours in 10 ml of Church buffer at 65°C. The membranes were hybridized overnight at 65°C with denatured [α-^{32}P]dCTP-labeled probes. The cDNA probes used were the human TC10Q75L sequence, a portion of the murine atrial natriuretic factor (ANF) sequence (amplified using the following primers: ANF forward 5'-AGACCACCTGGAGGAGG AGA-3' and ANF reverse 5'-ACTAGGCTGCAACAGCTTCC-3') and the murine GAPDH sequence, as a loading control. Labeled cDNA probes were generated as per manufacturer's instructions using the RediPrime II random prime labeling system (Amersham Pharmacia Biotech Inc., Piscataway, NJ, USA). Label incorporation was verified using a Beckman LS6500 Multi-Purpose Scintillation Counter. The membranes were then washed accordingly and exposed to x-ray film at –80°C for exposure times ranging from one to ten days.

2.6 Expression and purification of HIS-TC10wt fusion proteins

To generate HIS-fusion proteins, TC10wt was subcloned into the *BamHI/EcoRI* sites of pRSET A in-frame with the N-terminal HIS-tag. The nature of the DNA construct was verified by appropriate diagnostic restriction enzyme digests and the final sequence was confirmed by sequence analysis (Cortec DNA Service Laboratories, Inc., Kingston, ON, Canada).

HIS-TC10wt fusion proteins were chemically induced in bacterial cultures with 1 mM isopropyl β-D-thiogalactoside (IPTG) for 3 hours at 30°C in *E. coli* BL21DE3 pLysS cells (Novagen, Madison, WI, USA). Purification of HIS-fusion proteins was completed using the ProBond purification system, under denaturing conditions, according to the accompanying instructions (Invitrogen Life Technologies, Carlsbad, CA, USA). To eliminate contaminating urea from the sample, the recombinant fusion protein was dialyzed against 50 mM Tris-HCl (pH 8.0) with 0.1% Tween-20 overnight at 4°C. Protein concentrations were estimated by electrophoresing 10 µl of HIS-TC10wt fusion protein resuspended in water on a 12% polyacrylamide gel against known bovine serum albumin (BSA) standards. Protein expression was verified using 12% sodium dodecyl sulfate-polyacrylamide gel electrophoresis (SDS-PAGE), followed by Coomassie blue staining and western blotting techniques (see Section 2.8).

2.7 TC10wt polyclonal antibody production

Approximately 700 µg of recombinant HIS-TC10wt fusion protein was resolved using SDS-PAGE and the subsequent approximately 27 kDa fusion protein was excised from the gel and stored at –80°C. To produce a sheep polyclonal antibody against full-length human TC10, a standard 120-day immunization program was completed in a single sheep following injection of the TC10 fusion protein (Affinity Biologicals, Ancaster, ON, Canada). Whole immunoglobulin G (IgG) was fractionated from the resulting antiserum using a combination of octanoic acid precipitation and ammonium sulphate precipitations steps. The resulting sheep IgG concentration was 105.5 mg/ml in 0.01 M HEPES, 0.05 M NaCl, pH7.4, containing 50% glycerol.

2.8 Isolation of protein lysates and Western blot analysis

Freshly excised whole hearts from wild type and transgenic mice were rinsed twice in cold phosphate-buffered saline (PBS) containing the following phosphatase inhibitors: 100 mM sodium fluoride (NaF) and 1 mM sodium orthovanadate (Na_3VO_4). Tissues were then weighed and immediately flash frozen in liquid nitrogen. Frozen tissues were powdered and homogenized in ice-cold PLCγ lysis buffer (0.05 M HEPES, pH 7.5, 0.15 M NaCl, 10% glycerol, 1% Triton X-100, 1 mM EGTA, 1.5 mM $MgCl_2$, 0.02 M NaF, 0.01 sodium pyrophosphate) containing appropriate protease inhibitors (10μg/ml each of phenylmethylsulfonyl fluoride (PMSF), aprotinin, leupeptin and pepstatin). Lysates were then cleared by centrifugation and protein concentrations were determined by Bradford analysis, using BSA as a standard. One hundred micrograms of protein from each tissue sample was boiled with Laemmli buffer (0.31 M Tris-HCl, pH 6.8, 0.35 M SDS, 0.025% bromophenol blue, 25% β-mercaptoethanol) and separated by 12% SDS-polyacrylamide gel electrophoresis. Proteins were then transferred to an Immobilon-P membrane (Millipore Corp., Bedford, MA, USA) at 6V for 105 minutes. The efficacy of protein transfer and verification of equal protein loading were confirmed by Ponceau S staining of the membranes. Membranes were blocked at room temperature for one hour in 5% skim milk powder in TBS/0.1% Tween-20 (0.1% TBS-T) and incubated with polyclonal sheep anti-human TC10wt (custom whole IgG) at a dilution of 1:1500 overnight at 4°C. After several 5 minute washes with 0.1% TBS-T, membranes were incubated with horseradish peroxidase-conjugated anti-sheep antibody (Bio-Rad Laboratories, Hercules, CA, USA) at a dilution of 1:7500 in 5% skim milk powder for one hour at room temperature. Enhanced chemiluminescence was then performed using the ECL™

Western Blotting Detection Reagents, according to the manufacturer's directions (Amersham Pharmacia Biotech Inc., Piscataway, NJ, USA).

2.9 Global GTPase activity assay

The intrinsic global GTPase activities of extracted heart protein lysates from wild type and TC10Q75L transgenic littermates were measured as described previously by the nitrocellulose filter-binding method (Li et al., 1997). Briefly, 75 μg of freshly extracted heart protein lysates were preloaded with 10 μCi [γ-^{32}P]GTP (Amersham Pharmacia Biotech Inc., Piscataway, NJ, USA) in 40 μl of incubation buffer (50 mM HEPES, pH 7.6, 100 mM NaCl, 0.2 mg/ml BSA, and 0.5 mM EDTA) for 10 minutes at 20°C prior to the addition of $MgCl_2$ (5 mM). At specific time points (0, 5, 10, and 15 minutes), the reaction was terminated by filtering the entire reaction mixture through nitrocellulose filters, followed by 2X10 ml washes with ice-cold buffer (50 mM HEPES, pH 7.6, 100 mM NaCl, and 10 mM $MgCl_2$). The radioactivity retained on the filters was then subjected to quantification by scintillation in 10 ml of scintillation fluid (Ecoscint; DiaMed Lab Supplies Inc., Mississauga, ON, Canada) using a Beckman LS6500 Multi-Purpose Scintillation Counter.

2.10 JNK1 immunoprecipitation and *in vitro* kinase assay

To examine JNK1 activation in wild type versus transgenic hearts, JNK1 was immunoprecipitated from whole heart protein lysates and was subjected to an *in vitro* kinase assay for JNK1. For JNK1 immunoprecipitations (IPs), 5 μl of a mouse monoclonal JNK1 antibody (PharMingen International, San Diego, CA, USA) was added

to 500 μg of cardiac protein lysates in 750 μl of modified RIPA buffer (50 mM Tris-HCl, pH 7.4, 1% NP-40, 150 mM NaCl, 1 mM EDTA, and 1% glycerol), containing 10 mM Na_3VO_4 and 5 mM NaF. Immunoprecipitations proceeded at 4°C for 16 hours, before the addition of 30 μl of protein G sepharose beads (Amersham Biosciences, Corp., Piscataway, NJ, USA) for 2 hours at 4°C. The precipitates were then washed three times for 10 minutes each time with modified RIPA buffer containing 10 mM Na_3VO_4 and 5 mM NaF (800 μl/wash). Following the third wash, 30 μl of assay dilution buffer containing MBP (myelin basic protein, 0.02 mg/sample), as the exogenous substrate and 10 μCi [γ-^{32}P]ATP, was added to the JNK1 immunocomplex for 30-45 minutes at 30°C. The reactions were terminated by the addition of 20 μl of 5X SDS loading buffer and were resolved by 12% polyacrylamide gel electrophoresis. The gel was then stained with Coomassie blue for 30 minutes, destained and dried overnight using a Bio-Rad GelAir Dryer at room temperature. The dried gel was then exposed to film to visually analyze any differences in phosphorylated MBP between wild type and transgenic heart protein lysates.

2.11 Evans Blue Dye injections

Adult wild type and transgenic mice, ranging in age from 9 to 18 months, were injected with 1% Evans Blue Dye (EBD) in PBS (pH 7.5) sterilized by passage through a 0.22 μm filter (Millipore Corp., Bedford, MA, USA). Intraperitoneal EBD injections were made into the left side of the peritoneal cavity. The amount of EBD solution injected into each mouse was calculated according to body weight and was based on a 1% injection volume (i.e. 0.30 ml/30 g mouse). Following injections, mice were returned to their cages and

allowed unlimited food and water. At 24 hours post-injection, hearts were immediately removed, fixed in 4% paraformaldehyde (PFA) overnight and embedded in paraffin for histological analysis (see Section 2.12).

2.12 Histological analysis

Hearts were excised, rinsed in cold 1X PBS and fixed in 4% PFA/PBS for 2-4 days. Hearts were then embedded in paraffin, sectioned at 5 and 10 μm and counterstained with hematoxylin-eosin to allow for visualization of the nuclei and cytoplasm. To analyze EBD penetration into the cardiac tissue, hearts from EBD-injected mice were sectioned at 5 μm. Sections were dehydrated in a graded ethanol series ending in CitriSolv (Fisher Scientific Limited, Nepean, ON, Canada), and coverslipped prior to analysis using a Zeiss Axioscope microscope. Heart sections from wild type and transgenic mice were examined for gross morphological differences and variations in EBD penetration into cardiac cells using bright field and fluorescence microscopy, respectively.

2.13 Primary cardiomyocyte cell culture

Neonatal mouse cardiomyocytes were isolated from the ventricles of three- to seven-day old wild type and TC10Q75L transgenic mice and were maintained in primary culture as previously described (Argentin et al., 1994). In brief, the ventricles from eight to fifteen neonatal pups were isolated and immediately placed in Joklik's modified Eagle's medium (JMEM) on ice prior to enzymatic digestion (Invitrogen Life Technologies, Carlsbad, CA, USA). Upon completion of tissue collection, the ventricles were washed several times in cold JMEM to remove cellular debris and red blood cells. The ventricular tissue

was then subjected to multiple rounds of enzymatic digestions (4X15 minute) with 1% collagenase B (Roche, Nutley, NJ, USA) with gentle agitation at 37°C. Following each digestion, cells contained within the supernatant were transferred to a 50 ml Falcon tube containing 10 ml of cold fetal bovine serum (FBS) to halt further collagenase digestion. Cells were then collected by centrifugation at 200 g for 5 minutes at room temperature and were resuspended in Dulbecco's Modified Eagle Medium media (DMEM; Invitrogen Life Technologies, Carlsbad, CA, USA) supplemented with 10% FBS and 1X penicillin/streptomycin (growth media). Upon completion of enzymatic digestions, the four cell suspensions were pooled, cells were collected by centrifugation and resuspended in growth media. The cell suspension was then filtered using 74 μm inserts (Costar Netwell) to remove any undigested ventricular tissue and debris. Subsequently, the cells were differentially plated on uncoated cell culture dishes for two 20-minute incubations at 37°C to remove contaminating non-myocytes. The resulting cardiomyocytes were then counted and plated on collagen type-a coated glass chamber slides (Becton Dickinson, Bedford, MA, USA) at a density $5.0X10^5$ cells per chamber in growth media. Cardiomyocytes remained in growth media at 37°C for 16-24 hours, at which time the media was replaced with serum-free DMEM Nutrient Mixture F-12 (Invitrogen Life Technologies, Carlsbad, CA, USA) supplemented with 1X insulin/transferrin/selenium (Becton Dickinson, Bedford, MA, USA) and 1X penicillin/streptomycin (100U/ml pen/ 100μg/ml strep). Neonatal mouse ventricular cardiomyocytes were maintained in DMEM/F-12 media at 37°C in a carbon dioxide-enriched (5%), humid environment for three to seven days prior to fixation and immunofluorescence studies (See Section 2.15 for details of cell fixation and immunofluorecence experiments).

2.14 Cell Culture and transient transfections

Murine skeletal muscle myoblasts (C2C12), rat cardiomyocytes (H9C2) and African green monkey kidney cells (COS-1) (American Type Culture Collection, Manassas, VA, USA) were all cultured at 37°C in the presence of 5% CO_2 in DMEM supplemented with 10% FBS and 100U/ml penicillin/100 μg /ml streptomycin (growth media). Transient transfections of 70% confluent cell cultures (2 μg of plasmid per chamber of a 2-chamber glass slide or per well of a 6-well plate, 10 μg of plasmid per 10 cm dish) were performed in serum-free media using a standard calcium phosphate method. Sixteen hours post-transfection, media was removed, cells were washed twice with PBS and were incubated for 36 to 48 hours in fresh growth media. Cells lysates were then collected using PLCγ buffer containing 1 mM sodium orthovanadate and 10 μg/ml of each of the following protease inhibitors: aprotinin, phenylmethysulfonyl, leupeptin, and pepstatin. Cell lysates were used for Western blot analysis (see Section 2.8); alternatively, cells were fixed and subjected to immunofluorescent experiments (see Section 2.15).

2.15 Immunofluorescence

Neonatal mouse ventricular cardiomyocytes and transiently transfected immortalized cell lines (C2C12, H9C2, COS-1) were prepared for immunofluorescence as described above. All cells were washed twice in phosphate-buffered saline (PBS), fixed in 4% paraformaldehyde (in PBS) at room temperature for 10 minutes, washed twice in PBS, and then permeabilized for 10 minutes in 0.3% Triton X-100. Desmin detection was conducted in primary cardiomyocyte cultures blocked with 3% BSA in PBS overnight at 4°C, followed by a 2.5 hour incubation with an anti-desmin mouse monoclonal antibody

(DAKO Corporation, Carpinteria, CA, USA) at a dilution of 1:100. Detection of HA was performed in transiently transfected H9C2 and C2C12 cells incubated with blocking buffer (10% goat serum, 1% BSA, 0.02% NaN_3, 1X PBS) for one hour at room temperature, followed by an overnight incubation at 4°C with an anti-HA mouse monoclonal antibody (Cell Signaling Technologies, Inc., Beverly, MA, USA) at a dilution of 1:200. In both cases, immunofluorescent staining was conducted using a Cy3 conjugated goat anti-mouse secondary antibody (Chemicon International, Temecula, CA, USA) at a dilution of 1:50 for 45 minutes at room temperature in the dark. Filamentous actin (F-actin) was visualized using fluorescein-conjugated phalloidin (10 µl/200 µl PBS; Molecular Probes, Inc., Eugene, OR, USA), which was added directly to the secondary antibody dilution. Nuclei were stained with 4,6-Diamidino-2-Phenylindole (DAPI) diluted to 1:10000 in 1X PBS for 10 minutes at room temperature. Cells were mounted using DAKO fluorescent mounting medium (DAKO Corporation, Carpinteria, CA, USA) and were visualized by fluorescence microscopy using a Zeiss Axioscope microscope equipped with an ultraviolet light source. Images were acquired using Axiovision and were compiled using Adobe PhotoShop 7.0 software (Adobe Systems Inc., San Jose, CA, USA).

2.16 Statistical analysis

All data are presented as mean values ± SEM. Differences between wild type and transgenic mice were evaluated for statistical significance using two-tailed, unpaired Student's *t* tests. Differences were considered statistically significant at a p value less than 0.05.

CHAPTER 3

3.0 Results

3.1 Generation of TC10Q75L transgenic mice

The Rho GTPase family consists of small, widely expressed G proteins that perform a variety of functions within eukaryotic cells. However, TC10 expression is elevated in adult heart and skeletal muscle, which suggests a tissue-specific role for this Rho GTPase. While many other Rho GTPases have been extensively characterized and specific roles for these proteins have been defined, TC10 has only recently been described *in vitro* and has remained uncharacterized *in vivo*.

To investigate the role of TC10 in this context, I generated transgenic mice over-expressing a constitutively active form of TC10 (TC10Q75L) under the control of a cardiac specific promoter. The open reading frame of constitutively active, GTPase-defective TC10Q75L was cloned into a pBluescript II SK+ expression vector containing a human growth hormone poly (Hgh) A region, under the control of a murine alpha-myosin heavy chain promoter (α-MHC) promoter which mediates a post-natal, cardiac-specific expression pattern (Figure 2a) (Robbins et al., 1990; Subramaniam et al., 1991; Jones et al., 1994; Jones et al., 1996). The TC10Q75L transgene (Figure 3a) was injected into the pronuclei of one-cell mouse embryos, which were implanted into the oviducts of five pseudo-pregnant foster mothers. Nine of the thirty-six pups born were determined to contain the TC10Q75L transgene by polymerase chain reaction, using primers embedded in the TC10Q75L and Hgh poly A sequences (Figure 3b). The PCR genotyping results were confirmed by southern blot hybridization with an Hgh-specific probe (Figure 3c). Four independent TC10Q75L transgenic lines were successfully established.

Figure 2. Transgene maps for transgenic mouse line, protein purification and transient transfections.

a) Schematic representation of constitutively activated TC10Q75L cDNA inserted into a pBluescript II SK+ expression vector. The pronuclei of one-cell mouse embryos were injected with this construct to generate a TC10 gain-of-function transgenic mouse line. The murine α-myosin heavy chain promoter is shown in *yellow*, while the Hgh poly A region is shown in *green*. ***b)*** Schematic representation of the pRSET A vector containing the full-length cDNA for TC10wt. This construct was used to induce protein expression in a bacterial system. Subsequently, the purified HIS-TC10 fusion protein was used to immunize a sheep and produce a polyclonal antibody against full-length TC10wt. The bacterial pUC promoter is shown in *yellow*, while the amino-terminal His tag is shown in *purple*. ***c)*** Transgene map for the construct used to transiently transfect H9C2, C2C12, and COS-1 cells using the calcium phosphate method. This schematic shows the CMV promoter in *yellow*, the amino-terminal triple-HA tag in *red* and the SV40 poly A in *green*.

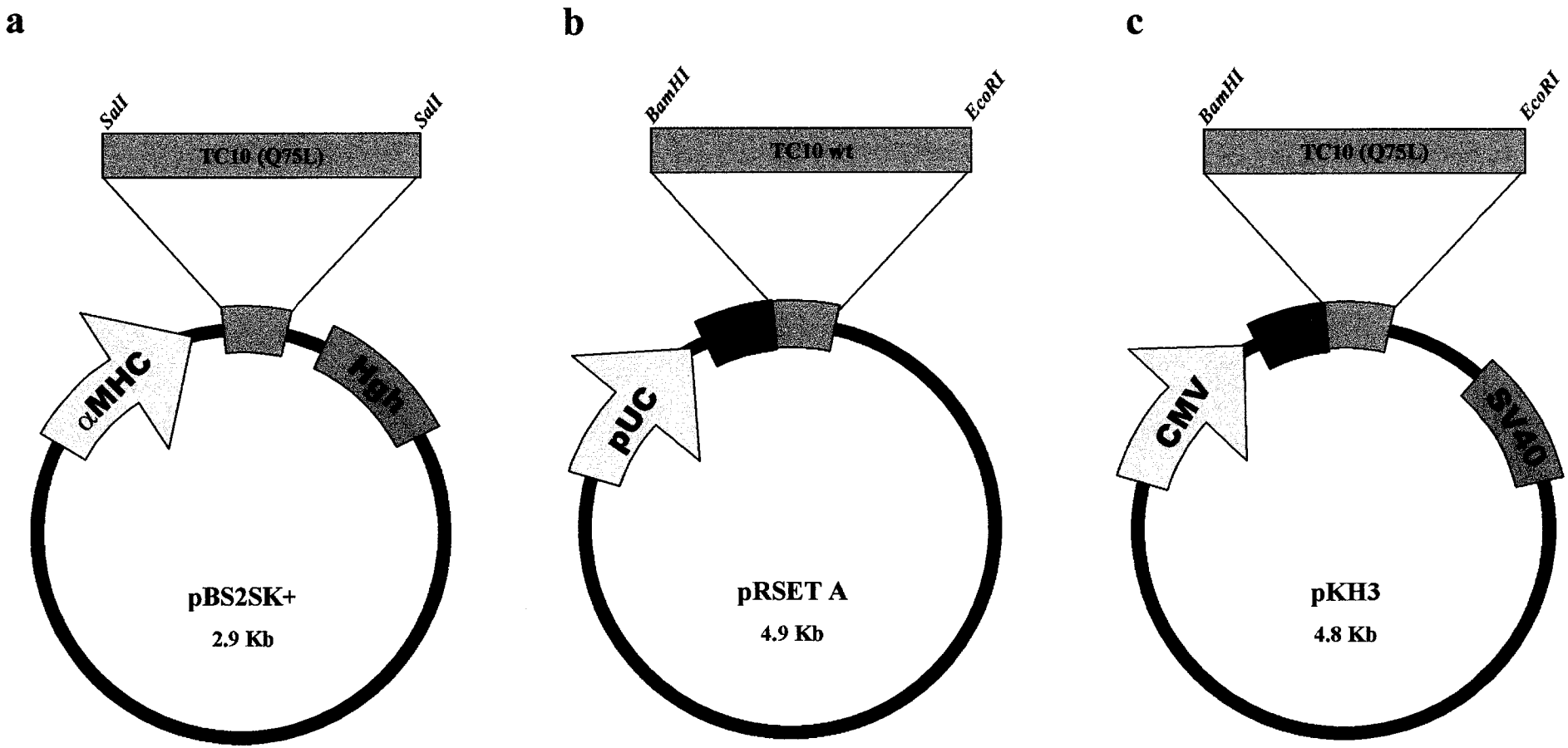
a
SalI
SalI
TC10 (Q75L)
αMHC
Hgh
pBS2SK+
2.9 Kb
b
BamHI
EcoRI
TC10 wt
pUC
pRSET A
4.9 Kb
c
BamHI
EcoRI
TC10 (Q75L)
CMV
SV40
pKH3
4.8 Kb

Figure 3. Identification of TC10Q75L transgenic founder lines.

a) Schematic of transgenic vector showing insertion of TC10Q75L cDNA under the α-MHC promoter and the location of primers used for genotyping by PCR. ***b)*** Representative PCR screening of wild type (wt) and transgenic (tg) mice using phenol:chloroform extracted genomic DNA. GAPDH was also amplified as a loading control (data not shown). PCR genotyping identified nine transgenic founder lines, which are identified with red asterisks. ***c)*** Southern blot confirmation of PCR genotyping results. Briefly, 10 μg of genomic DNA was digested overnight at 37°C using *EcoRI*. The digested tail DNA was separated on a 0.7% agarose gel and transferred to a nylon membrane. The Hgh poly A cDNA was used as a probe. The southern blot results confirmed the identification of nine transgenic founder lines, with varying copy numbers. A Trap3.1 probe was used as a loading control. The red asterisks identify the transgenic lines that were successfully established.

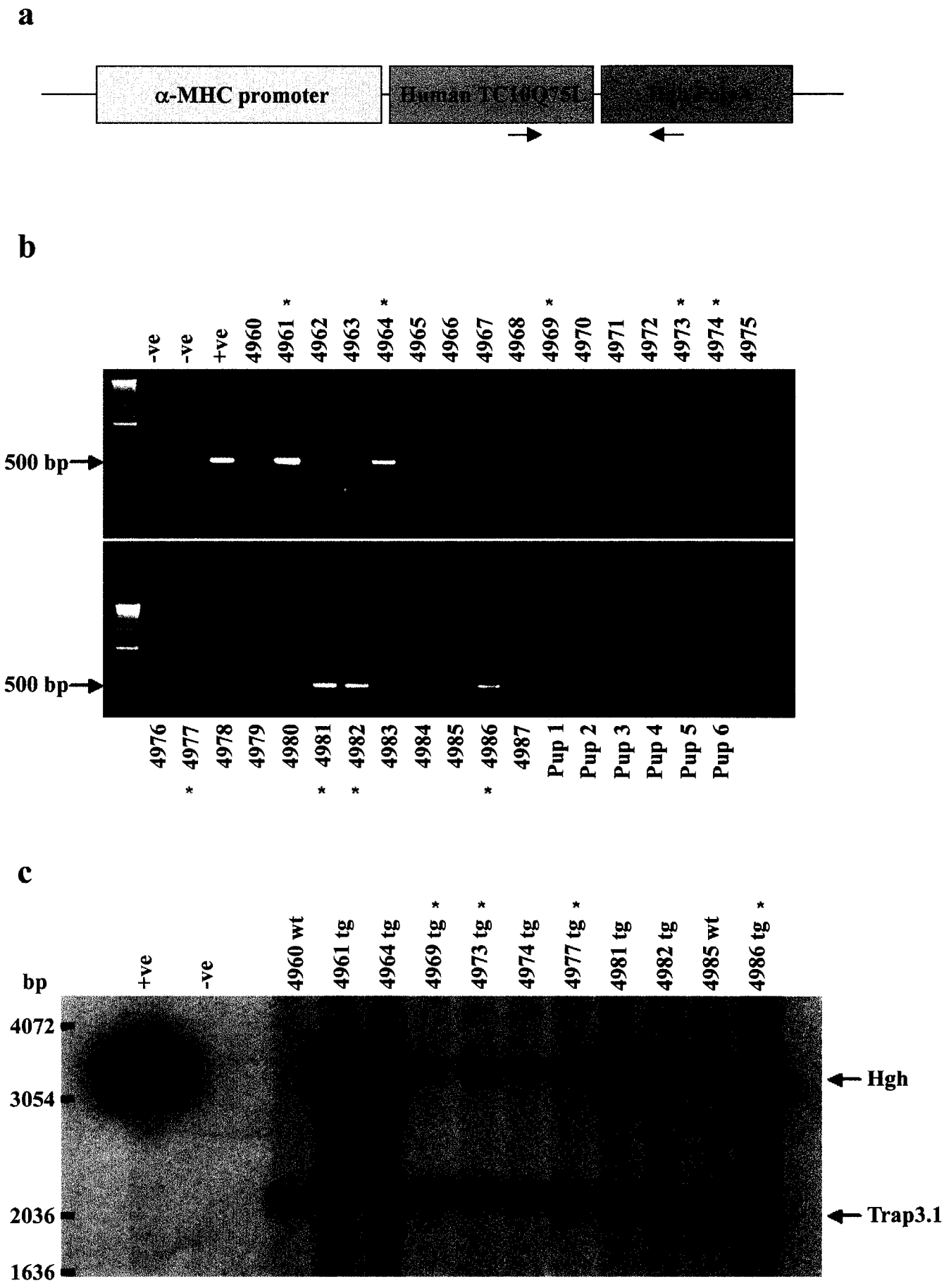
a
α-MHC promoter
Human TC14Q75L
b
-ve
-ve
+ve
4960
4961 *
4962
4963
4964 *
4965
4966
4967
4968
4969 *
4970
4971
4972
4973 *
4974 *
4975
500 bp
500 bp
4976
4977 *
4978
4979
4980
4981 *
4982 *
4983
4984
4985
4986 *
4987
Pup 1
Pup 2
Pup 3
Pup 4
Pup 5
Pup 6
c
bp
+ve
-ve
4960 wt
4961 tg
4964 tg
4969 tg *
4973 tg *
4974 tg
4977 tg *
4981 tg
4982 tg
4985 wt
4986 tg *
4072
3054
2036
1636
Hgh
Trap3.1

3.2 Transgenic viability is negatively affected by TC10Q75L over-expression in the murine heart

Two of the nine independent TC10Q75L transgenic founders generated were characterized by premature lethality at five and fifteen weeks of age, a phenomenon observed in transgenic lines with higher transgene integration numbers (4961 and 4964; Figure 3c). Interestingly, these transgenic founder mice expressed the transgene in tissues other than the heart in a limited fashion (as seen by RT-PCR, results not shown). Although exact copy numbers were not determined, this phenomenon was not observed in other founder lines or their offspring. Transgenic mouse # 4964, who died at five weeks of age, expressed the transgene in heart and skeletal muscle, while transgenic founder # 4961, who died at fifteen weeks of age, expressed TC10Q75L in skeletal muscle and brain tissue. In the latter instance, TC10Q75L message levels were not determined as the whole heart was used for histological analysis (see Section 3.5, Figure 8). However, it is a reasonable assumption that this transgenic mouse had high TC10Q75L transgene message levels, as the other founder with a similar, yet less severe phenotype also expressed the transgene to a high level (see Section 3.3, Figure 4). In addition, despite several attempts to create stable cell lines expressing constitutively active TC10, all attempts were unsuccessful. These observations suggest that the over-expression of activated TC10 was lethal/toxic under these circumstances. Further experimentation is necessary to confirm these observations.

3.3 Cardiac-specific expression of TC10Q75L in transgenic founder mice

To determine the level of TC10Q75L transgene message in the heart and skeletal muscle of each of the four established transgenic lines, northern blot hybridizations were performed using an activated TC10 probe. Transgenic line 4986 expressed the TC10Q75L transgene message to a high level, while the other three transgenic lines (4969, 4973 and 4977) expressed the transgene message at lower levels in the myocardium (Figure 4). TC10Q75L transgene message was not present in the skeletal muscle of these transgenic lines, demonstrating a cardiac-specific expression pattern (Figure 4). Using an activated TC10 probe, additional northern blot analyses revealed cardiac-specific expression profiles across several tissues of line 4969 (a randomly chosen low-expressing line) and line 4986 (the only high-expressing line). All other tissues examined (liver, brain, lung, spleen, skeletal muscle and kidney) did not express the TC10Q75L transgene message, which confirmed the cardiac specificity for the α-MHC promoter (Figure 5).

Figure 4. TC10Q75L transgene expression profile.

TC10Q75L transgene expression in adult heart and skeletal muscle from transgenic and age- and sex-matched wild type mice (lines 4969, 4973, 4977 and 4986). TC10Q75L transgene message was high in line 4986, and low in lines 4969, 4973 and 4977. Briefly, 15 μg of RNA isolated using the Trizol Reagent was subjected to northern blot analysis using an [α-^{32}P]dCTP-labeled TC10Q75L probe (*Li*, liver; *He*, heart; *Sk*, skeletal muscle). GAPDH was used as a loading control. Molecular masses (in kilobases) are indicated on the left.

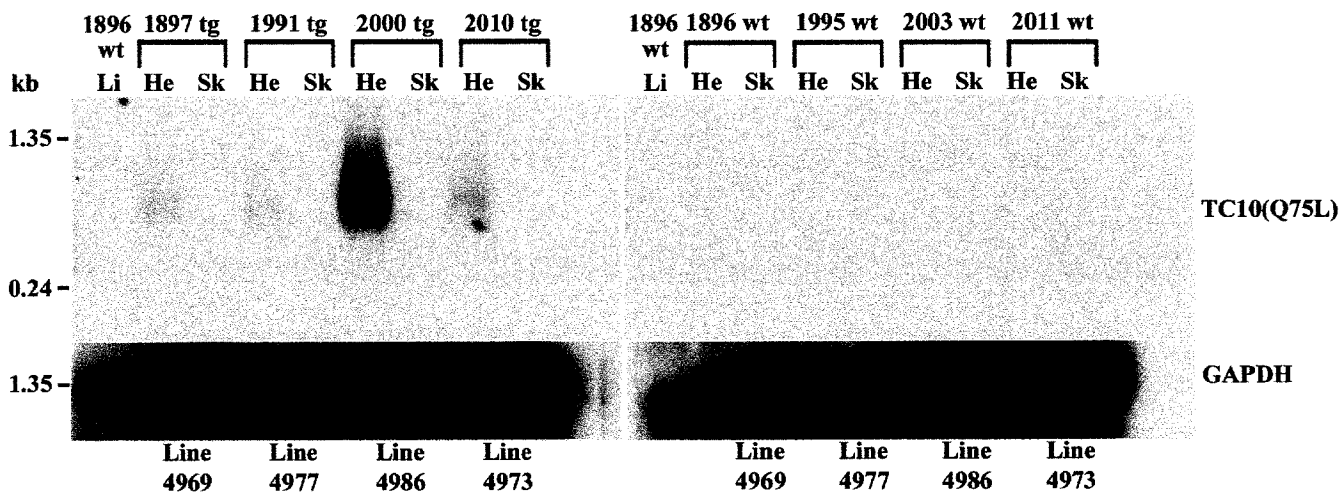
1896 wt
1897 tg
1991 tg
2000 tg
2010 tg
1896 wt
1896 wt
1995 wt
2003 wt
2011 wt
kb
Li
He
Sk
He
Sk
He
Sk
He
Sk
Li
He
Sk
He
Sk
He
Sk
He
Sk
1.35
0.24
1.35
TC10(Q75L)
GAPDH
Line 4969
Line 4977
Line 4986
Line 4973
Line 4969
Line 4977
Line 4986
Line 4973

Figure 5. TC10Q75L cardiac-specific transgene expression.

TC10Q75L transgene expression in various adult tissues from transgenic and age- and sex-matched wild type mice from line 4969 (low expression) and line 4986 (high expression). A northern blot (15 μg RNA/lane) was hybridized with an [α-^{32}P]dCTP-labeled TC10Q75L probe. Several tissues including: *Li*, liver; *Br*, brain; *Lu*, lung; *He*, heart; *Sp*, spleen; *Sk*, skeletal muscle and *Ki*, kidney, were analyzed. TC10Q75L transgene expression was restricted to the heart tissue of transgenic mice. To confirm RNA integrity and equal loading of the RNA gel, ethidium bromide staining of the RNA gels was performed. Sizes (in kilobases) are indicated on the left.

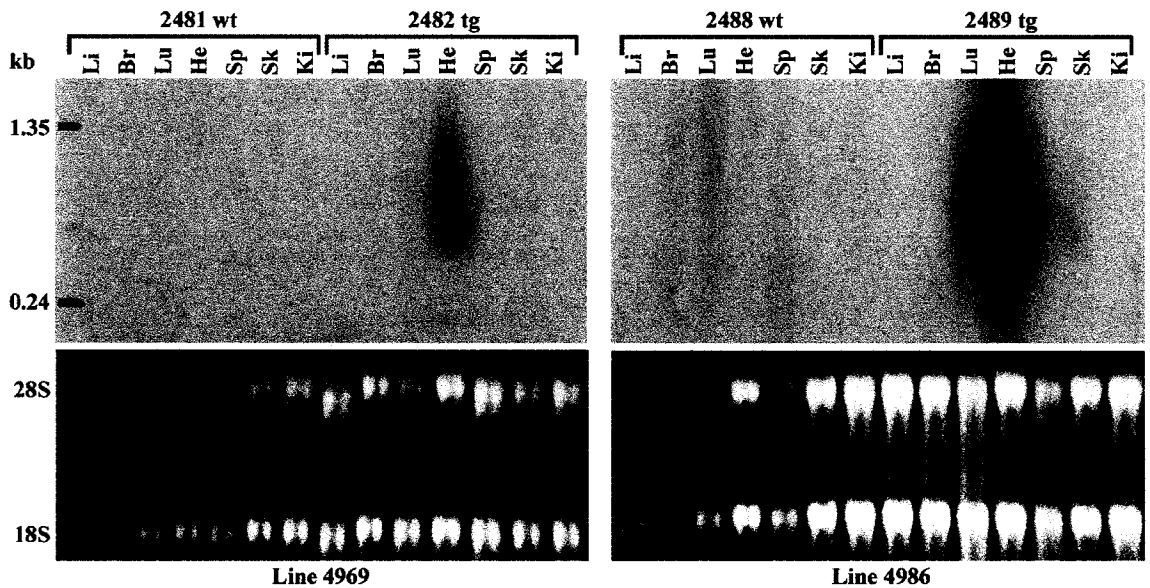
2481 wt
2482 tg
2488 wt
2489 tg
kb
Li Br Lu He Sp Sk Ki
1.35
0.24
28S
18S
Line 4969
Line 4986

3.4 Molecular characterization of TC10Q75L transgenic mice

To verify over-expression of the TC10Q75L transgene, protein extracts were generated from the hearts of seven-month-old mice from both the low-copy-number line (4969) and the high-copy-number line (4986). TC10 protein content in transgenic and wild type heart lysates was monitored with the sheep polyclonal TC10 antibody. HIS-tagged recombinant TC10 and COS-1 whole cell lysates, transiently transfected with HA-tagged TC10Q75L, were used as positive controls for western blot analyses. The discrepancy in the molecular mass of these tagged proteins is explained by the differences in the size of their corresponding tags, HA being larger than HIS. An increased amount of full-length TC10Q75L protein was observed in transgenic heart lysates from line 4969 in comparison to age- and sex-matched non-transgenic heart lysates (Figure 6). In addition, the presence of a large amount of breakdown product was routinely observed in the transgenic heart lysates from line 4986, the high expressing line. One possible explanation for this observation is that forcing the over-expression of a membrane-associated protein may cause the membrane to reach a saturation point, at which time any additional TC10Q75L would remain in the cytoplasm, where it would be subjected to degradation. Most Rho GTPases contain a carboxyl terminal CAAX box motif, indicating that they are subjected to isoprenylation of the cysteine, followed by proteolytic removal of the three terminal amino acids and carboxymethylation (Murphy et al., 2001). TC10 also has a CXXC sequence immediately upstream of the CAAX motif, allowing for palmitoylation of the two cysteine residues, which serves as a membrane-targeting signal (Abe et al., 2003). This series of post-translational

modifications suggests that TC10 is associated with cellular membranes for a period of time during its normal, regulated function (Murphy et al., 2001).

To verify that the TC10Q75L transgenic mice were indeed over-expressing a constitutively active, GTPase-defective form of the TC10 protein, a global GTPase activity assay was performed using wild type and transgenic heart lysates. Assuming all other GTPase activity is equal, global GTPase activity in the transgenic heart lysates should be lower than that of its wild type counterpart since TC10Q75L is GTPase-defective and thus is unable to be inactivated by GTPase-activating proteins and remains GTP-bound *in vivo*. Global GTPase activity was indeed lower in transgenic heart lysates at 5 min ($p<0.025$), 10 min ($p<0.01$) and 15 min ($p<0.05$) when compared to heart lysates generated from age-and sex-matched wild type mice (Table 1).

Table 1: Global GTPase activity comparison between wild type and TC10Q75L transgenic heart lysates.

Time (min)	Wt global GTPase activity (avg. cpm)	Tg global GTPase activity (avg. cpm)	Sample size	P value
0	1242909	1069491	n = 8	p=0.615
5	1850850	1203065	n = 6	p<0.025
10	1697232	1172425	n = 8	p<0.01
15	1368760	714169.6	n = 7	p<0.05

Briefly, 75 μg of heart lysates were preloaded with 10 μCi [γ-^{32}P]GTP in 40 μl of incubation buffer for 10 min at 20°C before the addition of $MgCl_2$ to a final concentration of 5 mM. At indicated time points, the reaction was terminated by filter binding to nitrocellulose filters, followed by 2-10 ml washes with ice-cold wash buffer. Radioactivity remaining on filters was quantified by scintillation counting. Values are indicated in counts per milliliter (cpm) and P values were calculated using a Student's t-test.

There were no significant differences observed between wild type and transgenic global GTPase activity in the heart at 0 min (p=0.615). This was an expected observation since

the magnesium chloride, a component necessary to maintain guanine nucleotide associated with TC10, was added just prior to filter binding and thus did not allow time for differences in the reaction to become apparent (Table 1) (Neudauer and Macara, 2000).

These observations suggest that the TC10Q75L transgenic mice were indeed over-expressing constitutively active TC10 in the heart in comparison to their non-transgenic counterparts.

Figure 6. Increased cardiac expression of TC10Q75L protein.

Western blot analysis revealed higher full-length TC10Q75L protein levels in transgenic (tg) versus wild type (wt) heart lysates in the low-expressing 4969 and the high-expressing 4986 transgenic lines, with the presence of a breakdown product apparent in the tg heart lysates from line 4986. Protein lysates derived from wt and tg whole hearts were separated on a 12% SDS-polyacrylamide gel (100 μg heart lysates/lane), transferred to a PVDF membrane, and immunoblotted with anti-TC10 antibody. 12.5 ng of recombinant HIS-TC10 fusion protein was used as a positive control, along with 50 μg of COS-1 lysates that had been transiently transfected with HA-TC10Q75L. 50 μg of COS-1 lysates were used as a negative control for TC10. Equal loading was verified by Ponceau S staining.

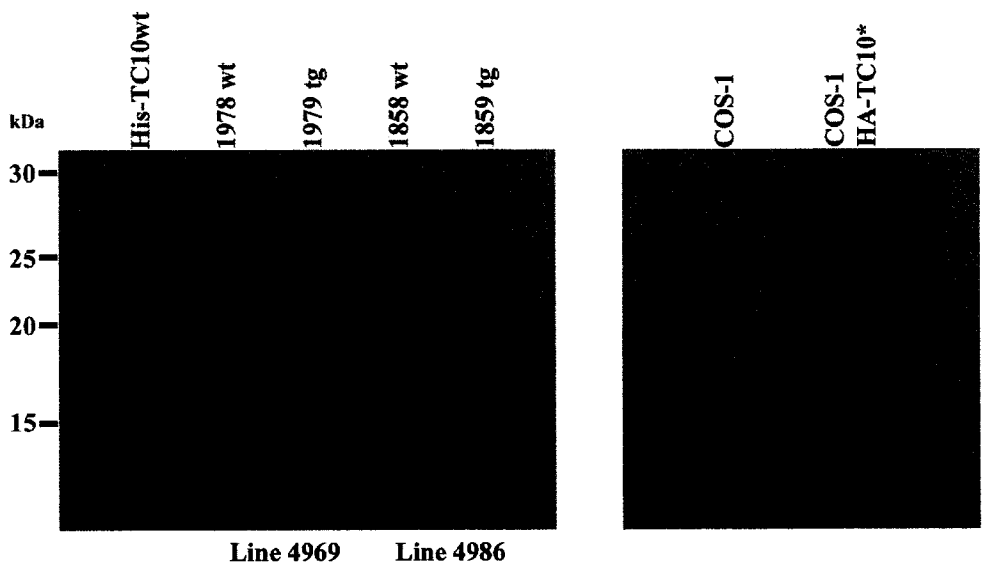
kDa
30
25
20
15
His-TC10wt
1978 wt
1979 tg
1858 wt
1859 tg
COS-1
COS-1
HA-TC10*
Line 4969
Line 4986

3.5 Over-expression of activated TC10 causes atrial and ventricular enlargement in transgenic mice

A histological comparison of wild type and transgenic founder hearts at 10.5 months of age revealed notable evidence of left ventricular hypertrophy, right ventricular dilatation, and atrial enlargement in the high-expressing TC10Q75L line 4986 (Figure 7). Evidence of similar cardiac pathologies was not as extensive in the hearts of the three low-expressing TC10Q75L transgenic founder mice (4969, 4973 and 4977), although hearts from founder mice 4969 and 4973 showed signs of slight atrial and ventricular enlargement, in addition to right ventricular dilatation. A similar cardiac phenotype was observed in established TC10Q75L transgenic lines (Figure 8). To obtain evidence of cardiac hypertrophy/dilatation, hearts from TC10Q75L transgenic mice were weighed and initially normalized to body weight. This morphometric ratio proved to be insignificant, which was later determined to be due to the moderate differences in the body weight measurements of TC10Q75L transgenic mice, compared to their wild type littermates. The observed increase in transgenic body weight could be as a result of a mild, generalized edema in the transgenic mice afflicted with a cardiac pathology. Indeed, edema is a common feature of congestive heart failure (Schiff et al., 2003), however further experimentation would be necessary to verify this phenomenon with certainty. Therefore, heart weights from TC10Q75L mice were normalized to tibia length as this proved to be a consistent internal standard between transgenic and non-transgenic mice. Hearts from TC10Q75L transgenic mice showed a moderate, but significant increase in heart weight to tibia length ratios lending evidence to the

hypothesis that cardiac over-expression of activated TC10 is detrimental to cardiac morphology over an extended period of time (Table 2).

Table 2: Morphometric analysis of wild type and TC10Q75L transgenic mice.

Ratio	Wild type	Transgenic	P value
Heart weight/ tibia length	0.008387 ± 0.000432 (n = 3)	0.010133 ± 0.00113 (n = 5)	$p < 0.025$

Whole hearts were excised from wild type (wt) and transgenic (tg) mice, weighed and normalized to tibia length. Data are presented as the mean ± SE. Statistical significance was determined with a Student's t-test.

Cardiac hypertrophy is an adaptive physiological response characterized by an increase in cardiomyocyte size and associated with altered expression of contractile or fetal genes in the heart. However, sustained hypertrophy can lead to dilated cardiomyopathy, heart failure, and sudden death. Increased atrial natriuretic factor (ANF) expression in the adult heart is often used as an index of myocyte hypertrophy. As such, ANF message levels were assessed in wild type and transgenic mice by Northern blot analysis. ANF expression levels were significantly higher in all transgenic animals studied between 5 and 18 months of age from both low- and high-expressing transgenic lines (Figure 8). This increase in ANF expression suggests that the molecular program for cardiac hypertrophy has been activated in TC10Q75L transgenic mice. These results lend support to the hypothesis that cardiac over-expression of activated TC10 is detrimental to cardiac muscle cells over an extended period of time.

Figure 7. Comparison of TC10Q75L transgenic founder hearts.

Cardiac histological analysis of TC10Q75L transgenic founder hearts, which were perfused and fixed in 4% paraformaldehyde, embedded in paraffin, sectioned at 5 μm and counterstained with hematoxylin and eosin. Hearts from a wild type age-matched mouse (*left*; 4962), from 3 low-expressing founder lines (*middle*; 4969, 4973, 4977) and from a high-expressing founder line (*right*; 4986) were examined for any evidence of cardiac pathology at ten and a half months of age. Cardiac hypertrophy and atrial enlargement were observed in line 4986 compared to the wild type heart, while two of the three low-expressing transgenic founder hearts are moderately enlarged with concomitant increase in chamber sizes (dilation) when compared to the wild type heart. Scale bar is indicated on the bottom left.

4962 wt

4969 tg

4973 tg

4977 tg

4986 tg

10 mm

Figure 8. Atrial enlargement and ventricular hypertrophy in transgenic hearts.

a) Intact whole hearts from 4-month-old wild type and transgenic mice (line 4961) were fixed in 4% PFA and photographed using a digital camera. Grossly enlarged atria and ventricles are observed in the tg versus the wt age- and sex-matched heart. ***b)*** Macroscopic hematoxylin- and eosin-stained histological heart section (10 μm) shows an extremely enlarged right atrium, right ventricular dilation, and signs of left ventricular hypertrophy. ***c)*** Cardiomyocyte hypertrophic marker analysis by ANF Northern blotting. 15 μg of RNA isolated from wt and tg mouse hearts of differing ages (1954wt, 1955tg, 1854tg, 1442tg: ≥1 yr old; 2483wt, 2477tg: 5 mo. old; 2304wt, 2305tg: 8 mo. old) was separated on a 1% agarose-formaldehyde gel and transferred to a nylon membrane. Northern blot was hybridized with an [α-^{32}P]dCTP-labeled ANF probe to analyze ANF expression, an index of myocyte hypertrophy. To confirm RNA integrity and equal loading of the RNA gels, ethidium bromide staining of RNA gels was performed. Sizes (in kilobases) are indicated on the left.

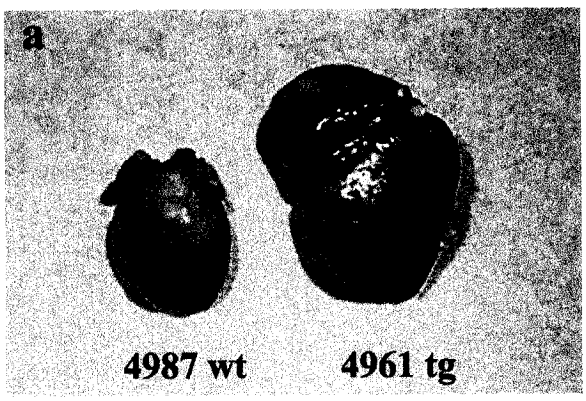
a
4987 wt
4961 tg

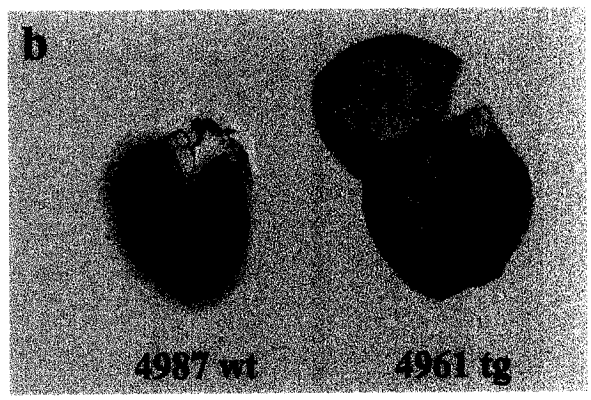
b
4987 wt
4961 tg

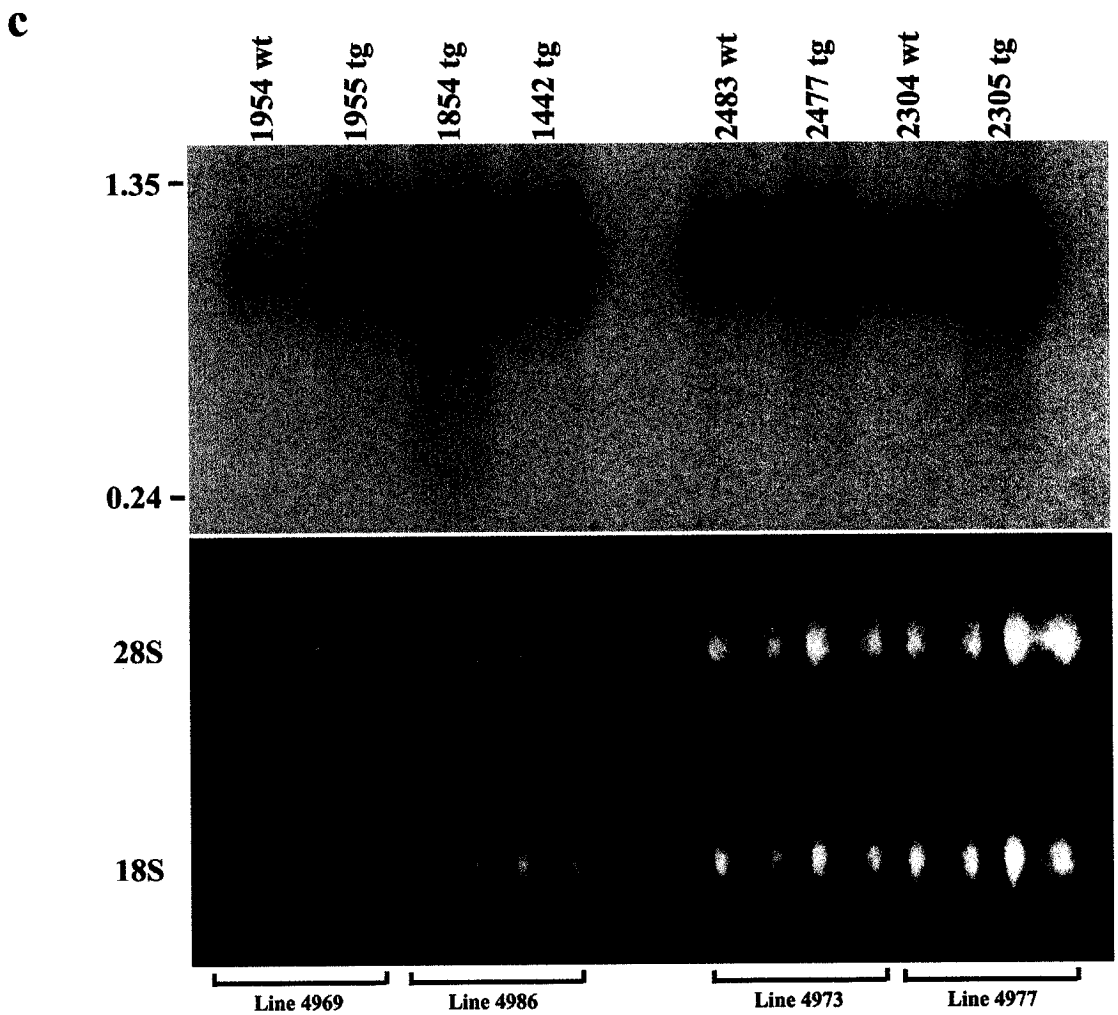
c
1954 wt
1955 tg
1854 tg
1442 tg
2483 wt
2477 tg
2304 wt
2305 tg
1.35
0.24
28S
18S
Line 4969
Line 4986
Line 4973
Line 4977

3.6 Cardiac hypertrophy in TC10Q75L transgenic mice may be mediated through the JNK1 signalling pathway

The signalling pathways activated by the TC10 GTPase in the context of cardiac adaptation are unknown. However, it is proposed that the mitogen-activated protein kinase (MAPK) signalling pathway may be responsible for the hypertrophic responses seen in TC10Q75L transgenic hearts. Specifically, TC10 has been shown to activate JNK1 *in vitro* by means of *in vitro* kinase and reporter assays (Murphy et al., 1999; Neudauer et al., 1998), and JNK1 activity has been shown to mediate cardiomyocyte hypertrophy (De Windt et al., 1999; Ramirez et al., 1997; Wang et al., 1998).

Initially, to investigate the role of JNK1 in the cardiac hypertrophic response of TC10Q75L transgenic mice, JNK1 phosphorylation status was assessed by immunoprecipitation (IP) with a monoclonal JNK1 antibody, followed by western blot analysis with a phospho-specific JNK antibody. Differences were noted in the banding pattern seen by IP-western blot between wild type and transgenic heart lysates, i.e. the antibody detected a slower migrating JNK1 isoform in the transgenic lysates. This altered migration pattern of JNK1 may be indicative of increased phosphorylation (lanes 10 and 13, compared to lanes 4 and 7; Figure 9).

To clarify whether in fact this MAPK signalling pathway was involved in the hypertrophic response of the TC10Q75L transgenic hearts, an *in vitro* kinase assay was performed to directly measure JNK1 kinase activity. The *in vitro* kinase assay revealed increased JNK1-directed phosphorylation of an MBP substrate in transgenic heart lysates,

compared to control lysates (Figure 10). These observations may in part explain the propensity of TC10Q75L to induce a detrimental cardiac phenotype.

Figure 9. JNK1 phosphorylation in transgenic and wild type heart protein lysates.

A difference is seen in JNK1 phosphorylation between whole heart lysates from wt and tg mice. JNK1 was assessed by immunoprecipitation with an anti-JNK1 antibody, followed by western blot analysis with a phosphospecific anti-JNK antibody. Lane *1*, no lysate negative control; lanes *2,5*, *8*, *11*, immunoprecipitation with a nonspecific GST antibody; lanes *3*, *6*, *9*, *12*, no antibody control; lanes *4*, *7*, *10*, *13*, JNK-1 antibody used for immunoprecipitation. Size markers (in kDa) are indicated on the left.

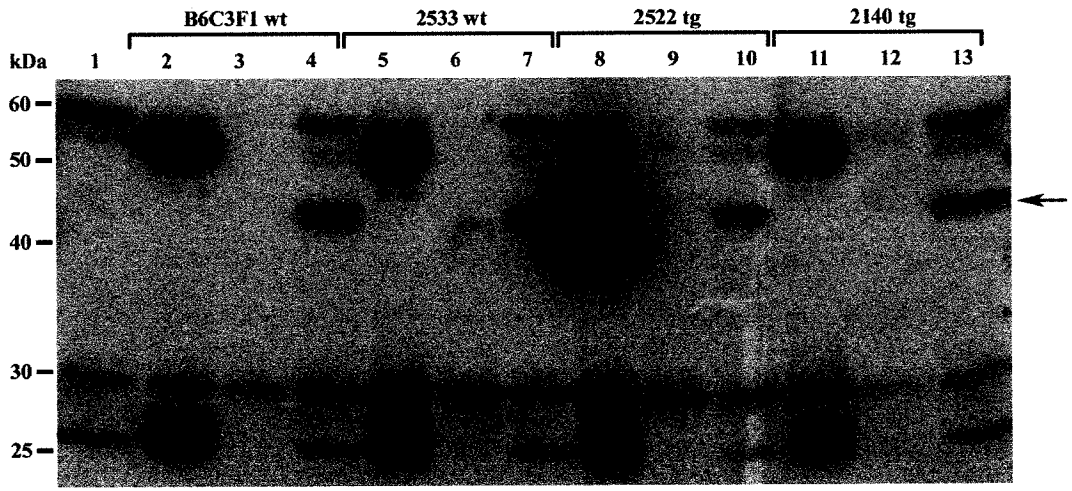
B6C3F1 wt
2533 wt
2522 tg
2140 tg
kDa
1
2
3
4
5
6
7
8
9
10
11
12
13
60
50
40
30
25

Figure 10. JNK1 activation is moderately increased in TC10Q75L transgenic heart lysates.

Heart lysates (500 μg/sample) derived from wild type and TC10Q75L transgenic mice were subjected to immunoprecipitation with a JNK1 antibody, followed by an *in vitro* kinase assay using MBP as an exogenous substrate. The positive control was an activated p38 recombinant protein (using MBP as the substrate) and a negative control was also included (no heart protein lysates). Size markers are indicated in kDa on the left.

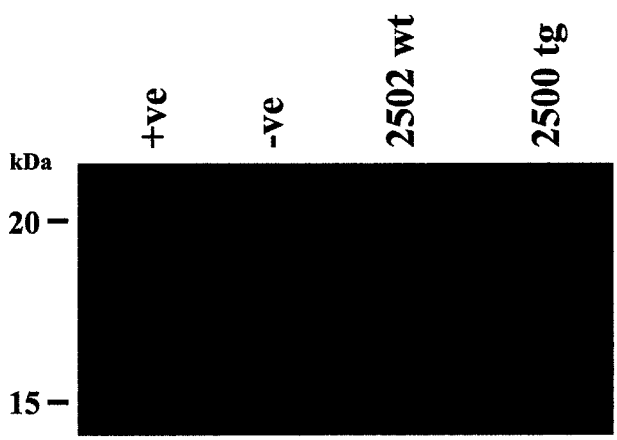
+ve
-ve
2502 wt
2500 tg
kDa
20
15

3.7 Cardiac over-expression of TC10Q75L induces the formation of actin-containing spikes and disrupts filamentous actin in transgenic cardiomyocytes

The actin cytoskeleton is central in defining many important cellular events, such as cell shape, morphology, and motility (Vidal et al., 2002). Rho GTPases are well-defined regulators of the actin cytoskeleton in all eukaryotic cells. In fibroblasts, activation of Rho causes increased actin stress fiber and focal adhesion complex formation, while the activation of Rac1 leads to the formation of lamellipodia and membrane ruffles, and Cdc42 activation prompts the formation of filopodial extensions and microspikes (Mackay and Hall, 1998; Schmitz et al., 2000). Therefore, to examine the relationship between TC10Q75L and the actin cytoskeleton, ventricular cardiomyocytes derived from wild type and transgenic hearts were maintained in primary culture and inspected for changes and/or disruptions in actin architecture. Filamentous actin was visualized by fluorescein-phalloidin staining. Over-expression of TC10Q75L transgene resulted in the reorganization of the actin cytoskeleton and the formation of actin-containing peripheral extensions (filopodia) of the cell membrane in primary cardiomyocytes (Figure 11). The formation of filopodia was observed in ventricular primary cardiomyocytes derived from both low- and high-expressing transgenic animals, when compared to their non-transgenic counterparts. The effects of TC10Q75L on the actin cytoskeleton was correlated with the level of transgene expression, as twenty-four percent of cells derived from the high-expressing transgenic cells from line 4986 consistently displayed peripheral membrane extensions, in comparison to fourteen percent of cardiomyocytes derived from the low-expressing transgenic line 4969 and only five percent of wild type cardiomyocytes (~100 cells from each line were counted) (Figure 12).

In addition, constitutively active TC10 caused the disassembly of actin stress fibers and the formation of actin aggregates in cardiomyocytes derived from TC10Q75L transgenic mice (eight percent of cardiomyocytes from line 4969 and thirteen percent from line 4986), compared to only four percent of their wild type counterparts (Figures 12 and 13).

Figure 11. Reorganization of the actin cytoskeleton in TC10Q75L transgenic mice. Ventricular cardiomyocytes from wild type, and transgenic TC10Q75L lines 4969 (low expresser) and 4986 (high expresser) were cultured on collagen-coated glass 2-well chamber slides. Cells were maintained in DMEM/F-12 media for 7 days, fixed in 4% PFA, and incubated with a mouse anti-desmin antibody and fluorescein phalloidin, and stained with a Cy3-conjugated anti-mouse antibody. The first column of photomicrographs shows the anti-desmin stain to identify cardiomyocytes, the second column depicts the phalloidin stain to identify actin and the third column depicts the nuclear DAPI staining. A lower percentage of cells from wild type mice displayed filopodial extensions (5%), compared to cells from TC10Q75L transgenic lines 4969 and 4986 (14% and 24%, respectively). All photomicrographs were taken at identical magnifications (40X).

Desmin
Phalloidin
DAPI
wt
4969
4986
4986

Figure 12. Quantification of actin reorganization in wild type and transgenic cardiomyocytes by TC10Q75L.

The percentage of cardiomyocytes containing filopodial extensions or actin aggregation was calculated for comparison between wild type and low- and high-expressing TC10Q75L transgenic mice (line 4969 and line 4986, respectively). A total of ~100 cells from two separate experiments were analysed for the presence of peripheral membrane extensions (filopodia) or actin aggregation (percentages are the means obtained). Wild type counts are shown in *blue*, line 4969 in *burgundy* and line 4986 in *yellow*.

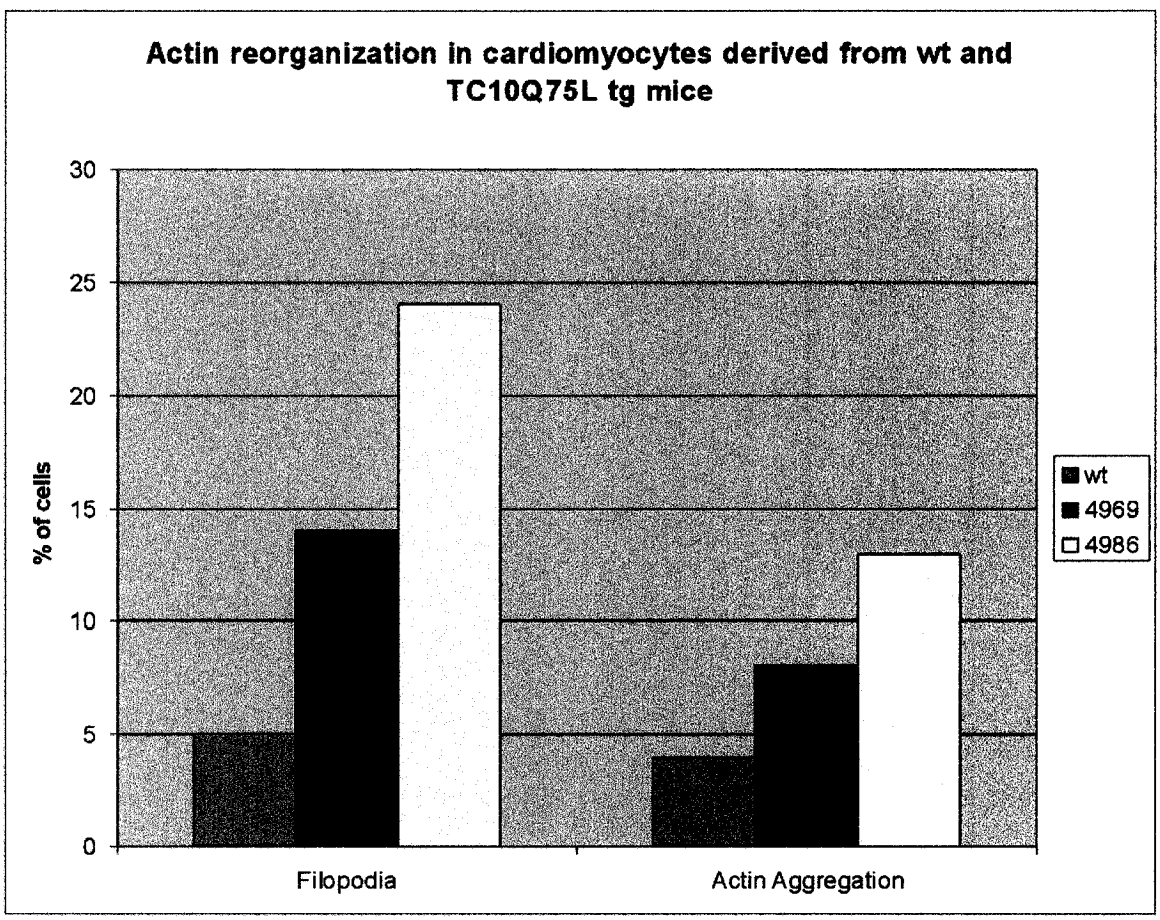
Actin reorganization in cardiomyocytes derived from wt and TC10Q75L tg mice
% of cells
30
25
20
15
10
5
0
Filopodia
Actin Aggregation
wt
4969
4986

Figure 13. Actin aggregation in TC10Q75L transgenic cardiomyocytes.

Neonatal mouse ventricular cardiomyocytes from wild type and TC10Q75L transgenic animals from lines 4969 (low expresser) and 4986 (high expresser) were cultured on collagen-coated glass 2-well chamber slides. Cells were maintained in DMEM/F-12 media for 7 days, fixed in 4% paraformaldehyde, and incubated with a mouse anti-desmin antibody and fluorescein phalloidin, and stained with a Cy3-conjugated anti-mouse antibody. The first column of photomicrographs shows the anti-desmin stain to visualize cardiomyocytes, the second column depicts the phalloidin stain to visualize actin, the third column depicts the nuclear DAPI staining and the last shows the bright field picture of the cells. Cardiomyocytes from wild type animals generally contained well-ordered actin structures, with little or no actin aggregation (only 4% displayed evidence of actin aggregation). In contrast, cardiomyocytes from transgenic mice from both line 4969 and 4986 often showed evidence of actin aggregation (8% and 13%, respectively). All photomicrographs were taken at the same magnification (63X).

Phase
DAPI
Phalloidin
Desmin
wt
4969
4986

3.8 Reorganization of the actin cytoskeleton by TC10Q75L increases transgenic cardiomyocyte membrane permeability to Evans Blue Dye

To determine whether TC10-mediated reorganization and disruption of the actin cytoskeleton changed cardiomyocyte membrane permeability, Evans blue dye (EBD) injections were performed on wild type and transgenic mice between 9 and 18 months of age. Evans blue dye is a nontoxic dye that is widely used to study cellular membrane integrity and has recently been utilized as an *in vivo* marker of myofiber damage and membrane fragility (Hamer et al., 2002).

Low- and high-expressing TC10Q75L transgenic hearts from aged mice (greater than one year) revealed greater EBD permeability than did their wild type counterparts (Figure 14, top two panels). Additionally, line 4986, the high-expressing transgenic line, appeared to demonstrate greater ventricular EBD penetration than did the low-expressing line, line 4969, as evidenced by a stronger auto-fluorescent signal from the dye (Figure 14, panels e and f). Although there was evidence of increased membrane permeability to EBD by 9 months of age (Figure 14, bottom panels), cardiomyocyte membrane permeability to the dye was most pronounced in aged mice (> 1 year) (Figure 14, panels b, c, e, f).

The increased EBD penetration in TC10Q75L transgenic ventricles and the formation of peripheral membrane extensions seen in cardiomyocytes derived from TC10Q75L transgenic mice, indicates that over-expression of activated TC10 perturbs the plasma membrane, which in turn leads to a compromise in overall muscle cell integrity.

Figure 14. Increased Evans Blue Dye penetration in TC10Q75L transgenic hearts. EBD injections revealed greater dye permeability in TC10Q75L transgenic cardiac tissue compared to age- and sex-matched wild type hearts. Mice were injected (i.p.) with 1% EBD 24 h prior to sampling. Murine hearts were fixed in 4% paraformaldehyde, embedded in paraffin, sectioned at 5 μm and visualized by fluorescence microscopy using a Zeiss Axioscope microscope equipped with an ultraviolet light source. Top two rows of photomicrographs, mice were greater than one year of age; bottom row of photomicrographs, mice were 9 months of age. All photographs were taken at the same exposure time and in a similar area of the left ventricle to ensure reliable comparisons of EBD penetration between wild type and transgenic hearts.

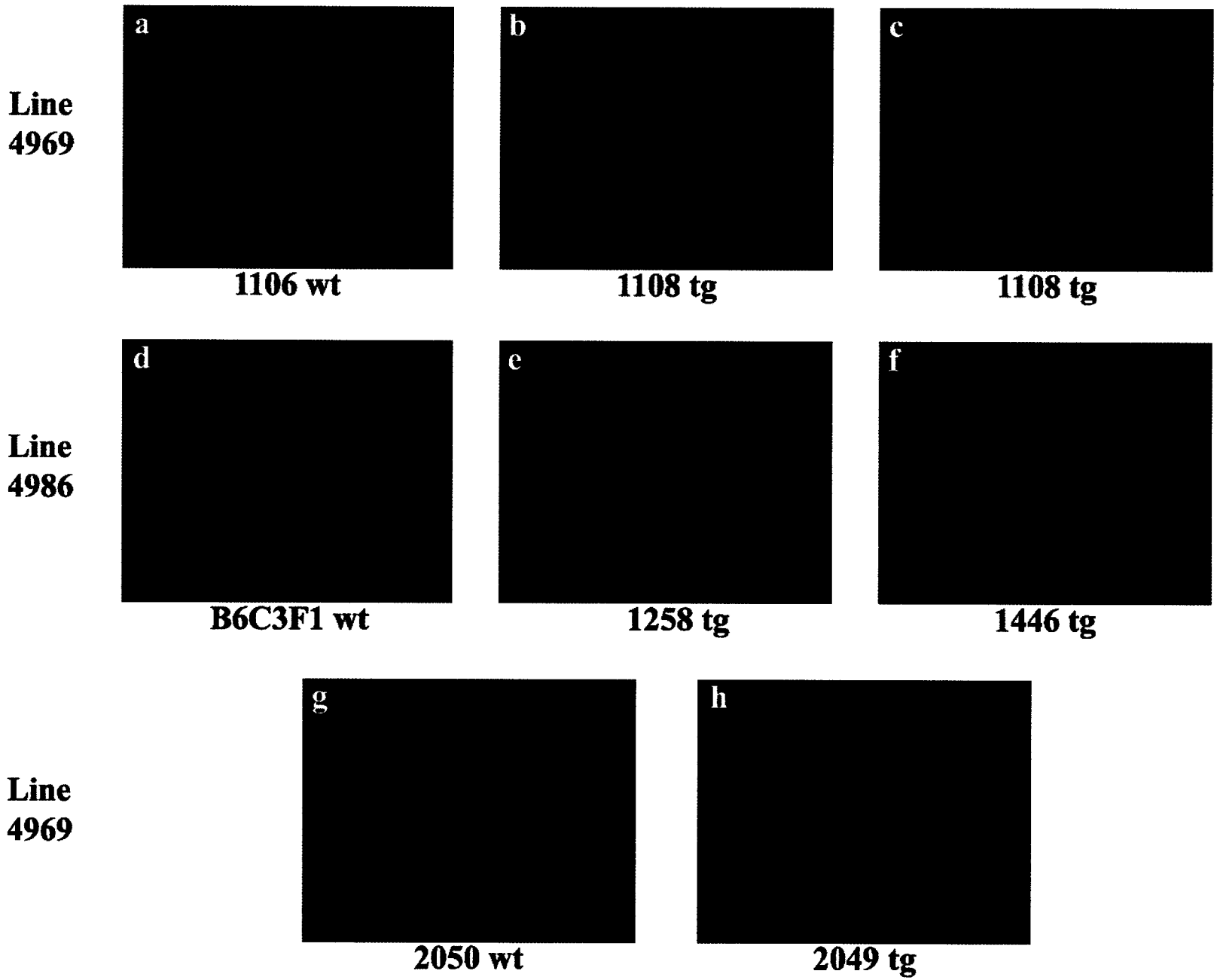
Line 4969
a
1106 wt
b
1108 tg
c
1108 tg
Line 4986
d
B6C3F1 wt
e
1258 tg
f
1446 tg
Line 4969
g
2050 wt
h
2049 tg

3.9 Over-expression of activated TC10 disrupts filamentous actin and induces peripheral membrane extensions in C2C12 skeletal muscle myoblasts

To determine whether the effects of over-expressing TC10Q75L were specific to cardiomyocytes, transient transfections with HA-tagged TC10Q75L were performed in an immortalized mouse myoblast cell line (C2C12), as muscle tissue normally expresses TC10 (Abe et al., 2003). To date, research conducted with TC10 has focused on the protein's function in cell lines that do not normally express this Rho GTPase, such as fibroblast and kidney cells.

In C2C12 myoblasts, TC10Q75L induced the formation of peripheral extensions and disrupted filamentous actin, leading to the disassembly of actin stress fibers and actin aggregation (Figure 15). The effects of TC10Q75L over-expression in C2C12 cells were comparable to the phenotypic consequences observed in TC10Q75L transgenic cardiomyocytes. These results confirm the hypothesis that the over-expression of activated TC10 *in vitro* leads to actin cytoskeleton reorganization, which perturbs the plasma membrane in C2C12 myoblasts. The subcellular localization of HA-tagged TC10Q75L was also verified in C2C12 skeletal muscle myoblasts. Activated TC10 was detected in the perinuclear region and in the cell periphery, which is consistent with the reported localization of TC10 in other cell types, such as HeLa cells, with different tags, such as green fluorescent protein (GFP; Murphy et al., 2001) (Figure 16).

Figure 15. Peripheral membrane extensions and increased actin aggregation in HA-TC10Q75L C2C12 cells.

C2C12 cells were transfected with 2 μg pKH3-TC10Q75L or pKH3-TC10wt on two-well glass chamber slides. Cells expressing triple-HA-tagged TC10Q75L were stained using an anti-HA monoclonal primary antibody, followed by a Cy3-conjugated anti-mouse secondary antibody. F-actin was visualized with fluorescein-phalloidin and the nuclei were detected with DAPI. The top two rows of images were taken of cells transfected with pKH3-TC10Q75L and the bottom row of cells were transfected with pKH3-TC10wt. All pictures were taken at identical magnifications (40X).

Phase
DAPI
Phalloidin
HA
HA-TC10(Q75L)
HA-TC10wt

Figure 16. Subcellular localization of HA-TC10Q75L in C2C12 myoblasts.

Activated TC10 was detected in the perinuclear region and in the cell periphery of transiently transfected C2C12 cells. C2C12 myoblasts actively growing in medium containing 10% FBS were transfected with HA-TC10Q75L using the calcium phosphate method in serum free media. After 16 hours, the transfection media was removed and cells were transferred into fresh DMEM with 10% FBS. Twenty-four hours following the removal of the transfection media, cells were fixed with 4% PFA and subjected to immunoflourescent studies. Cells expressing triple-HA-tagged TC10Q75L were stained using an anti-HA monoclonal primary antibody, followed by a Cy3-conjugated anti-mouse secondary antibody (*top left panel*). F-actin was visualized with fluorescein-phalloidin (*top right*) and the nuclei were detected with DAPI (*bottom left*). The bright field picture of the cell is seen in the *bottom right*. All pictures were taken at identical magnifications (40X).

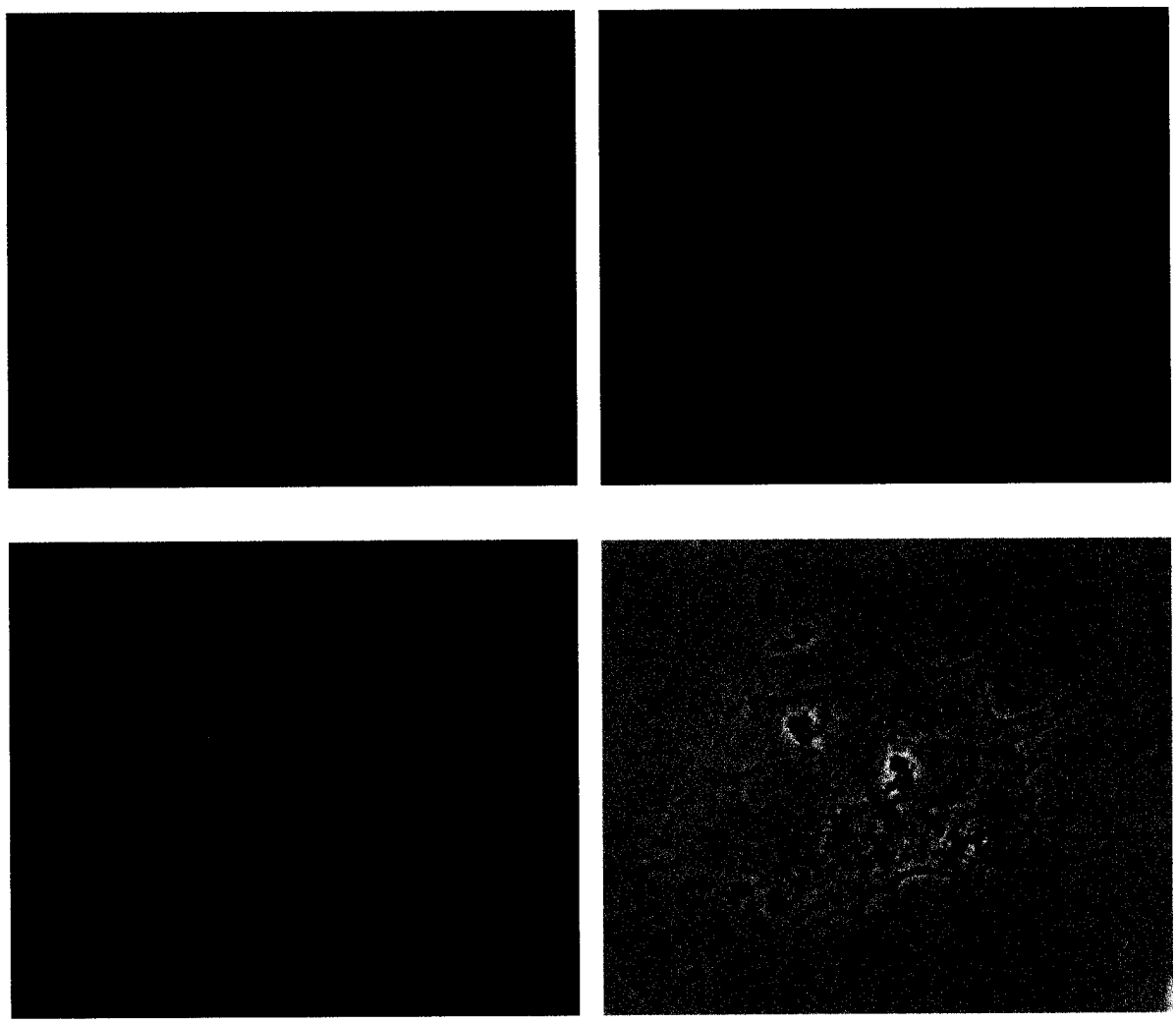

3.10 TC10Q75L increases peripheral membrane ruffling and the formation of actin stress fibers in H9C2 cells

To determine the cytoskeletal effects of TC10Q75L in another relevant cell type, mutated TC10 was transfected into an immortalized rat cardiomyocyte cell line (H9C2). In H9C2 cells, activated TC10 caused increased membrane ruffling, cell rounding and an increase in actin stress fibers (top two rows, Figure 17) compared to the typical phenotype seen in H9C2 cells transfected with wild type TC10 (bottom row, Figure 17). In this cell type, TC10Q75L also affected filamentous actin, as was observed in C2C12 cells and cardiomyocytes derived from TC10Q75L transgenic animals. However, the TC10-induced phenotype in transfected H9C2 myoblasts varied considerably from that observed in C2C12 cells, i.e. actin aggregation and actin stress fiber disassembly were not observed.

Figure 17. Peripheral membrane ruffling and increased actin stress fibers in HA-TC10Q75L H9C2 cells.

H9C2 cells were transfected with 2 μg pKH3-TC10Q75L or pKH3-TC10wt on two-well glass chamber slides. Cells expressing triple-HA-tagged TC10Q75L were stained using an anti-HA monoclonal primary antibody, followed by a Cy3-conjugated anti-mouse secondary antibody. F-actin was visualized with fluorescein-phalloidin and the nuclei were detected with DAPI. The top two rows of images were taken of cells transfected with pKH3-TC10Q75L and the bottom row of cells were transfected with pKH3-TC10wt. All pictures were taken at identical magnifications (63X).

Phase
DAPI
Phalloidin
HA
HA-TC10(Q75L)
HA-TC10wt

CHAPTER 4

4.0 Discussion

4.1 Cardiac-specific functions of TC10

The basis for any physiological differences between closely related Rho GTPases remains unknown. However, based on unique tissue and cellular expression patterns, we hypothesized that TC10 may have a striated muscle-specific function. To investigate the potential cardiac-specific functions of TC10 *in vivo*, we generated gain-of-function TC10 transgenic mice under the control of the cardiac-specific α-MHC promoter. By over-expressing constitutively active, GTPase-defective TC10Q75L in the post-natal myocardium, we were able to assess the function of this particular Rho GTPase in an appropriate tissue locale. Transgenic mice expressing high levels of TC10Q75L showed pronounced atrial enlargement, evidence of ventricular hypertrophy and dilatation and diminished cardiomyocyte membrane integrity *in vivo*. Two of the nine transgenic lines generated were also characterized by premature lethality. *In vitro*, transgenic cardiomyocytes in primary culture showed marked reorganization of the actin cytoskeleton, leading to the formation of filopodial extensions, actin aggregation and loss of stress fibers. Taken together, these observations demonstrate that TC10, a mammalian Rho GTPase, does indeed have a cardiac-specific function in the post-natal heart and suggests that TC10 functions to regulate cellular signalling to the actin cytoskeleton and processes associated with cellular growth.

The results presented in this study do indeed support the hypothesis that TC10 has a tissue-specific role in the post-natal myocardium. Previous studies have documented that TC10 is involved in actin cytoskeleton reorganization, stimulation of transcription mediated by nuclear factor κB (NF-κB), serum response factor (SRF), and the cyclin D1

promoter, and activation of JNK kinases (Murphy et al., 1999; Murphy et al., 2001; Abe et al., 2003). Given that TC10 shares a largely overlapping set of effectors with Cdc42 and a phenotype most closely related to this isoform when over-expressed *in vitro*, a plausible explanation for any physiological differences remains to be proven with certainty (Neudauer et al., 1998). Nevertheless, the different physiological roles of closely related Rho GTPases may in fact result from preferential tissue localization, developmental and/or differentiation stage specificity. Subcellular localization, specific post-translational modifications and interaction with target effectors and regulatory proteins may underlie the differences observed in the physiological functions of similar Rho GTPases (Abe et al., 2003). As such, additional experiments will be required to gain a better understanding of the role of TC10 in the adult myocardium and the signalling pathways which mediate the cardiac-specific responses observed in the present study.

4.2 Over-expression of activated TC10

Transient over-expression experiments in different cell lines have shown that TC10 is involved in a multitude of complex cellular events from actin remodeling to the activation of transcription factors. However, few experiments have studied TC10 in cell lines in which this Rho GTPase is normally expressed. Furthermore, the precise role of TC10 in an *in vivo* system has yet to be examined. Therefore to address the *in vivo* function of TC10, we chose to generate transgenic mice over-expressing constitutively active, GTPase-defective TC10Q75L in the post-natal murine heart.

Alternatively, other models could be employed to test TC10 function *in vivo*. For example, we could have attempted to disrupt endogenous TC10 activity by over-expressing the effector domain of TC10. Such a truncated protein would be hypothesized to sequester endogenous TC10 effectors, rendering the endogenous TC10 unable to complete its effector-driven functions. However there is significant overlap observed in the effectors of TC10 and Cdc42 (Neudauer et al., 1998; Kjøller and Hall, 1999). Therefore in using such a model system, it would have been difficult to determine whether any perturbations were the result of impaired TC10, Cdc42, and/or other closely related Rho GTPase proteins, i.e. experimental observations have demonstrated that TC10 and Cdc42 interact with many common effectors, including IQGAP1, α-, β- and γPAK, MRCKα/β, MLK2, N-WASP and Borg5 (Neudauer et al., 1998; Neudauer et al., 2001; Joberty et al., 1999; Osada et al., 2000; Abe et al., 2003). Moreover, the majority of these effectors contain a well-defined CRIB domain, which is necessary and sufficient for GTP-bound Rho GTPases to associate with their effectors (Joberty et al., 1999; Burbelo et al, 1995; Neudauer et al., 1998), thus making it difficult to inhibit the activity of only one specific Rho GTPase at a time.

More recently, the roles of Rho GTPases in murine cardiac development were explored using a reverse genetic approach, i.e. over-expressing Rho GDIα in a cardiac-specific manner (Wei et al., 2002). While Rho GDIα specifically inhibits RhoA, Rac1 and Cdc42 Rho family proteins, experimental evidence has demonstrated that TC10, in contrast to Cdc42 and Rac1, does not interact with RhoGDIα (Murphy et al., 2001). Hence, until specific TC10 inhibitors are identified, such an approach to study the role of TC10 in the

adult myocardium is not a feasible option. Presently, a TC10 knockout mouse does not exist. While this model would allow us to obliterate the function of TC10 in the heart to provide insight into its cardiac-specific functions, it would be a difficult strategy to pursue, as any early lethality owing to TC10 deletion would prevent the study of its role in the adult myocardium. Therefore, given the nature of Rho GTPases and their various functions in eukaryotic cell types, over-expression of activated TC10 in the post-natal heart was the most appropriate model system to employ.

4.3 Phenotypic consequences of TC10Q75L over-expression in the adult heart

4.3.1 TC10Q75L transgenic mice display cardiac hypertrophy and dilatation

A significant finding of the present study is that over-expression of activated TC10Q75L *in vivo* results in cardiac hypertrophy with associated dilatation. A pronounced cardiac phenotype developed only in the highest-expressing TC10Q75L transgenic mice, with a much milder cardiac phenotype in the lower-expressing transgenic mice. Thus, phenotypic manifestations of TC10Q75L over-expression were observed in at least three of the four established transgenic lines and appear to be dependent on a threshold level of transgene expression, a similar trend as that observed with RhoA transgenic mice (Sah et al., 1999).

4.3.2 Atrial enlargement in TC10Q75L transgenic hearts

The α-MHC promoter is typically used to direct transgene expression to the post-natal ventricles. However, in instances of elevated TC10Q75L transgene expression, an atrial phenotype was observed, i.e. pronounced atrial enlargement. This is not an unexpected

observation as the α-MHC promoter is expressed in the atria during embryonic development and also in a limited manner in the post-natal atria (Subramaniam et al., 1991; Jones et al., 1996). Similar atrial phenotypes have been observed in other cardiac-specific over-expression transgenic models, such as angiotensin AT_1 receptor and calmodulin transgenic mice, with varying alterations in heart rate and/or rhythm (Gruver et al., 1993; Hein et al., 1997). Specifically, cardiac-specific over-expression of RhoA resulted in pronounced atrial enlargement, ventricular dilatation and dysfunction, bradycardia, atrial fibrillation and atrioventricular block, suggesting that RhoA may be involved in the regulation of cardiac sinus and atrioventricular nodal function (Sah et al., 1999).

These observations beg the question: Are atrial myocytes more susceptible than ventricular myocytes to the effects of altered GTPase activity? The myocardium of higher vertebrates consists of only three distinct cell types, atrial and ventricular myocytes, in addition to endocardial endothelia. Atrial and ventricular myocytes originate from different regions of the presumptive myocardium during the linear tube stage of heart development. Whereas, cells in the rostral region become ventricular mycoytes, cells in the caudal region differentiate into atrial myocytes. These cells are distinguished based on electrophysiological characteristics and the expression of contractile proteins (Mikawa in Harvey and Rosenthall, 1999). Indeed, differences in the cellular origins of atrial and ventricular myoctes may account for the perceived differences observed in atrial versus ventricular mycoyte susceptibility to increased Rho GTPase activity. It will be interesting to pursue the functional consequences of the atrial

enlargement and ventricular hypertrophy/dilation observed in TC10Q75L transgenic hearts to verify whether it has similar functional consequences as the closely related RhoA isoform.

4.4 Premature mortality in TC10Q75L transgenic mice

Of the nine TC10Q75L transgenic founder lines identified, premature mortality was observed in two lines, or approximately 20% of these mice. Interestingly, in each instance in which TC10Q75L over-expression was associated with early lethality, these mice also expressed the transgene in tissues other than the myocardium (i.e., brain and/or skeletal muscle). This phenomenon was not observed in the viable TC10Q75L transgenic lines. In the first instance of premature mortality, the TC10Q75L transgenic founder mouse appeared to have multiple or altered sites of transgene integration, leading to severe health complications, stunted growth and hydrocephalus. In the second instance of premature death, this TC10Q75L transgenic founder appeared to legitimately over-express the TC10Q75L transgene in the adult myocardium, as this animal's heart showed signs of pronounced atrial and ventricular enlargement, increased heart weight and dilatation of ventricular chambers. Unfortunately, transcript expression was not determined as the whole hearts were used for histological purposes and viable offspring were not produced. It would be interesting to generate TC10Q75L transgenic mice with the use of cre-lox technology. The use of such an inducible system would circumvent limitations arising from temporal and spatial transgene control and would allow us to properly characterize the cardiac-specific consequences of TC10Q75L over-expression.

4.5 Over-expression of TC10Q75L in the myocardium does not affect whole body glucose metabolism or insulin sensitivity

Insulin stimulates glucose uptake in adipocytes and muscle cells by recruiting the GLUT-4 facilitative glucose transporter from intracellular compartments to the plasma membrane (as reviewed in Watson et al., 2003). Evidence from earlier research suggested that the well-characterized PI3K-dependent signalling pathway was necessary, but not sufficient to regulate this biological process (Isakoff et al., 1995; Krook et al., 1997). Recently, the activation of TC10 was also found to be involved in insulin-stimulated glucose uptake via GLUT-4 translocation. This novel insulin signalling pathway functions in parallel with the PI3K-dependent pathway, to fully stimulate GLUT-4 translocation in response to insulin (Chiang et al., 2001). Furthermore, recent data have clearly demonstrated the importance of spatial separation and distinct compartmentalization of TC10 during insulin stimulated GLUT-4 translocation (Watson et al., 2001). The compartmentalization of TC10 within lipid raft microdomains was recently found to be necessary for insulin-dependent activation of TC10 and GLUT-4 translocation (Watson et al., 2001). Specifically, expression of chimeric TC10 proteins containing the COOH-terminal domains of H-Ras, which directs the protein to the lipid raft microdomains, and K-Ras, which targets the protein to the non-lipid raft microdomains, demonstrated the importance of proper compartmentalization during TC10 function. The TC10/H-Ras chimeric protein disrupted GLUT-4 translocation; whereas, a TC10/K-Ras chimera, was unaffected by insulin and did not alter GLUT-4 translocation events (Watson et al., 2001). Furthermore, these data offered evidence supporting the importance of precise cellular localization of TC10 in signalling cascades

and provided a molecular basis for the specificity of insulin signalling with respect to glucose transport (Watson et al., 2001).

To investigate the role of TC10 in regulating glucose metabolism and insulin sensitivity, we compared body weight, fasting blood glucose and insulin tolerance measurements in wild type versus TC10Q75L transgenic mice. Preliminary results revealed consistently higher body weight measurements in TC10Q75L transgenic mice, with no significant differences in fasting blood glucose levels or insulin tolerance between wild type and transgenic mice. This confirms the notion that it is unlikely that over-expression of activated TC10 in the heart alone is sufficient to perturb whole body glucose regulation/insulin sensitivity. Furthermore, the discrepancies observed in body weight measurements are likely the result of generalized edema, a symptom often associated with decompensated heart failure (Schiff et al., 2003), which would be an obvious outcome of the cardiac phenotype noted in TC10Q75L transgenic mice. This phenotype was also noted in transgenic mice over-expressing RhoA in the adult myocardium (Sah et al., 1999), although further experimentation would be necessary to confirm this observation with certainty in TC10Q75L transgenic mice. In order to effectively assess the impact of TC10 on global glucose metabolism and insulin sensitivity, transgenic mice over-expressing the TC10Q75L transgene in adipocytes and skeletal muscle should be generated.

4.6 TC10 and actin cytoskeletal reorganization

The Rho family of GTPases exerts powerful effects upon the actin cytoskeleton and thus cellular structure. However, the precise molecular pathway that connects TC10 activity to cytoskeletal remodeling has not been fully elucidated. Although this study did not pursue the signalling aspect of this phenomenon, it is likely that TC10 impacts the actin cytoskeleton through several different signalling pathways, including the PAKs, IQGAPs and N-WASP (Figure 18) (Krebs et al., 2001; Olson, 2003; Bokoch, 2003; Johnson, 1999). However, the results of this study clearly support the role of TC10 in actin cytoskeleton reorganization, with evidence of filopodial extensions, loss of stress fibers and actin aggregation in TC10Q75L transgenic cardiomyocytes in primary culture. Given that actin reorganization is a fundamental process involved in cardiomyocyte hypertrophy, it is possible that TC10 plays a critical role in actin cytoskeleton remodeling leading to cardiomyocyte hypertrophy.

Similar cardiac phenotypes have been observed following the over-expression of Rho GTPases in cardiac cells. Specifically, in activated RhoA-infected neonatal rat ventricular myocytes, a striking increase in the assembly and organization of distinct sarcomeric units was observed, along with an increase in ANF expression (Hoshijima et al., 1998). In contrast, transgenic mice expressing constitutively active Rac1 resulted in two distinct cardiac phenotypes dependent upon temporal activation of the transgene. In neonates, a lethal dilated cardiomyopathy was observed, whereas transient cardiac hypertrophy was observed among juvenile mice, a condition that resolved with age (Sussman et al., 2000). Interestingly, neither phenotype displayed signs of myofibril

disarray suggesting that Rac1 is also involved in reorganization of the actin cytoskeleton. Additional studies are needed to investigate the role of TC10 in signalling to the actin cytoskeleton during cardiac remodeling events and to assess the participation of the aforementioned families of proteins.

Figure 18. Mammalian targets of the TC10 GTPase involved in transcriptional activation and actin rearrangements.

This is a schematic representation of the probable signalling pathways that are activated by TC10. Inactive TC10·GDP is shown in *red* and active TC10·GTP is shown in *green*. TC10 cycles between inactive and active states, regulated by TC10 GAPs, which inactivate TC10, and GEFs, which activate TC10. The kinases belonging to the MAPK and PAK families are shown in *yellow*, while additional targets of TC10 are depicted in *blue*. For simplicity and for the lack of fully identified signalling pathways, not all components of the JNK kinase cascade or the actin cytoskeleton cascade are shown. This figure was adapted from: Johnson, 1999.

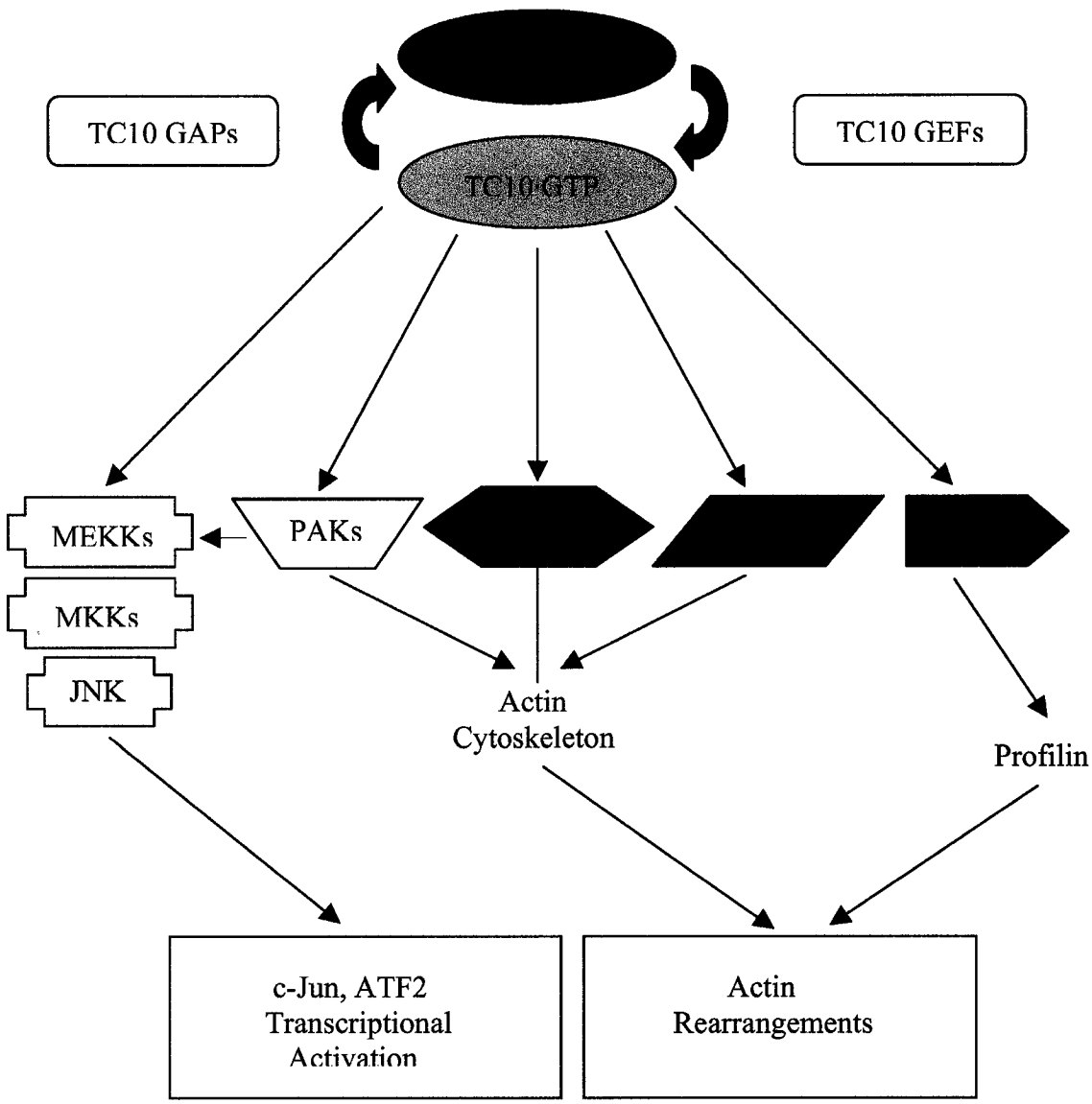

Adapted from Johnson, 1999.

4.7 Discrepancy in C2C12 and H9C2 phenotypes following transient transfection

Phenotypic differences were noted following transient transfections with HA-tagged TC10Q75L in C2C12 myoblasts and H9C2 cardiomyocytes. In C2C12 cells, over-expression of activated TC10 disrupted filamentous actin and induced peripheral membrane extensions, similar to the phenotypic consequences observed in TC10Q75L transgenic cardiomyocytes. However, TC10Q75L over-expression in H9C2 cells led to cell rounding, peripheral membrane ruffling and the formation of actin stress fibers. This discrepancy could possibly be due to the unusual nature of the H9C2 immortalized cell line, i.e., these cardiomyocytes fuse *in vitro* to form myotube structures, a feature uncharacteristic to cardiac myocytes *in vivo* or primary cardiac myocytes *in vitro*. Additionally, it is difficult to control the experimental parameters following transient transfections, as protein levels can diminish rapidly and/or the protein may not be available for enough time to exert its true biological effects. Nevertheless, it is clear from the transient transfection studies that TC10 is indeed intertwined in signalling events that regulate the actin cytoskeleton.

4.8 TC10 and JNK1 in cardiac hypertrophy and dilated cardiomyopathy

4.8.1 Regulation of JNK1 activation by TC10Q75L

Cdc42 and Rac1 provide inductive signals for the JNK and p38 kinase cascades (Minden et al., 1995; Moriguchi et al., 1995; Frost et al., 1996). This activation is likely mediated through the PAKs (Bagrodia et al., 1999; Daniels et al., 1999). Experimental evidence has also implicated TC10 in the stimulation of JNK and PAK kinase activities (Neudauer et al., 1998; Murphy et al., 1999). However, the vast majority of these conclusions have

been drawn from transfection experiments. While this type of experiment is beneficial in establishing active signalling pathways in cells, over-expression of signalling intermediates may inappropriately activate or inhibit other signal pathways, not normally associated with the biological processes being examined (Clerk et al., 2001).

To begin to characterize the role of TC10 activation of JNK1 during cardiac growth, JNK1 phosphorylation and activation were assessed in wild type and TC10Q75L transgenic heart protein lysates. Indeed, JNK1 activity was higher in TC10Q75L transgenic protein heart lysates compared to wild type counterparts. These findings suggest a model whereby TC10-induced cardiac hypertrophy/dilation may be dependent on the stimulation of JNK1 kinase activity.

Although conflicting evidence has emerged surrounding the role of JNK in hypertrophic signalling in the heart, it is perhaps an indication of the complexity of MAPK signalling in this response. Nonetheless, more recent *in vivo* and *in vitro* experimental evidence strongly implicates JNK activation as a necessary component of the cardiomyocyte hypertrophic response (Molkentin and Dorn II, 2001). Collectively, these observations suggest that elevated JNK activity may promote the cardiomyocyte hypertrophy observed in TC10Q75L transgenic mice. More importantly, it has been suggested that JNK activity may promote the transition from a hypertrophic to a dilated state (Molkentin and Dorn II, 2001). This hypothesis is certainly consistent with observations in the current study.

4.8.2 Rho family activation of JNK1 in the cardiac lineage

There is considerable debate surrounding the intracellular signalling pathways that regulate the hypertrophic response in cardiomyoyctes (Sugden and Clerk, 1998; Sugden, 1999). Rho GTPases are widely accepted as key regulators of the actin cytoskeleton. Consequently, this family of small proteins has become the focus of considerable attention, as remodeling of the actin cytoskeleton into distinct sarcomeric structures is a hallmark of cardiomyocyte hypertrophy (Clerk and Sugden, 2000; Clerk et al., 2001). Previous experimental evidence supports a role for RhoA and Rac1 in cardiomyocyte hypertrophy, as activation mutants induce a hypertrophic pattern of gene expression and inhibitory mutants decrease the response to phenylephrine-induced hypertrophy (Thorburn et al., 1997; Pracyk et al., 1998; Hoshijima et al., 1998; Hines et al., 1998). Indeed, the hypertrophy observed in TC10Q75L transgenic hearts mirrors the reported effects of the Rho family.

Recent evidence implicating Rho GTPases in cell growth came following injection of RhoA, Rac1 and Cdc42 in Swiss 3T3 fibroblasts, which stimulated cell cycle progression through the G_1 phase and subsequent DNA synthesis (Olsen et al., 1995; Van Aelst and D'Souza-Schorey, 1997). Likewise, activated TC10 has been shown to stimulate transcription of the cyclin D1 promoter, an indication that perhaps this Rho GTPase is also involved in the regulation of cell growth (Murphy et al., 2001). Furthermore, providing the effector domains are intact, activated TC10, like Rac1 and Cdc42, has been shown to activate JNK (Murphy et al., 1999; Neudauer et al., 1998; Minden et al., 1995; Coso et al., 1995; Teramoto et al., 1996). Although the transcription factors that respond

to JNK activation by TC10 have not been identified, it is possible that, in the heart, the zinc finger-containing GATA subfamily of transcription factors (GATA4/5/6) are involved (Liang et al., 2001). This speculation is based on the fact that GATA4 was recently identified as a nuclear mediator of RhoA signalling in the heart, controlling sarcomeric assembly in cardiomyocytes (Charron et al., 2001; Liang et al., 2001). Additionally, cardiac-specific over-expression of GATA4 in transgenic mice resulted in cardiac hypertrophy and functional impairment (Charron et al., 2001; Liang et al., 2001). Further experimentation in TC10Q75L transgenic mice will need to be performed in order to confirm or refute the role of GATA transcription factors in any putative TC10/JNK cascade.

4.9 Conclusions and future research directions

Similar to other Rho GTPases, TC10 is involved in a vast array of cellular processes. This study, the first known examination of TC10-mediated effects *in vivo*, reinforces the hypothesis that GTPase function is determined in part by tissue specificity and cellular localization. In reference to TC10, a definitive role for this Rho GTPase has been established for the processes associated with actin cytoskeleton reorganization and cardiac growth. Vigorous exploration of the precise signalling intermediates involved in these phenotypes will be needed to determine the molecular basis for actin rearrangement and cellular growth. Finally, over-expression of different mutant forms of the TC10 protein, individually and in combination, will continue to provide insight into the tissue-specific roles for this protein *in vivo*.

References

Abe T, Kato M, Miki H, Takenawa T, and Endo T. (2003). Small GTPase TC10 and its homologue RhoT induce N-WASP-mediated long process formation and neurite outgrowth. *J Cell Sci* 116: 155-168.

Aikawa R, Komuro I, Yamazaki T, Zou Y, Kudoh S, Zhu W, Kadowaki T, and Yazaki Y. (1999). Rho family small G proteins play critical roles in mechanical stress-induced hypertrophic responses in cardiac myocytes. *Circ Res* 84: 458-466.

Aoki H, Richmond M, Izumo S, and Sadoshima J. (2000). Specific role of the extracellular signal-regulated kinase pathway in angiotensin II-induced cardiac hypertrophy in vitro. *Biochem J* 347: 275-284.

Argentin S, Ardati A, Tremblay S, Lihrmann I, Robitaille L, Drouin J, and Nemer M. (1994). Developmental stage-specific regulation of atrial natriuretic factor gene transcription in cardiac cells. *Mol Cell Biol* 14: 777-790.

Bagrodia S, Bailey D, Lenard Z, Hart M, Guan JL, Premont RT, Taylor SJ and Cerione RA. (1999). A tyrosine-phosphorylated protein that binds to an important regulatory region on the cool family of p21-activated kinase-binding proteins. *J Biol Chem* 274(32): 22393-22400.

Bar-Sagi D and Hall A. (2000). Ras and Rho GTPases: A family reunion. *Cell* 103: 227-238.

Bishop AL and Hall A. (2000). Rho GTPases and their effector proteins. *Biochem J* 348: 241-255.

Bogoyevitch MA, Gillespie-Brown J, Ketterman AJ, Fuller SJ, Ben-Levy R, Ashworth A, Marshall CS, and Sugden PH. (1996). Stimulation of the stress-activated mitogen-activated protein kinase subfamilies in perfused heart. p38/RK mitogen-activated protein

kinases and c-Jun N-terminal kinases are activated by ischemia/reperfusion. *Circ Res* 79: 162-73.

Bokoch, GM. (2003). Biology of the p21-activated kinases. *Annu Rev Biochem* 72: 743-781.

Bueno OF, De Windt LJ, Tymitz KM, Witt SA, Kimball TR, Klevitsky R, Hewett TE, Jones SP, Lefer DJ, Peng CF, Kitsis RN, and Molkentin JD. (2000). The MEK1-ERK1/2 signaling pathway promotes compensated hypertrophy in transgenic mice. *EMBO* 19(23): 6341-6350.

Burbelo PD, Drechsel D, and Hall A. (1995). A conserved binding motif defines numerous candidate target proteins for both Cdc42 and Rac GTPases. *J Biol Chem* 270(49): 29071-29074.

Chang L, Adams RD, and Saltiel AR. (2002). The TC10-interacting protein CIP4/2 is required for insulin-stimulated Glut4 translocation in 3T3L1 adipocytes. *PNAS*: 99(20): 12835-12840.

Chang L and Karin M. (2001). Mammalian MAP kinase signalling cascades. *Nature* 410: 37-40.

Charron F, Tsimiklis G, Arcand M, Robitaille L, Liang Q, Molkentin JD, Meloche S, and Nemer M. (2001). Tissue-specific GATA factors are transcriptional effectors of the small GTPase RhoA. *Genes Dev* 15: 2702-2719.

Chiang S-H, Baumann CA, Kanzaki M, Thurmond DC, Watson RT, Neudauer CL, Macara IG, Pessin JE, and Saltiel AR. (2001). Insulin-stimulated GLUT4 translocation requires the CAP-dependent activation of TC10. *Nature* 410: 944-948.

Chiang S-H, Hou JC, Hwang J, Pessin JE, and Saltiel AR. (2002). Cloning and functional characterization of related TC10 isoforms, a subfamily of Rho proteins involved in

insulin-stimulated glucose transport. *J Biol Chem* 277(15): 13067-13073.

Choukroun G, Hajjar R, Fry S, del Monte F, Haq S, Guerrero JL, Picard M, Rosenzweig A, and Force T. (1999). Regulation of cardiac hypertrophy in vivo by the stress-activated protein kinases/c-Jun NH_2-terminal kinases. *J Clin Invest* 104: 391-398.

Clerk A, Pham FH, Fuller SJ, Sahai E, Aktories K, Marais R, Marshall C, and Sugden PH. (2001). Regulation of the Mitogen-Activated Protein Kinases in cardiac myocytes through the small G protein Rac1. *Mol Cell Biol* 21(4): 1173-1184.

Clerk A and Sugden PH. (2000). Small guanine nucleotide-binding proteins and myocardial hypertrophy. *Circ Res* 86: 1019-1023.

Coso OA, Chiariello M, Yu JC, Teramoto H, Crespo P, Xu N, Miki T, and Gutkind JS. (1995). The small GTP-binding proteins Rac1 and Cdc42 regulate the activity of the JNK/SAPK signaling pathway. *Cell* 81: 1137-1146.

Daniels RH, Zenke FT, and Bokoch GM. (1999). alphaPix stimulates p21-activated kinase activity through exchange factor-dependent and –independent mechanisms. *J Biol Chem* 274: 6047-6050.

Davis RJ. (2000). Signal transduction by the JNK group of MAP kinases. *Cell* 103: 239-252.

De Windt LJ, Lim HW, Haq S, Force T, and Molkentin JD. (2000). Calcineurin promotes protein kinase C and c-Jun NH_2-terminal kinase activation in the heart: Cross-talk between cardiac hypertrophic signaling pathways. *J Biol Chem* 275(18): 13571-13579.

DiDonato CJ, Lorson CL, De Repentigny Y, Simard L, Chartrand C, Androphy EJ, and Kothary R. (2001). Regulation of murine survival motor neuron (Smn) protein levels by modifying Smn exon 7 splicing. *Hum Mol Genet* 10(23): 2727-2736.

Drivas GT, Shih A, Coutavas E, Rush MG, and D'Eustachio P. (1990). Characterization of four

novel ras-like genes expressed in a human teratocarcinoma cell line. *Mol Cell Biol* 10(4): 1793-1798.

Etienne-Manneville S and Hall A. (2002). Rho GTPases in cell biology. *Nature* 420: 629-635.

Fidyk NJ and Cerione RA. (2002). Understanding the catalytic mechanism of GTPase-activating proteins: Demonstration of the importance of switch domain stabilization in the stimulation of GTP hydrolysis. *Biochem* 41: 15644-15653.

Finkel T. (1999). Myocyte hypertrophy: the long and winding RhoA'd. *J Clin Inv* 103(12): 1619-1620.

Frost JA, Xu S, Hutchison MR, Marcus S, and Cobb MH. (1996). Actions of Rho family small G proteins and p21-activated protein kinases on mitogen-activated protein kinase family members. *Mol Cell Biol* 16(7): 3707-3713.

Galbiati F, Ranzani B, and Lisanti MP. (2001). Emerging themes in lipid rafts and caveolae. *Cell* 106: 403-411.

Gruver CL, DeMayo F, Goldstein MA, and Means AR. (1993). Targeted developmental overexpression of calmodulin induces proliferative and hypertrophic growth of cardiomyocytes in transgenic mice. *Endocrinology* 133(1): 376-388.

Gual P, Shigematsu S, Kanzaki M, Grémeaux T, Gonzalez T, Pessin JE, Le Marchand-Brustel Y, and Tanti J-F. (2002). A Crk-II/TC10 signaling pathway is required for osmotic shock-stimulated glucose transport. *J Biol Chem* 277(46): 43980-43986.

Hamer PW, McGeachie JM, Davies MJ, and Grounds MD. (2002). Evans Blue Dye as an *in vivo* marker of myofibre damage: Optimising parameters for detecting initial myofibre membrane permeability. *J Anat* 200: 69-79.

Hart MJ, Eva A, Zangrilli D, Aaronson SA, Evans T, Cerione RA, and Zheng Y. (1994).

Cellular transformation and guanine nucleotide exchange activity are catalyzed by a common domain on the dbl oncogene product. *J Biol Chem* 269(1): 62-65.

Harvey RP and Rosenthal N. (1999). Heart Development (1 ed.). Academic Press, CA, USA: 19-33.

Hein L, Stevens ME, Barsh GS, Pratt RE, Kobilka BK, and Dzau VJ. (1997). Overexpression of angiotensin AT_1 receptor transgene in the mouse myocardium produces a lethal phenotype associated with myocyte hyperplasia and heart block. *Proc Natl Acad Sci* 94: 6391-6396.

Heo WD and Meyer T. (2003). Switch-of-function mutants based on morphology classification of Ras superfamily small GTPases. *Cell* 113: 315-328.

Hines WA and Thorburn A. (1998). Ras and Rho are required for Gαq-induced hypertrophic gene expression in neonatal rat cardiac myocytes. *J Mol Cell Cardiology* 30: 485-494.

Hoffman GR, Nassar N, and Cerione RA. (2000). Structure of the Rho family GTP-binding protein Cdc42 in complex with the multifunctional regulator RhoGDI. *Cell* 100: 345-356.

Hogan B, Beddington R, Costantini F, and Lacy E. (1994). Manipulating the mouse embryo: A laboratory manual (2 ed.). Cold Spring Harbor Laboratory Press, NY, USA: 217-250.

Hogan B and Tilly R. (1977). In vitro culture and differentiation on normal mouse blastocysts. *Nature* 265: 626-629.

Hoshijima M, Sah VP, Wang Y, Chien KR, and Heller Brown J. (1998). The low molecular weight GPase Rho regulates myofibril formation and organization in neonatal rat ventricular myocytes: Involvement of Rho kinase. *J Biol Chem* 273(13): 7725-7730.

Hunter JJ, Tanaka N, Rockman HA, Ross Jr. J, and Chien KR. (1995). Ventricular expression of a MLC-2*v*-*ras* fusion gene induces cardiac hypertrophy and selective diastolic dysfunction in transgenic mice. *J Biol Chem* 270(39): 23173-23178.

Ichida M and Finkel T. (2001). Ras regulates NFAT3 activity in cardiac myocytes. *J Biol Chem* 276(5): 3524-3530.

Inoue M, Chang L, Hwang J, Chiang S-H, and Saltiel AR. (2003). The exocyst complex is required for targeting of Glut4 to the plasma membrane by insulin. *Nature* 422: 629-633.

Isakoff SJ, Taha C, Rose E, Marcusohn J, Klip A, and Skolnik EY. (1995). The inability of phosphatidylinositol 3-kinase activation to stimulate GLUT4 translocation indicates additional signaling pathways are required for insulin-stimulated glucose uptake. *Proc Natl Acad Sci* 92: 10247-10251.

Joberty G, Perlungher RR, and Macara IG. (1999). The Borgs, a new family of Cdc42 and TC10 GTPase-interacting proteins. *Mol Cell Biol* 19(10): 6585-6597.

Johnson DI. (1999). Cdc42: An essential Rho-type GTPase controlling eukaryotic cell polarity. *Microbiol Mol Biol Rev* 63(1): 54-105.

Jones WK, Grupp IL, Doetschman T, Grupp G, Osinska H, Hewett TE, Boivin G, Gulick J, Ng WA, and Robbins J. (1996). Ablation of the murine α myosin heavy chain gene leads to dosage effects and functional deficits in the heart. *J Clin Inv* 98(8): 1906-1917.

Jones WK, Sánchez A, and Robbins J. (1994). Murine pulmonary myocardium: Developmental analysis of cardiac gene expression. *Devel Dynamics* 200: 117-128.

Kanzaki M and Pessin JE. (2002). Caveolin-associated filamentous actin (Cav-actin) defines a novel F-actin structure in adipocytes. *J Biol Chem* 277(29): 25867-25869.

Kanzaki M, Watson RT, Hou JC, Stamnes M, Saltiel AR, and Pessin JE. (2002). Small GTP-binding protein TC10 differentially regulates two distinct populations of filamentous actin on 3T3L1 adipocytes. *Mol Biol Cell* 13: 2334-2346.

Khan AH and Pessin JE. (2002). Insulin regulation of glucose uptake: a complex interplay of intracellular signalling pathways. *Diabetologia* 45: 1475-1483.

Kjφller L and Hall A. (1999). Signaling to Rho GTPases. *Exp Cell Res* 253: 166-179.

Kolodziejczyk SM, Walsh GS, Balazsi K, Seale P, Sandoz J, Hierlihy AM, Rudnicki MA, Chamberlain JS, Miller FD, and Megeney LA. (2001). Activation of JNK1 contributes to dystrophic muscle pathogenesis. *Curr Biol* 11: 1-20.

Kolodziejczyk SM, Wang L, Balazsi K, DeRepentigny Y, Kothary R, and Megeny LA. (1999). MEF2 is upregulated during cardiac hypertrophy and is required for normal post-natal growth of the myocardium. *Curr Biol* 9: 1203-1206.

Krebs A, Rothkegel M, Klar M, and Jockusch BM. (2001). Characterization of functional domains of mDia1, a link between the small GTPase Rho and the actin cytoskeleton. *J Cell Sci* 114: 3663-3672.

Krook A, Whitehead JP, Dobson SP, Griffiths MR, Ouwens M, Baker C, Hayward AC, Sen SK, Maassen JA, Siddle K, Tavaré JM, and O'Rahilly S. (1997). Two naturally occurring insulin receptor tyrosine kinase domain mutants provide evidence that phosphatidylinositol 3-kinase activation is not sufficient for the mediation of insulin's metabolic and mitogenic effects. *J Biol Chem* 272(48): 30208-30214.

Li R, Zhang B, and Zheng Y. (1997). Structural determinants required for the interaction between Rho GTPase and the GTPase-activating domain of p190. *J Biol Chem* 272(52): 32830-32835.

Liang Q, De Windt LJ, Witt SA, Kimball TR, Markham BE, and Molkentin JD. (2001). The transcriptional factors GATA4 and GATA6 regulate cardiomyocyte hypertrophy *in vitro* and *in vivo*. *J Biol Chem* 276(32): 30245-30253.

Mackay DJG and Hall A. (1998). Rho GTPases. *J Biol Chem* 273(33): 20685-20688.

Megeney LA, Kablar B, Perry RLS, Ying C, May L, and Rudnicki MA. (1999). Severe cardiomyopathy in mice lacking dystophin and MyoD. *Proc Natl Acad Sci* 96: 220-225.

Michaelson D, Silletti J, Murphy G, D'Eustachio P, Rush M, and Philips MR. (2001). Differential localization of Rho GTPases in live cells: Regualtion by hypervariable regions and RhoGDI binding. *J Cell Biol* 152(1): 111-126.

Minden A, Lin A, Claret F-X, Abo A, and Karin M. (1995). Selective activation of the JNK signaling cascade and c-Jun transcriptional activity by the small GTPases Rac and Cdc42Hs. *Cell* 81: 1147-1157.

Molkentin JD. (2000). Calcineurin and beyond: Cardiac hypertrophic signaling pathway. *Circ Res* 87: 731-738.

Molkentin JD and Dorn II GW. (2001). Cytoplasmic signaling pathways that regulate cardiac hypertrophy. *Annu Rev Physiol* 63: 391-426.

Molkentin JD, Lu J-R, Antos CL, Markham B, Richardson J, Robbins J, Grant SR, and Olson EN. (1998). A calcineurin-dependent transcriptional pathway for cardiac hypertrophy. *Cell* 93: 215-228.

Moon SY and Zheng Y. (2003). Rho GTPase-activating proteins in cell regulation. *Trends Cell Biol* 13(1): 13-22.

Moriguchi T, Kawasaki H, Matsuda S, Gotoh Y, and Nishida E. (1995). Evidence for multiple activators for stress-activated protein kinases/c-Jun amino-terminal kinases. *J Biol Chem* 270(22): 12969-12972.

Murphy GA, Jillian SA, Michaelson D, Philips MR, D'Eustachio P, and Rush MG. (2001). Signaling mediated by the closely related mammalian Rho family GTPases TC10 and Cdc42 suggests distinct functional pathways. *Cell Growth Differ* 12: 157-167.

Murphy GA, Solski PA, Jillian SA, Pérez de la Ossa P, D'Eustachio P, Der CJ, and Rush MG. (1999). Cellular functions of TC10, a Rho family GTPase: regulation of morphology, signal transduction and cell growth. *Oncogene* 18: 3831-3845.

Nemoto S, Sheng Z, and Lin A. (1998). Opposing effects of Jun kinase and p38 mitogen-activated protein kinases on cardiomyocyte hypertrophy. *Mol Cell Biol* 18(6): 3518-3526.

Neudauer CL, Joberty G, and Macara IG. (2001). PIST: A novel PDZ/coiled-coil domain binding partner for the Rho-family GTPase TC10. *Biochem Biophys Res Comm* 280: 541-547.

Neudauer CL, Joberty G, and Macara IG. (2000). Purification and biochemical characterization of TC10. *Methods Enzymol* 325: 3-14.

Neudauer CL, Joberty G, Tatsis N, and Macara IG. (1998). Distinct cellular effects and interactions of the Rho-family GTPase TC10. *Curr Biol* 8: 1151-1160.

Olson MF. (2003). GTPase signalling: New functions for diaphanous-related formins. *Curr Biol* 13: R360-362.

Olson MF, Ashworth A, and Hall A. (1995). An essential role for Rho, Rac, and Cdc42 GTPases in cell cycle progression through G1. *Science* 269: 1270-1272.

Osada N, Kusuda J, Suzuki Y, Sugano S, and Hashimoto K. (2000). Sequence analysis, gene expression, and chromosomal assignment of mouse *Borg4* gene and its human orthologue. *J Human Genet* 45(6): 374-377.

Pracyk JB, Tanaka K, Hegland DD, Kim K-S, Sethi R., Rovira II, Blazina DR, Lee L, Bruder JT, Kovesdi I, Goldschmidt-Clermont PJ, Irani K, and Finkel T. (1998). A requirement for the Rac1 GTPase in the signal transduction pathway leading to cardiac myocyte hypertrophy. *J Clin Invest* 102(5): 929-937.

Ramirez MT, Sah VP, Zhao XL, Hunter JJ, Chien KR, and Brown JH. (1997). The MEKK-JNK pathway is stimulated by α_1-adrenergic receptor and Ras activation and is associated with in vitro and in vivo cardiac hypertrophy. *J Biol Chem* 272(22): 14057-14061.

Ren Y, Li R, Zheng Y, and Busch H. (1998). Cloning and characterization of GEF-H1, a microtubule-associated guanine nucleotide exchange factor for Rac and Rho GTPases. *J Biol Chem* 273(52): 34954-34960.

Ridley A. (2000). Rho GTPases: Integrating integrin signaling. *J Cell Biol* 150(4): F107-109.

Robbins J, Gulick J, Sanchez A, Howles P, and Doetschman T. (1990). Mouse embryonic stem cells express the cardiac myosin heavy chain genes during development *in vitro*. *J Biol Chem* 265(20): 11905-11909.

Sah VP, Hoshijima M, Chien KR, and Heller Brown J. (1996). Rho is required for $G\alpha_q$ and α_1-adrenergic receptor signaling in cardiomyocytes: Dissociation of Ras and Rho pathways. *J Biol Chem* 271(49): 31185-31190.

Sah VP, Minamisawa S, Tam SP, Wu TH, Dorn II GW, Ross Jr. J, Chien KR, and Heller Brown J. (1999). Cardiac-specific overexpression of RhoA results in sinus and atrioventricular nodal dysfunction and contractile failure. *J Clin Inv* 103(12): 1627-1634.

Saltiel AR and Pessin JE. (2002). Insulin signaling pathways in time and space. *Trends Cell Biol* 12(2): 65-71.

Schiff GD, Fung S, Speroff T, and McNutt RA. (2003). Decompensated heart failure: Symptoms, patterns of onset, and contributing factors. *Am J Med* 114: 625-630.

Schmitz AAP, Govek E-E, Böttner B, and Van Aelst L. (2000). Rho GTPases: Signaling, migration, and invasion. *Exp Cell Res* 261: 1-12.

Subramaniam A, Jones WK, Gulick J, Wert S, Neumann J, and Robbins J. (1991). Tissue-specific regulation of the α-myosin heavy chain gene promoter in transgenic mice. *J Biol Chem* 266(36): 24613-24620.

Sugden PH. (1999). Signaling in myocardial hypertrophy: Life after calcineurin? *Circ Res* 84: 633-646.

Sugden PH and Clerk A. (1998). "Stress-responsive" mitogen-activated protein kinases (c-Jun N-terminal kinases and p38 mitogen-activated protein kinases) in the myocardium. *Circ Res* 83: 345-352.

Sussman MA, Welch S, Walker A, Klevitsky R, Hewett TE, Price RL, Schaefer E, and Yager K. (2000). Altered focal adhesion regulation correlates with cardiomyopathy in mice expressing constitutively active rac1. *J Clin Invest* 105: 875-886.

Tanabe K, Tachibana T, Yamashita T, Che YH, Yoneda Y, Ochi T, Tohyama M, Yoshikawa H, and Kiyama H. (2000). The small GTP-binding protein TC10 promotes nerve elongation in neuronal cells, and its expression is induced during nerve regeneration in rats. *J Neurosci* 20(11): 4138-4144.

Teramoto H, Coso OA, Miyata H, Igishi T, Miki T, and Gutkind JS. (1996). Signaling from the small GTP-binding proteins Rac1 and Cdc42 to the c-Jun N-terminal Kinase/Stress-

Activated Protein Kinase pathway. *J Biol Chem* 271(44): 27225-27228.

Teramoto H, Crespo P, Coso OA, Igishi T, Xu N, and Gutkind JS. (1996). The small GTP-binding protein Rho activates c-Jun N-terminal Kinases/Stress-Activated Protein Kinases in human kidney 293T cells. *J Biol Chem* 271(42): 25731-25734.

Thorburn A, Thorburn J, Chen S-Y, Powers S, Shubeita HE, Feramisco JR, and Chien KR. (1993). HRas-dependent pathways can activate morphological and genetic markers of cardiac muscle cell hypertrophy. *J Biol Chem* 268(3): 2244-2249.

Thorburn J, Xu S, and Thorburn A. (1997). MAP kinase- and Rho-dependent signals interact to regulate gene expression but not actin morphology in cardiac muscle cells. *EMBO* 16(8): 1888-1900.

Van Aelst L and D'Souza-Schorey C. (1997). Rho GTPases and signaling networks. *Genes Devel* 11: 2295-2322.

Vidal C, Geny B, Melle J, Jandrot-Perrus M, and Fontenay-Roupie M. (2002). Cdc42/Rac1-dependent activation of the p21-activated kinase (PAK) regulates human platelet lamellipodia spreading: implication of the cortical-actin binding protein cortactin. *Blood* 100(13): 4462-4469.

Vignal E, De Toledo M, Comunale F, Ladopoulou A, Gauthier-Rouviere C, Blangy A, and Fort P. (2000). Characterization of TCL, a new GTPase of the Rho Family related to TC10 and Cdc42. *J Biol Chem* 275(46): 36457-36464.

Wang Y, Su B, Sah VP, Brown JH, Han J, and Chien KR. (1998). Cardiac hypertrophy induced by mitogen-activated protein kinase kinase 7, a specific activator for c-Jun NH2-terminal kinase in ventricular muscle cells. *J Biol Chem* 273(10): 5423-5426.

Wang S-W, Tsai Y-J, Jiang M-J, and Tseng Y-Z. (1997). Studies on the function of Rho A

protein in cardiac myofibrillogenesis. *J Cel Biochem* 66: 43-53.

Watson RT, Furukawa M, Chiang S-H, Boeglin D, Kanzaki M, Saltiel AR, and Pessin JE. (2003). The exocytotic trafficking of TC10 occurs through both classical and nonclassical secretory transport pathways in 3T3L1 adipocytes. *Mol Cell Biol* 23(3): 961-974.

Watson RT, Shigematsu S, Chiang S-H, Mora S, Kanzaki M, Macara IG, Saltiel AR, and Pessin JE. (2001). Lipid raft microdomain compartmentalization of TC10 is required for insulin signaling and GLUT4 translocation. *J Cell Biol* 154: 829-840.

Wei L, Imanaka-Yoshida K, Wang L, Zhan S, Schneider MD, DeMayo FJ, and Schwartz RJ. (2002). Inhibition of Rho family GTPases by Rho GDP dissociation inhibitor disrupts cardiac morphogenesis and inhibits cardiomyocyte proliferation. *Development* 129: 1705-1714.

Wu W-J, Leonard DA, Cerione RA, and Manor D. (1997). Interaction between Cdc42Hs and Rho GDI is mediated through the Rho insert region. *J Biol Chem* 272(42): 26153-26158.

Zhang S, Han J, Sells MA, Chernoff J, Knaus UG, Ulevitch RJ, and Bokoch GM. (1995). Rho family GTPases regulate p38 mitogen-activated protein kinase through the downstream mediator Pak1. *J Biol Chem* 270(41): 23934-23936.

Zhao Y-Y, Liu Y, Stan R-V, Fan L, Gu Y, Dalton N, Chu P-H, Peterson K, Ross Jr. J, and Chien KR. (2002). Defects in caveloin-1 cause dilated cardiomyopathy and pulmonary hypertension in knockout mice. *PNAS* 99(17): 11375-11380.

Zheng Y, Olson MF, Hall A, Cerione RA, and Toksoz D. (1995). Direct involvement of the small GTP-binding protein Rho in lbc oncogene function. *J Biol Chem* 270(16): 9031-9034.

Zhou K, Wang Y, Gorski JL, Nomura N, Collard J, and Bokoch GM. (1998). Guanine nucleotide exchange factors regulate specificity of downstream signaling from Rac and Cdc42. *J Biol Chem* 273(27): 16782-16786.

APPENDICES

Appendix A: Human TC10 Clone

A) Complete mRNA sequence (642 bp), NCBI accession # M31470

```
  1 atgcccggag ccggccgcag cagcatggct cacgggcccg gcgcgctgat gctcaagtgc
 61 gtggtggtcg gcgacggggc ggtgggcaag acgtgcctac tcatgagcta tgccaacgac
121 gccttcccgg aggagtacgt gcccaccgtc ttcgaccact acgcagtcag cgtcaccgtg
181 gggggcaagc agtacctcct aggactctat gacacggccg gacaggaaga ctatgaccgt
241 ctgaggcctt tatcttaccc aatgaccgat gtcttcctta tatgcttctc ggtggtaaat
301 ccagcctcat ttcaaaatgt gaaagaggag tgggtaccgg aacttaagga atacgcacca
361 aatgtaccct ttttattaat aggaactcag attgatctcc gagatgaccc caaaacttta
421 gcaagactga atgatatgaa agaaaaacct atatgtgtgg aacaaggaca gaaactagca
481 aaagagatag gagcatgctg ctatgtggaa tgttcagctt taacccagaa gggattgaag
541 actgtttttg atgaggctat catagccatt ttaactccaa agaaacacac tgtaaaaaaa
601 agaataggat caagatgtat aaactgttgt ttaattacgt ga
```

B) Complete amino acid sequence (213 amino acids)

```
MPGAGRSSMAHGPGALMLKCVVVGDGAVGKTCLLMSYANDAFPEEYVPTVFDHYAVSVTVGGKQYLLGLYD
TAGQEDYDRLRPLSYPMTDVFLICFSVVNPASFQNVKEEWVPELKEYAPNVPFLLIGTQIDLRDDPKTLAR
LNDMKEKPICVEQGQKLAKEIGACCYVECSALTQKGLKTVFDEAIIAILTPKKHTVKKRIGSRCINCCLIT
```

The constitutively active, GTPase-defective TC10 mutant, TC10Q75L, was accomplished as follows:

cag→cug (a to u base substitution at nucleotide 224) resulting in a Q to L amino acid substitution at amino acid 75

Note: the bases and amino acids of interest are underlined.

Complete Lineage List 4969

Mouse ID	tg/wt	Sex	Birth Date	Death Date	Female Parent	Male Parent
4969	tg	M	16-May-01	02-Apr-02	Surrogate	N/A
1105	tg	M	17-Jul-01	03-Jan-02	wt	4969
1106	wt	M	17-Jul-01	17-Jan-03	wt	4969
1110	tg	F	17-Jul-01	16-Oct-01	wt	4969
1453	tg	F	17-Jul-01	29-May-03	wt	4969
1600	tg	F	17-Jul-01	29-May-03	wt	4969
1862	tg	M	17-Jul-01	26-Jun-02	wt	4969
1863	tg	F	17-Jul-01	29-May-03	wt	4969
1864	wt	F	17-Jul-01	29-May-03	wt	4969
2066	tg	M	17-Jul-01	17-Jan-03	wt	4969
1158	wt	M	08-Aug-01	08-Jan-02	wt	4969
1159	tg	M	08-Aug-01	08-Jan-02	wt	4969
1160	wt	M	08-Aug-01	12-Sep-01	wt	4969
1161	wt	M	08-Aug-01	12-Sep-01	wt	4969
1162	wt	F	08-Aug-01	12-Sep-01	wt	4969
1163	wt	F	08-Aug-01	12-Sep-01	wt	4969
1164	wt	F	08-Aug-01	12-Sep-01	wt	4969
1165	wt	F	08-Aug-01	12-Sep-01	wt	4969
1166	wt	F	08-Aug-01	12-Sep-01	wt	4969
1359	wt	M	14-Sep-01	04-Oct-01	wt	4969
1360	wt	M	14-Sep-01	04-Oct-01	wt	4969
1361	wt	M	14-Sep-01	04-Oct-01	wt	4969
1362	wt	M	14-Sep-01	04-Oct-01	wt	4969
1363	wt	M	14-Sep-01	04-Oct-01	wt	4969
1364	wt	M	14-Sep-01	07-Nov-01	wt	4969
1365	wt	F	14-Sep-01	17-Jan-03	wt	4969
1366	wt	M	14-Sep-01	07-Nov-01	wt	4969
2138	tg	F	14-Sep-01	17-Jan-03	wt	4969
1899	wt	F	25-Mar-02	13-May-02	wt	1107
1900	wt	F	25-Mar-02	13-May-02	wt	1107
1960	wt	M	25-Mar-02	06-Aug-02	wt	1107

Appendix B: TC10Q75L Mouse Colony Information

Mouse ID	tg/wt	Sex	Birth Date	Death Date	Female Parent	Male Parent
1961	tg	M	25-Mar-02	29-May-03	wt	1107
1962	wt	M	25-Mar-02	29-May-03	wt	1107
1963	wt	M	25-Mar-02	06-Aug-02	wt	1107
1896	wt	M	27-Mar-02	27-May-02	1600	wt
1897	tg	M	27-Mar-02	27-May-02	1600	wt
1898	tg	M	27-Mar-02	27-May-02	1600	wt
1974	tg	M	27-Mar-02	29-May-03	wt	1107
1975	wt	M	27-Mar-02	29-May-03	wt	1107
1976	wt	M	27-Mar-02	06-Aug-02	wt	1107
1977	wt	F	27-Mar-02	06-Aug-02	wt	1107
1978	wt	F	27-Mar-02	21-Oct-02	wt	1107
1979	tg	F	27-Mar-02	21-Oct-02	wt	1107
1951	wt	M	28-Mar-02	13-May-02	1453	wt
1952	wt	M	28-Mar-02	13-May-02	1453	wt
1953	wt	M	28-Mar-02	13-May-02	1453	wt
1954	wt	M	28-Mar-02	04-Mar-03	1453	wt
1955	tg	M	28-Mar-02	04-Mar-03	1453	wt
1956	wt	M	28-Mar-02	06-Aug-02	1453	wt
1957	wt	F	28-Mar-02	13-May-02	1453	wt
1958	wt	F	28-Mar-02	13-May-02	1453	wt
1959	wt	F	28-Mar-02	13-May-02	1453	wt
1964	tg	M	29-Mar-02	29-May-03	wt	1107
1965	tg	M	29-Mar-02	29-May-03	wt	1107
1966	wt	M	29-Mar-02	29-May-03	wt	1107
1967	wt	M	29-Mar-02	29-May-03	wt	1107
1969	wt	F	29-Mar-02	06-Aug-02	wt	1107
1971	wt	F	29-Mar-02	09-Dec-02	wt	1107
2149	tg	F	29-Mar-02	09-Dec-02	wt	1107
2162	tg	M	29-Mar-02	29-May-03	wt	1107
2045	tg	M	15-Apr-02	29-May-03	wt	1107
2046	tg	M	15-Apr-02	29-May-03	wt	1107
2047	tg	M	15-Apr-02	29-May-03	wt	1107
2048	tg	F	15-Apr-02	29-May-03	wt	1107
2049	tg	F	15-Apr-02	17-Jan-03	wt	1107

Appendix B: TC10Q75L Mouse Colony Information

Mouse ID	tg/wt	Sex	Birth Date	Death Date	Female Parent	Male Parent
2050	wt	F	15-Apr-02	17-Jan-03	wt	1107
2479	wt	M	02-Oct-02	14-Nov-02	2048	wt
2480	wt	M	02-Oct-02	14-Nov-02	2062	wt
2481	wt	M	02-Oct-02	14-Nov-02	2048	wt
2482	tg	M	02-Oct-02	14-Nov-02	2048	wt
2483	wt	F	02-Oct-02	04-Mar-03	2048	wt
2496	tg	M	14-Oct-02	29-May-03	2045	wt
2497	wt	F	14-Oct-02	11-Feb-03	2045	wt
2498	tg	F	14-Oct-02	11-Feb-03	2045	wt
2504	tg	F	14-Oct-02		2045	wt
2505	wt	F	14-Oct-02	26-Mar-03	2045	wt
2506	wt	F	14-Oct-02		2045	wt
2499	tg	M	25-Oct-02	29-May-03	2048	wt
2500	tg	M	25-Oct-02		2048	wt
2501	tg	M	25-Oct-02	29-May-03	2048	wt
2502	wt	M	25-Oct-02		2048	wt
2503	wt	F	25-Oct-02	20-Dec-02	2048	wt
2692	wt	M	05-Feb-03	26-Mar-03	2504	wt
2693	tg	F	05-Feb-03		2504	wt
2694	wt	F	05-Feb-03		2504	wt
2695	wt	F	05-Feb-03		2504	wt
2696	wt	F	05-Feb-03		2504	wt
2777	wt	M	25-Feb-03		2504	wt
2778	tg	M	25-Feb-03		2504	wt
2779	tg	M	25-Feb-03		2504	wt
2780	wt?	M	25-Feb-03		2504	wt
2781	tg	M	25-Feb-03		2504	wt
2782	wt	M	25-Feb-03		2504	wt
2783	tg	M	25-Feb-03		2504	wt
2784	wt	M	25-Feb-03		2504	wt
2785	wt	F	25-Feb-03		2504	wt
2786	wt	F	25-Feb-03		2504	wt
2787	tg	F	25-Feb-03		2504	wt

Complete Lineage List 4973

Mouse ID	tg/wt	Sex	Birth Date	Death Date	Female Parent	Male Parent
4973	tg	F	16-May-01	02-Apr-02	Surrogate	N/A
1132	wt	F	21-Jul-01	12-Sep-01	1706	wt
1133	wt	F	21-Jul-01	12-Sep-01	1706	wt
1134	wt	M	21-Jul-01	12-Sep-01	1706	wt
1135	wt	M	21-Jul-01	12-Sep-01	1706	wt
1136	wt	M	21-Jul-01	12-Sep-01	1706	wt
1137	wt	M	21-Jul-01	12-Sep-01	1706	wt
1138	wt	M	21-Jul-01	12-Sep-01	1706	wt
1139	wt	M	21-Jul-01	12-Sep-01	1706	wt
1140	wt	M	21-Jul-01	12-Sep-01	1706	wt
1141	wt	M	21-Jul-01	12-Sep-01	1706	wt
1240	wt	M	13-Aug-01	12-Sep-01	1706	wt
1241	wt	M	13-Aug-01	12-Sep-01	1706	wt
1243	wt	M	13-Aug-01	12-Sep-02	1706	wt
1244	wt	F	13-Aug-01	12-Sep-01	1706	wt
1245	wt	F	13-Aug-01	12-Sep-01	1706	wt
1246	wt	F	13-Aug-01	12-Sep-01	1706	wt
1247	wt	F	13-Aug-01	12-Sep-01	1706	wt
1248	wt	F	13-Aug-01	12-Sep-01	1706	wt
1249	wt	F	13-Aug-01	12-Sep-01	1706	wt
1250	wt	F	13-Aug-01	12-Sep-01	1706	wt
1251	wt	F	13-Aug-01	12-Sep-01	1706	wt
1870	tg	M	13-Aug-01	12-Sep-02	1706	wt
1337	wt	M	06-Sep-01	04-Oct-01	1706	wt
1338	wt	M	06-Sep-01	04-Oct-01	1706	wt
1339	wt	M	06-Sep-01	04-Oct-01	1706	wt
1340	wt	M	06-Sep-01	04-Oct-01	1706	wt
1341	wt	M	06-Sep-01	04-Oct-01	1706	wt
1342	wt	M	06-Sep-01	04-Oct-01	1706	wt
1343	wt	M	06-Sep-01	04-Oct-01	1706	wt
1344	wt	F	06-Sep-01	04-Oct-01	1706	wt

Appendix B: TC10Q75L Mouse Colony Information

Mouse ID	tg/wt	Sex	Birth Date	Death Date	Female Parent	Male Parent
1345	wt	F	06-Sep-01	04-Oct-01	1706	wt
1346	wt	F	06-Sep-01	04-Oct-01	1706	wt
1347	wt	F	06-Sep-01	04-Oct-01	1706	wt
2009	wt	M	01-Apr-02	27-May-02	wt	1242
2010	tg	M	01-Apr-02	27-May-02	wt	1242
2011	wt	M	01-Apr-02	27-May-02	wt	1242
2012	tg	M	01-Apr-02	27-May-02	wt	1242
2013	wt	M	01-Apr-02	12-Sep-02	wt	1242
2015	tg	M	01-Apr-02	12-Sep-02	wt	1242
2017	wt	F	01-Apr-02	12-Sep-02	wt	1242
2019	tg	F	01-Apr-02	12-Sep-02	wt	1242
2020	wt	F	01-Apr-02	12-Sep-02	wt	1242
2022	wt	F	01-Apr-02	13-May-02	wt	1242
2023	wt	F	01-Apr-02	13-May-02	wt	1242
2024	wt	F	01-Apr-02	13-May-02	wt	1242
2025	wt	F	01-Apr-02	13-May-02	wt	1242
2337	wt	M	01-Apr-02	12-Sep-02	wt	1242
2338	tg	M	01-Apr-02	12-Sep-02	wt	1242
2339	wt	F	01-Apr-02	12-Sep-02	wt	1242
2340	tg	F	01-Apr-02	12-Sep-02	wt	1242
2051	wt	M	22-Apr-02	12-Sep-02	wt	1870
2052	tg	M	22-Apr-02	21-Nov-02	wt	1870
2054	wt	F	22-Apr-02	06-Aug-02	wt	1870
2055	tg	F	22-Apr-02	12-Sep-02	wt	1870
2056	tg	F	22-Apr-02	12-Sep-02	wt	1870
2057	wt	F	22-Apr-02	12-Sep-02	wt	1870
2058	wt	F	22-Apr-02	12-Sep-02	wt	1870
2059	tg	F	22-Apr-02	12-Sep-02	wt	1870
2060	tg	F	22-Apr-02	12-Sep-02	wt	1870
2061	tg	F	22-Apr-02	12-Sep-02	wt	1870
2062	tg	F	22-Apr-02	29-May-03	wt	1870
2143	wt	M	22-Apr-02	06-Aug-02	wt	1870
2471	tg	M	03-Oct-02	29-May-03	2062	wt
2472	tg	M	03-Oct-02	29-May-03	2062	wt

Appendix B: TC10Q75L Mouse Colony Information

Mouse ID	tg/wt	Sex	Birth Date	Death Date	Female Parent	Male Parent
2473	tg	M	03-Oct-02	29-May-03	2062	wt
2474	wt	M	03-Oct-02	14-Nov-02	2062	wt
2475	wt	M	03-Oct-02	14-Nov-02	2062	wt
2476	tg	M	03-Oct-02	14-Nov-02	2062	wt
2477	tg	F	03-Oct-02	04-Mar-03	2062	wt
2478	wt	F	03-Oct-02		2062	wt
2788	wt	M	01-Mar-03		wt	2473
2789	wt	M	01-Mar-03		wt	2473
2790	wt	M	01-Mar-03		wt	2473
2791	wt	M	01-Mar-03		wt	2473
2792	tg	M	01-Mar-03		wt	2473
2793	tg	F	01-Mar-03		wt	2473
2794	wt	F	01-Mar-03		wt	2473
2795	tg	F	01-Mar-03		wt	2473
2796	wt	F	01-Mar-03		wt	2473

Complete Lineage List 4977

Mouse ID	tg/wt	Sex	Birth Date	Death Date	Female Parent	Male Parent
4977	tg	M	16-May-01	02-Apr-02	Surrogate	N/A
1114	wt	M	19-Jul-01	12-Sep-01	wt	4977
1115	wt	M	19-Jul-01		wt	4977
1118	wt	M	19-Jul-01	12-Sep-01	wt	4977
1119	wt	M	19-Jul-01		wt	4977
1120	wt	F	19-Jul-01	12-Sep-01	wt	4977
1121	wt	F	19-Jul-01	16-Oct-01	wt	4977
1122	tg	F	19-Jul-01	16-Oct-01	wt	4977
1123	tg	F	19-Jul-01	20-Dec-02	wt	4977
1695	tg	M	19-Jul-01	29-May-03	wt	4977
1696	tg	M	19-Jul-01	29-May-03	wt	4977
1231	wt	M	13-Aug-01	12-Sep-01	wt	4977
1232	wt	M	13-Aug-01	12-Sep-01	wt	4977
1233	wt	M	13-Aug-01	12-Sep-01	wt	4977
1237	tg	F	13-Aug-01	05-May-03	wt	4977
1238	tg	F	13-Aug-01	05-May-03	wt	4977
1239	tg	F	13-Aug-01	05-May-03	wt	4977
1698	wt	F	13-Aug-01	22-Feb-02	wt	4977
1699	tg	F	13-Aug-01	22-Feb-02	wt	4977
1868	wt	F	13-Aug-01	05-May-03	wt	4977
1425	wt	M	28-Sep-01		wt	4977
1426	tg	M	28-Sep-01	22-Aug-02	wt	4977
1866	tg	F	28-Sep-01	20-Dec-02	wt	4977
2147	tg	F	28-Sep-01	20-Dec-02	wt	4977
2148	wt	F	28-Sep-01	20-Dec-02	wt	4977
1629	wt	M	20-Oct-01	15-Feb-02	wt	4977
1630	wt	M	20-Oct-01	15-Feb-02	wt	4977
1869	tg	F	20-Oct-01		wt	4977
2026	wt	M	02-Apr-02	13-May-02	1427	wt
2027	wt	M	02-Apr-02	13-May-02	1427	wt
2028	wt	M	02-Apr-02	13-May-02	1427	wt

Appendix B: TC10Q75L Mouse Colony Information

Mouse ID	tg/wt	Sex	Birth Date	Death Date	Female Parent	Male Parent
2029	wt	M	02-Apr-02	13-May-02	1427	wt
2030	wt	M	02-Apr-02	13-May-02	1427	wt
2031	wt	M	02-Apr-02	13-May-02	1427	wt
2032	wt	F	02-Apr-02	13-May-02	1427	wt
2033	wt	F	02-Apr-02	13-May-02	1427	wt
2034	wt	F	02-Apr-02	13-May-02	1427	wt
2035	wt	F	02-Apr-02	13-May-02	1427	wt
2036	wt	F	02-Apr-02	13-May-02	1427	wt
1991	tg	M	04-Apr-02	29-May-02	1123	wt
1992	wt	M	04-Apr-02	29-May-02	1123	wt
1993	wt	M	04-Apr-02	29-May-02	1123	wt
1994	wt	M	04-Apr-02	29-May-02	1123	wt
1995	wt	M	04-Apr-02	29-May-02	1123	wt
1997	wt	F	04-Apr-02	20-Dec-02	1123	wt
1998	wt	F	04-Apr-02	06-Aug-02	1123	wt
1999	tg	F	04-Apr-02	20-Dec-02	1123	wt
2163	wt	F	04-Apr-02	06-Aug-02	1123	wt
2151		M	12-Jun-02	20-Dec-02	1999	wt
2152		M	12-Jun-02		1999	wt
2153		M	12-Jun-02	20-Dec-02	1999	wt
2154		M	12-Jun-02	06-Aug-02	1999	wt
2155		F	12-Jun-02	20-Dec-02	1999	wt
2156		F	12-Jun-02	20-Dec-02	1999	wt
2157		F	12-Jun-02	20-Dec-02	1999	wt
2301	tg	F	06-Jul-02		1999	wt
2302	wt	F	06-Jul-02		1999	wt
2303	wt	F	06-Jul-02		1999	wt
2304	wt	F	06-Jul-02	04-Mar-03	1999	wt
2305	tg	F	06-Jul-02	04-Mar-03	1999	wt
2306	tg	M	06-Jul-02		1999	wt
2307	wt	M	06-Jul-02		1999	wt
2308	tg	M	06-Jul-02		1999	wt
2797	wt	F	03-Mar-03		wt	2306
2798	tg	F	03-Mar-03		wt	2306

Appendix B: TC10Q75L Mouse Colony Information

Mouse ID	tg/wt	Sex	Birth Date	Death Date	Female Parent	Male Parent
2799	tg	F	03-Mar-03		wt	2306
2800	tg	F	03-Mar-03		wt	2306
2801	tg	M	03-Mar-03		wt	2306
2802	wt	M	03-Mar-03		wt	2306
2803	tg	M	03-Mar-03		wt	2306
2804	wt	M	03-Mar-03		wt	2306
2805	wt	M	03-Mar-03		wt	2306

Complete Lineage List 4986

Mouse ID	tg/wt	Sex	Birth Date	Death Date	Female Parent	Male Parent
4986	tg	M	16-May-01	02-Apr-02	Surrogate	N/A
1142	tg	M	17-Jul-01	01-Oct-02	4986	wt
1143	wt	F	17-Jul-01	23-Aug-02	4986	wt
1144	tg	F	17-Jul-01	16-Oct-01	4986	wt
1145	wt	F	17-Jul-01	12-Sep-01	4986	wt
1697	tg	F	17-Jul-01	23-Aug-02	4986	wt
1167	tg	M	07-Aug-01	06-Jan-03	4986	wt
1168	wt	M	07-Aug-01	12-Sep-01	4986	wt
1169	wt	M	07-Aug-01	06-Jan-03	4986	wt
1170	wt	M	07-Aug-01	12-Sep-01	4986	wt
1171	wt	M	07-Aug-01	12-Sep-01	4986	wt
1258	tg	M	29-Aug-01	17-Jan-03	4986	wt
1259	tg	M	29-Aug-01	09-Apr-02	4986	wt
1440	tg	M	28-Sep-01	12-Mar-03	4986	wt
1441	tg	M	28-Sep-01	17-Jan-03	4986	wt
1442	tg	M	28-Sep-01	13-Feb-03	4986	wt
1443	tg	M	28-Sep-01	17-Jan-03	4986	wt
1444	tg	F	28-Sep-01	16-Sep-02	4986	wt
1445	tg	F	28-Sep-01		4986	wt
1446	tg	F	28-Sep-01	17-Jan-03	4986	wt
1853	tg	M	12-Mar-02	29-May-03	wt	1258
1854	tg	M	12-Mar-02	04-Mar-03	wt	1258
1855	tg	F	12-Mar-02	29-May-03	wt	1258
1856	tg	F	12-Mar-02	29-May-03	wt	1258
1858	wt	F	12-Mar-02	15-Oct-02	wt	1258
1859	tg	F	12-Mar-02	15-Oct-02	wt	1258
1860	tg	F	12-Mar-02	17-Jan-03	wt	1258
1861	wt	F	12-Mar-02	17-Jan-03	wt	1258
2140	tg	F	12-Mar-02	20-Jan-03	wt	1258
2000	tg	M	31-Mar-02	28-May-02	wt	1258
2001	tg	M	31-Mar-02	28-May-02	wt	1258

Appendix B: TC10Q75L Mouse Colony Information

Mouse ID	tg/wt	Sex	Birth Date	Death Date	Female Parent	Male Parent
2002	wt	M	31-Mar-02	28-May-02	wt	1258
2003	tg	M	31-Mar-02	28-May-02	wt	1258
2004	wt	M	31-Mar-02	28-May-02	wt	1258
2005	tg	F	31-Mar-02	09-Dec-02	wt	1258
2006	wt	F	31-Mar-02	06-Aug-02	wt	1258
2007	wt	F	31-Mar-02	06-Aug-02	wt	1258
2008	wt	F	31-Mar-02	09-Dec-02	wt	1258
2484	tg	M	04-Oct-02		wt	1853
2485	wt	M	04-Oct-02		wt	1853
2486	tg	M	04-Oct-02		wt	1853
2487	tg	M	04-Oct-02	14-Nov-02	wt	1853
2488	wt	M	04-Oct-02	14-Nov-02	wt	1853
2489	tg	M	04-Oct-02	14-Nov-02	wt	1853
2490	wt	F	04-Oct-02		wt	1853
2491	wt	F	04-Oct-02	11-Feb-03	wt	1853
2492	tg	F	04-Oct-02	11-Feb-03	wt	1853
2518	wt	M	24-Oct-02	26-Mar-03	2005	wt
2519	wt	M	24-Oct-02		2005	wt
2520	??	M	24-Oct-02		2005	wt
2521	wt	M	24-Oct-02		2005	wt
2522	tg	F	24-Oct-02	20-Jan-03	2005	wt
2523	tg	F	24-Oct-02		2005	wt
2524	tg	F	24-Oct-02		2005	wt
2525	wt	M	28-Oct-02		wt	1853
2526	tg	M	28-Oct-02		wt	1853
2527	tg	M	28-Oct-02		wt	1853
2528	??	M	28-Oct-02		wt	1853
2529	wt	M	28-Oct-02		wt	1853
2530	tg	F	28-Oct-02		wt	1853
2531	tg	F	28-Oct-02		wt	1853
2532	tg	F	28-Oct-02		wt	1853
2533	wt	F	28-Oct-02	20-Jan-03	wt	1853
2534	wt	F	28-Oct-02		wt	1853
2535	wt	F	28-Oct-02		wt	1853

Appendix B: TC10Q75L Mouse Colony Information

Mouse ID	tg/wt	Sex	Birth Date	Death Date	Female Parent	Male Parent
2669	wt	F	04-Feb-03	26-Mar-03	2523	wt
2670	wt	F	04-Feb-03	26-Mar-03	2523	wt
2671	wt	F	04-Feb-03	26-Mar-03	2523	wt
2672	wt	F	04-Feb-03	26-Mar-03	2523	wt
2673	wt	F	04-Feb-03	26-Mar-03	2523	wt
2674	tg	M	04-Feb-03		2523	wt
2675	wt	M	04-Feb-03	26-Mar-03	2523	wt
2676	wt	M	04-Feb-03		2523	wt
2677	wt	M	04-Feb-03	26-Mar-03	2523	wt
2678	wt	M	04-Feb-03	26-Mar-03	2524	wt
2679	wt	M	04-Feb-03		2524	wt
2680	tg	M	04-Feb-03		2524	wt
2681	wt	M	04-Feb-03	26-Mar-03	2524	wt
2682	wt	F	04-Feb-03		2524	wt
2683	wt	F	04-Feb-03		2524	wt
2684	tg	F	04-Feb-03		2524	wt
2685	tg	F	04-Feb-03		2524	wt
2758	tg	M	28-Feb-03		2523	wt
2759	wt	M	28-Feb-03		2523	wt
2760	wt	M	28-Feb-03		2523	wt
2761	tg	M	28-Feb-03		2523	wt
2762	tg	M	28-Feb-03		2523	wt
2763	tg	M	28-Feb-03		2523	wt
2764	tg	F	28-Feb-03		2523	wt
2765	wt	F	28-Feb-03		2523	wt
2766	wt	F	28-Feb-03		2523	wt
2767	tg	F	28-Feb-03		2523	wt
2768	wt	M	02-Mar-03		2524	wt
2769	wt	M	02-Mar-03		2524	wt
2770	tg	M	02-Mar-03		2524	wt
2771	wt	F	02-Mar-03		2524	wt
2772	tg	F	02-Mar-03		2524	wt
2773	tg	F	02-Mar-03		2524	wt
2774	wt	F	02-Mar-03		2524	wt

Appendix B: TC10Q75L Mouse Colony Information

Mouse ID	tg/wt	Sex	Birth Date	Death Date	Female Parent	Male Parent
2775	tg	F	02-Mar-03		2524	wt
2776	tg	F	02-Mar-03		2524	wt